SAND2014-2497C

Sensitive Detection: Cavity Ring-Down Spectroscopy and Crucial Intermediates Monitoring in Fuel Oxidation Chemistry

Haifeng Huang

March 13, 2014

Argonne National Laboratory

Princeton University

Acknowledgements

- Prof. Kevin Lehmann
- Prof. Giacinto Scoles
- Sco-Lehmann Group members
- and many others

- Prof. Brooks Pate
- Group members
- Charles Lam

- Lisa Bergson
- Dr. Wen-Bin Yan
- Dr. Yu Chen
- and others

- Drs. Judit Zádor, David Osborn, Craig Taatjes, Lenny Sheps (ZOTS)
- Drs. Tom Settersten, David Chandler
- Drs. Scott Bisson, Tom Kulp
- Howard Johnsen, Brian Patterson, Paul Fugazzi, Len Jusinski, Max Sloss
- Drs. Oliver Welz, John Savee, Arkke Eskola, Adam Scheer, Brandon Rotavera, Ivan Antonov, Ewa Papajak
- and many others

$$$

- NSF
- Princeton Institute for the Science & Technology of Materials (PRISM)
- University of Virginia

Outline

- Cavity Ring-down Spectroscopy (CRDS)
- Challenges in CRDS Technique
  - Higher order transverse mode interference
  - Linear birefringence and dichroism of supermirrors
  - Finite extinction ratio in CW-CRDS
- Trace Methane (63 pptv) Detection by CW-CRDS
- Ultimate Sensitivity Limits of CRDS Method
- Alkane Oxidation: Probing OH and ROO (308 nm)
- OH Detection (2.9 μm) in QOOH Chemistry
- Conclusions

Cavity Ring-Down Spectroscopy

In 1980s, dielectric coated "**supermirrors**" with **very high reflectivity (> 0.99)**

measuring **lifetime of trapped photon** in a high finesse cavity

Cavity ring-down optical spectrometer for absorption measurements using pulsed laser sources

Anthony O'Keefe and David A. G. Deacon

Deacon Research, 900 Welch Road, Palo Alto, California 94304

(Received 28 March 1988; accepted for publication 27 July 1988)

J. M. Herbelin, J. A. M ncer, and D. J. Benard

First spectroscopic cavity ring-down with pulsed-laser sources

Fig. 1. Typical cavity decay curve from a two-mirrored 10-m cavity having a fall time of 23.2 μsec starts on the left-hand side as the lower of the two curves. The second curve is the decay from a RC network having the same decay constant. The decays from the two events are perfectly merged showing that the cavity decay is indeed exponential.

CRDS has been *widely* employed for > 25 years.

- **Spectroscopy**
  - **Cu_2, Cu_3** — CPL **172**, 214 (1990) — O'Keefe *et al.*
- **Chemical kinetics**
  - **Phenyl** — JACS **115**, 4371 (1993) — Lin *et al.*
- **Analytical chemistry**
  - **$^{13}C/^{12}C$** — Anal. Chem. **74**, 2003 (2002) — Crosson *et al.*
  - **Trace H_2O** — Anal. Chem. **75**, 4599 (2003) — Dudek *et al.*
- **Combustion diagnostics**
  - **$^1CH_2$** — CPL **296**, 151 (1998) — McIlroy, A.
- **Medical gas diagnosis**
  - **NO** — Appl. Opt. **43**, 2257 (2004) — Bakhirkin *et al.*
- **and more**

CRDS: Basic Ideas

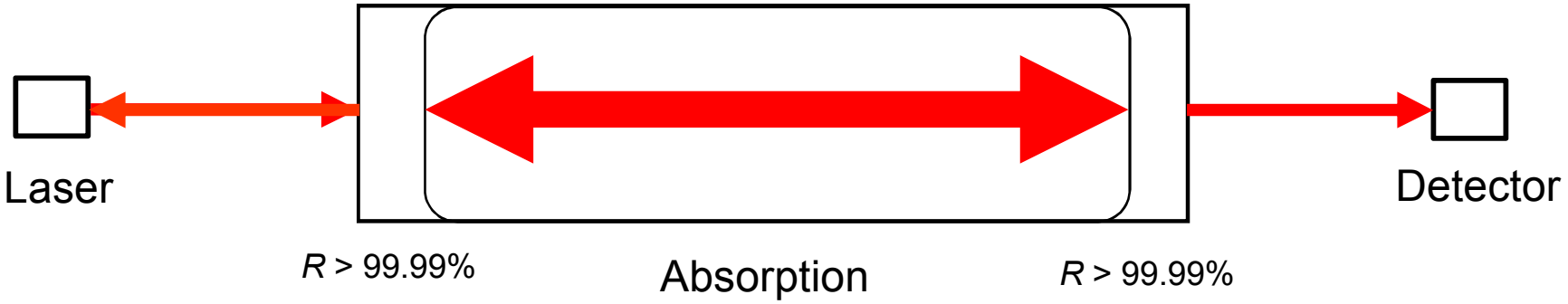

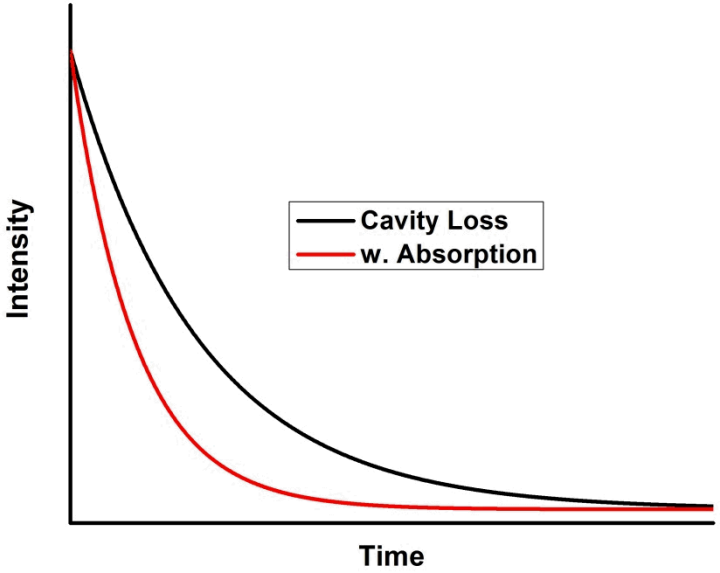

$$I(t) = Ae^{-kt} + B + \text{noise}$$

$$\tau = 1/k$$

$$\tau = \frac{L}{c(1 - R + \alpha L)}$$

Advantages of CRDS Method

- Much longer path lengths than traditional multi-pass cells

  $L_{eff} \sim 100\ \mu s \cdot c = 30\ km$

- Ring-down decay rate is **immune to the amplitude noise** of incident laser
- Very high sensitivity

  $\alpha_{min} \sim 10^{-6} - 10^{-12}\ cm^{-1}$

  single pass $\alpha L \sim 10^{-5} - 10^{-11}$ **if** $L = 30$ **cm**
- Method is calibration free if absorption cross section σ is known
- Cell is very compact; light contained in narrow spot of ~ 1 mm^2

Sensitive detection methods such as CRDS are *essential* for probing very weak absorption features or detecting species of very low concentrations.

Typical CW-CRDS Setup

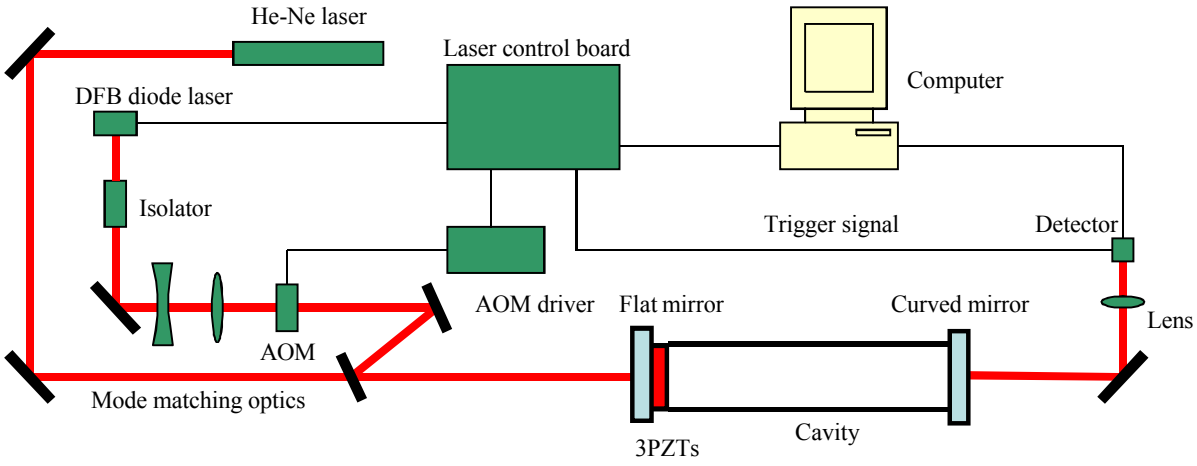

Key Parts:

- CW laser source
- Stable ring-down cavity
- Fast light switch
- Fast detector
- Piezo transducer (PZT)

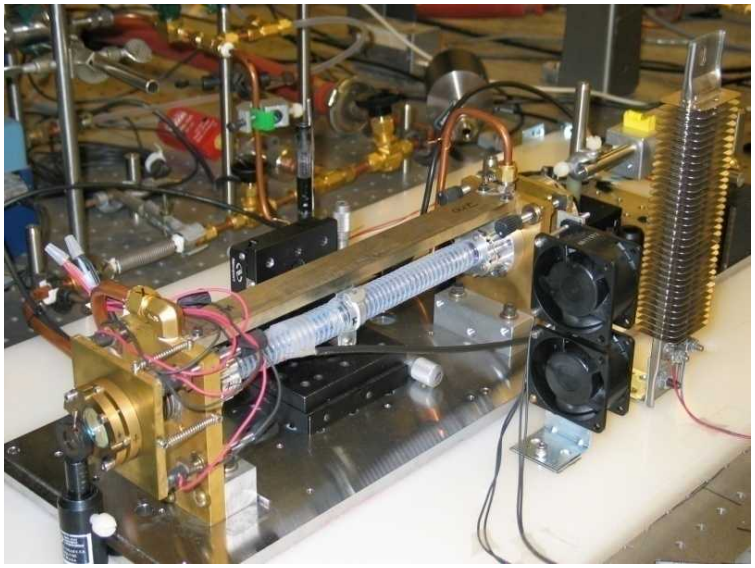

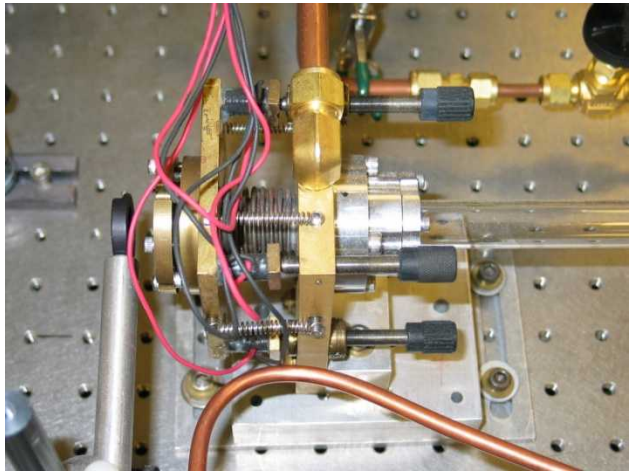

Eigenmodes in a Stable Optical Cavity

A. E. Siegman, "Lasers", 1986

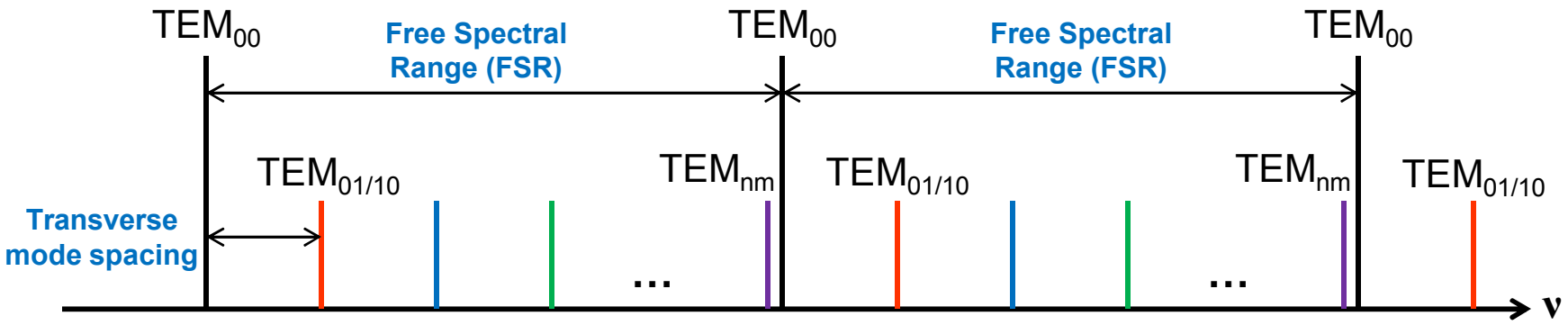

Single mode excitation produces exactly single exponential decay.
Multimode excitation can cause mode beating in decay signal.

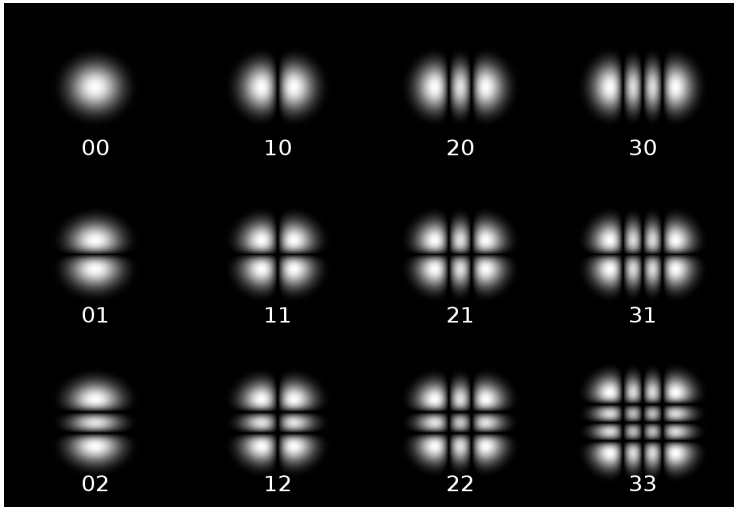

Wikipedia

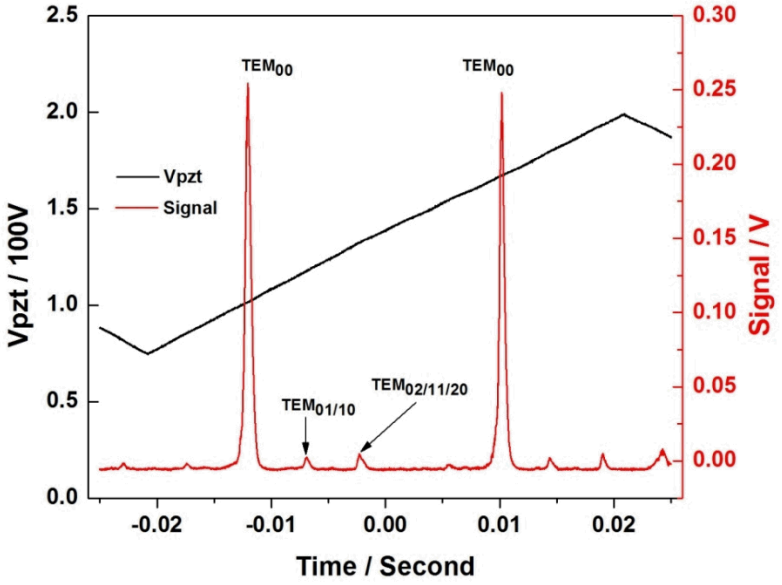

Empty cavity decay time constant "decreased" a lot!

$$\chi^2 = \frac{1}{(N-3)\sigma^2}\sum_{i=0}^{N-1}\left[y_i - B - A\exp(-i\Delta t/\tau)\right]^2$$

Reduced χ^2 should be close to one.

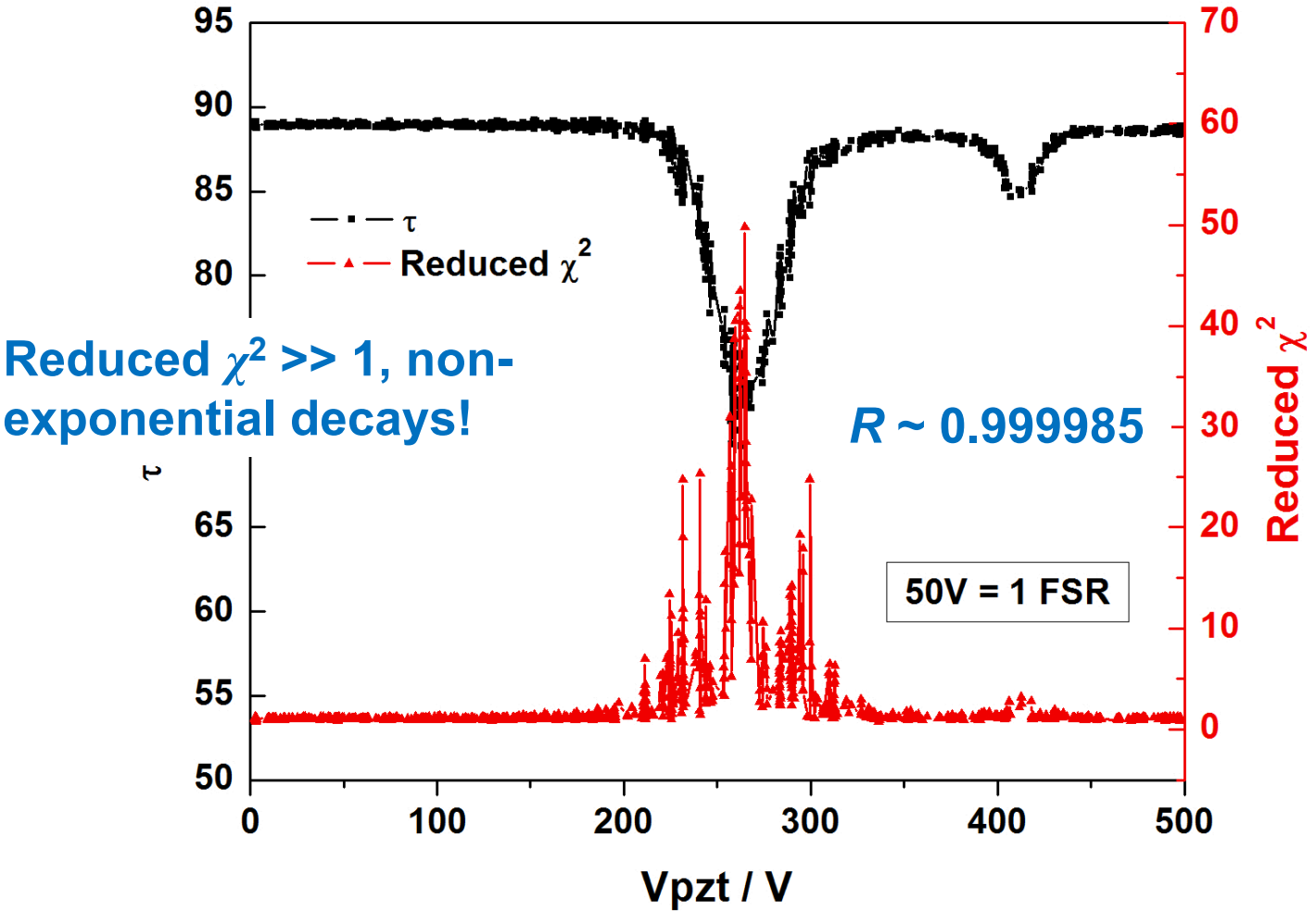

Reduced χ^2 >> 1, non-exponential decays!

R ~ 0.999985

50V = 1 FSR

The noisy decay signal is described by a two-mode beating model perfectly.

$$y(t) = A + B_1 \exp(-k_1 t) + B_2 \exp(-k_2 t) + 2\sqrt{B_1 B_2}\, \exp(-\frac{k_1 t}{2}) \exp(-\frac{k_2 t}{2}) \cos(2\pi \cdot \Delta\nu \cdot t + \Delta\varphi)$$

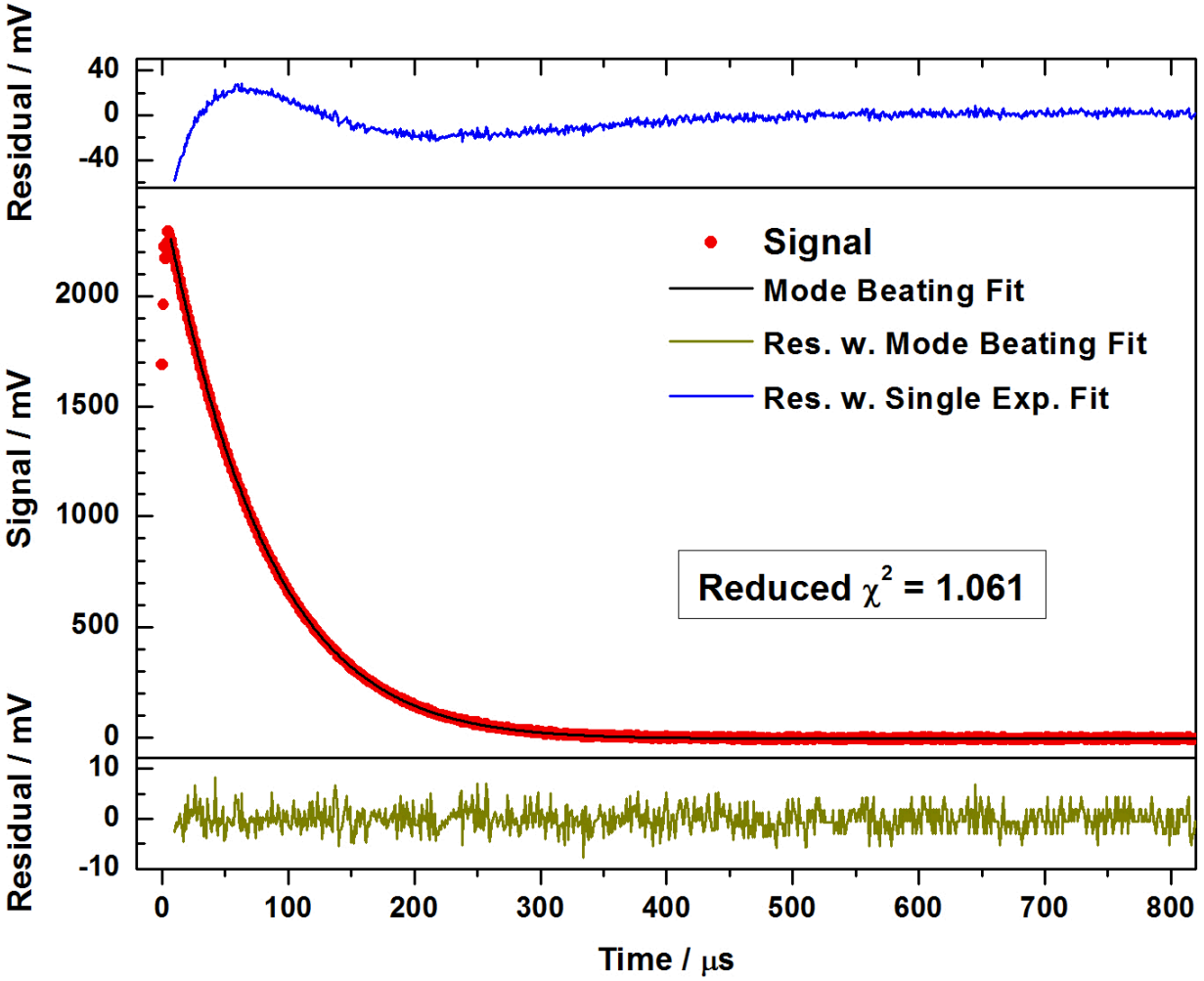

Data analysis shows signs of resonance by tuning.

- 50V = 1.0 FSR, laser λ = 1.652 μm
- Δν tuning rate 120 Hz/V, or **7.22 kHz/μm**

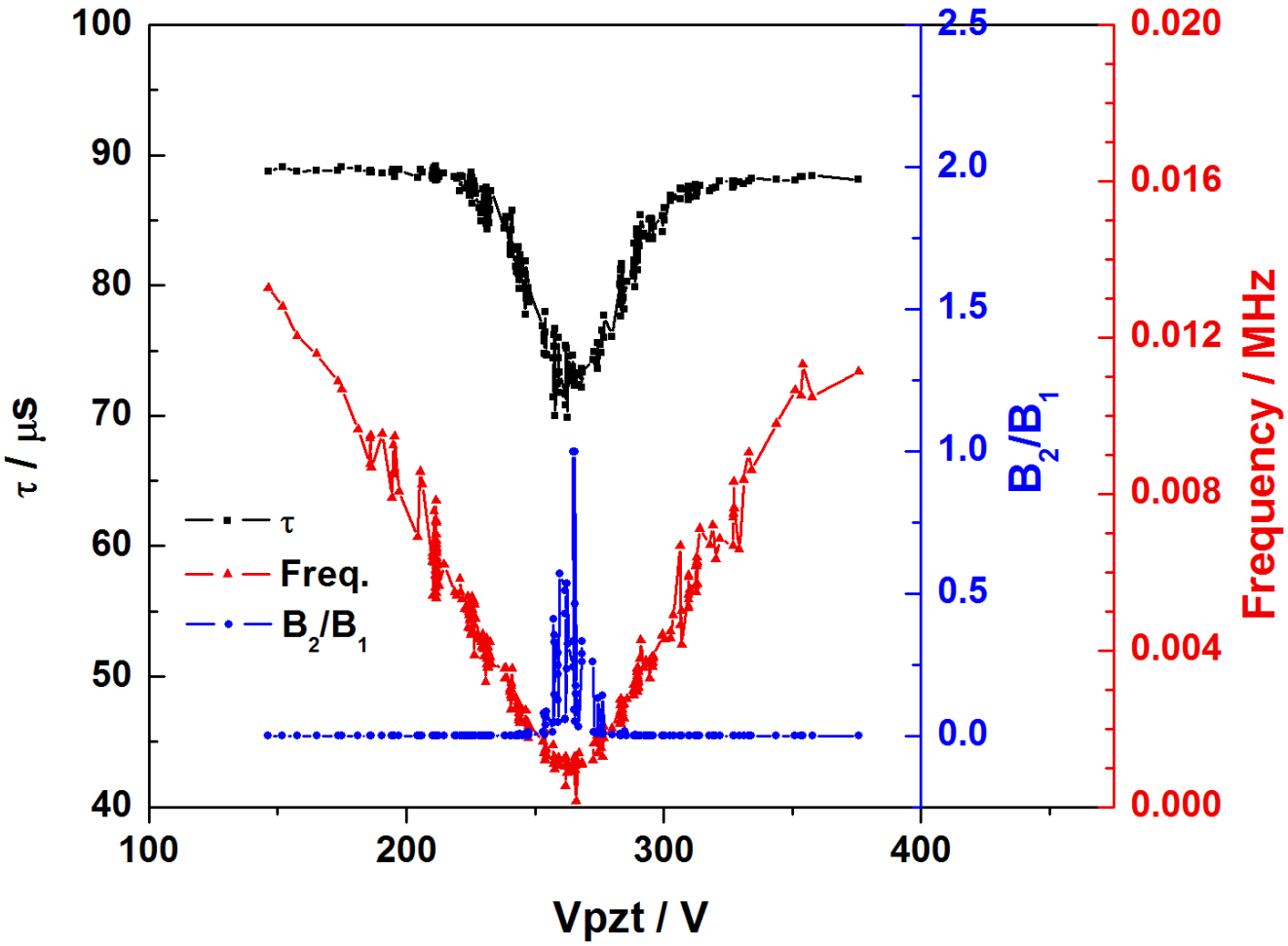

Images of very high order transverse mode have been captured by an IR camera.

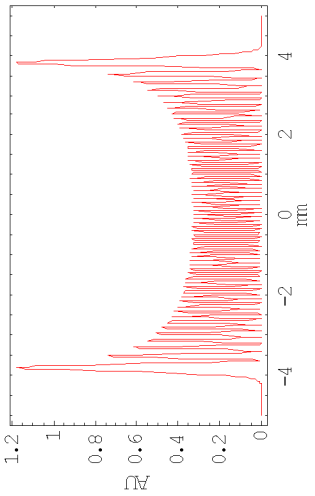

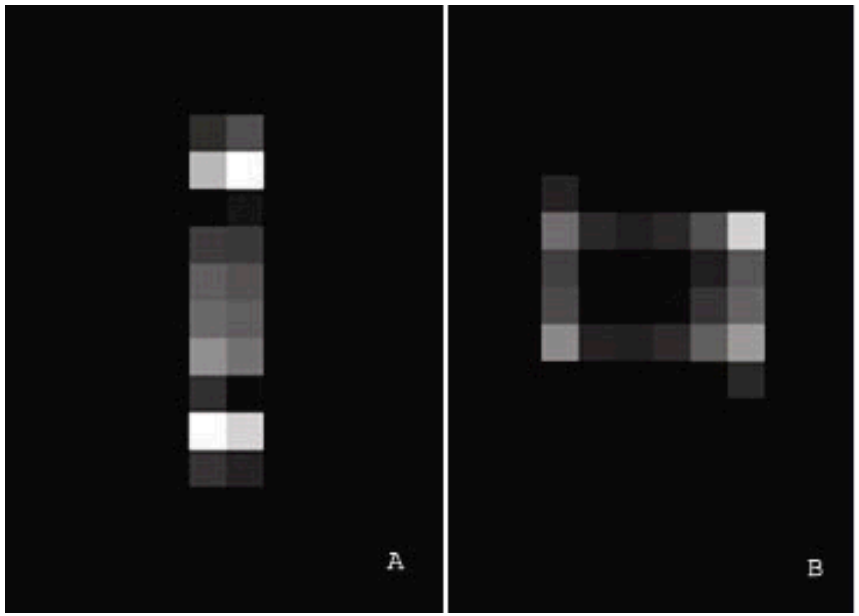

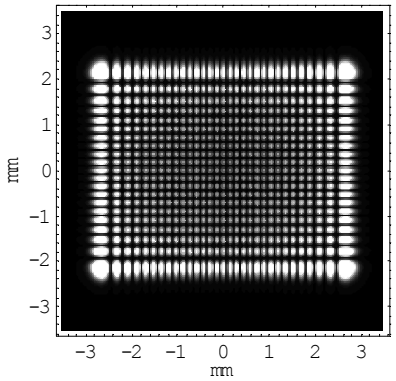

TEM_{nm} mode size:

$$\sqrt{n+m+1}\,\omega_{00}, \quad \omega_{00} = 0.507mm$$

- TEM_{00} mode diameter ~ **1 pixel**
- Mode size of A and B: ~ **4mm** and **3.6mm**
- Index n+m: ~ **60** for A and ~ **50** for B

A. Yariv, ***Quantum Electronics***, 2nd Edition, John Wiley & Sons, 1989

The excitation of very high order transverse modes is caused by mode crossing from cavity length tuning.

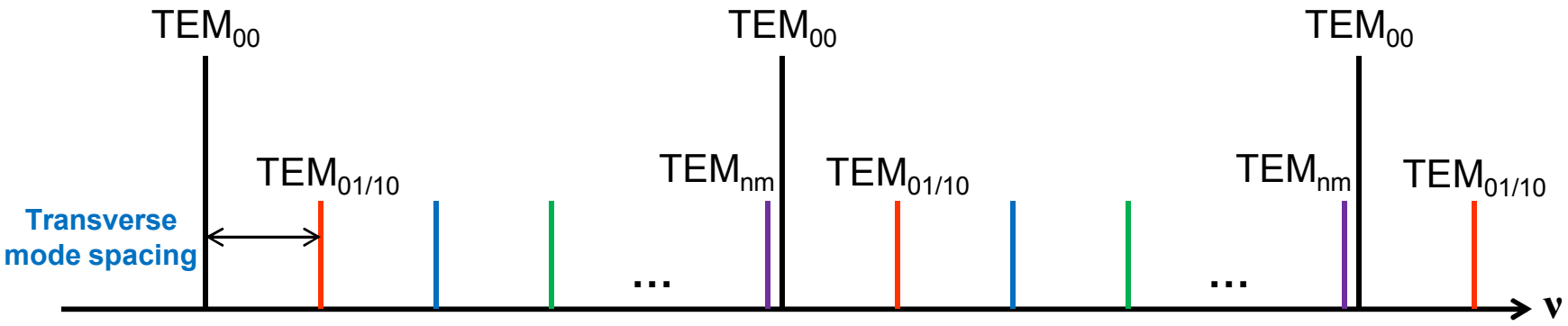

$$\frac{d\nu_{qnm}}{dL} = -\frac{\nu_{qnm}}{L} + \frac{c}{2n_0 L}\frac{n+m+1}{2\pi\sqrt{L(R_c - L)}}$$

Relative tuning rate:

$$123\,(n+m)\,\mathrm{Hz}/\mu\mathrm{m}$$

PZT scan:	**7.22kHz/μm**	n+m ~ **59**
Higher order mode images		n+m ~ **60, 50**
Cavity length 39.604 cm		n+m ~ 60
Cell inner radius 7.6 mm		n+m < 135
4 mm diameter aperture		n+m < **14**

A. Yariv, ***Quantum Electronics***, 2nd Edition, John Wiley & Sons, 1989

Those high order TEM_{nm} modes are excited through surface scattering coupling.

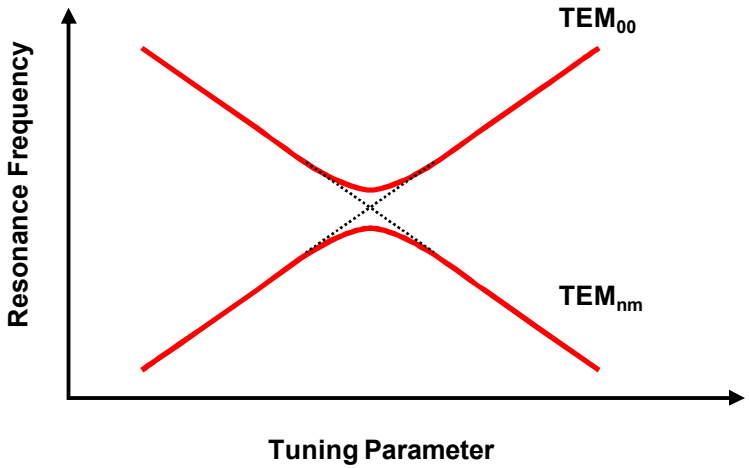

$$L_s = 1 - R - T \sim 10^{-6}$$
$$\Delta\Omega \sim \pi(\lambda/\pi\omega_{00})^2 = 3\times10^{-6}$$
$$L_s \Delta\Omega / 2\pi \sim 10^{-12}$$

$$\Delta\nu_{\min} = 2\left|S_1 + S_2\right| / t_r$$
$$\Delta\nu_{\min} \approx 1\,\text{kHz}$$
$$t_r = 2.63\,\text{ns}$$
$$\left|S_1\right|^2, \left|S_2\right|^2 \sim 10^{-12}$$

Relative Intensity of excited TEM_{nm} mode through coupling:

$$\sim (\Delta\nu_{\min}\tau_{nm})^2$$
$$\tau_{nm} \approx 50\,\mu\text{s} \quad \sim \underline{10}^{-3}$$
10 micron
$$\tau_{nm} \approx 100\,t_r \quad \sim 10^{-10}$$

Not B_1/B_2 !

Klaassen T. *et al.*, ***Optics Letters*** **30** 1959 (2005)

Paschotta R. ***Optics Express*** **14** 6069 (2006)

Huang & Lehmann, ***Optics Express*** **15**(14), 8745-8759 (2007)

Sub-ppbv Methane Detection

Methane at ppbv level has been found in the atmosphere of Mars but the source of it is still under debate.

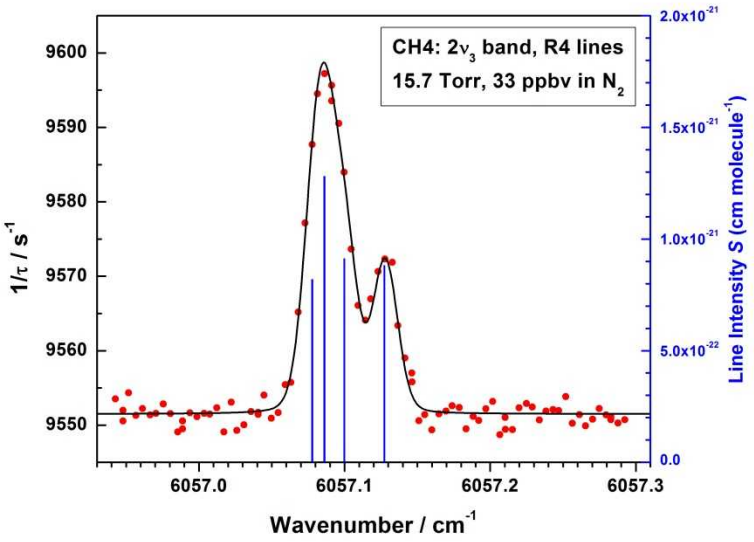

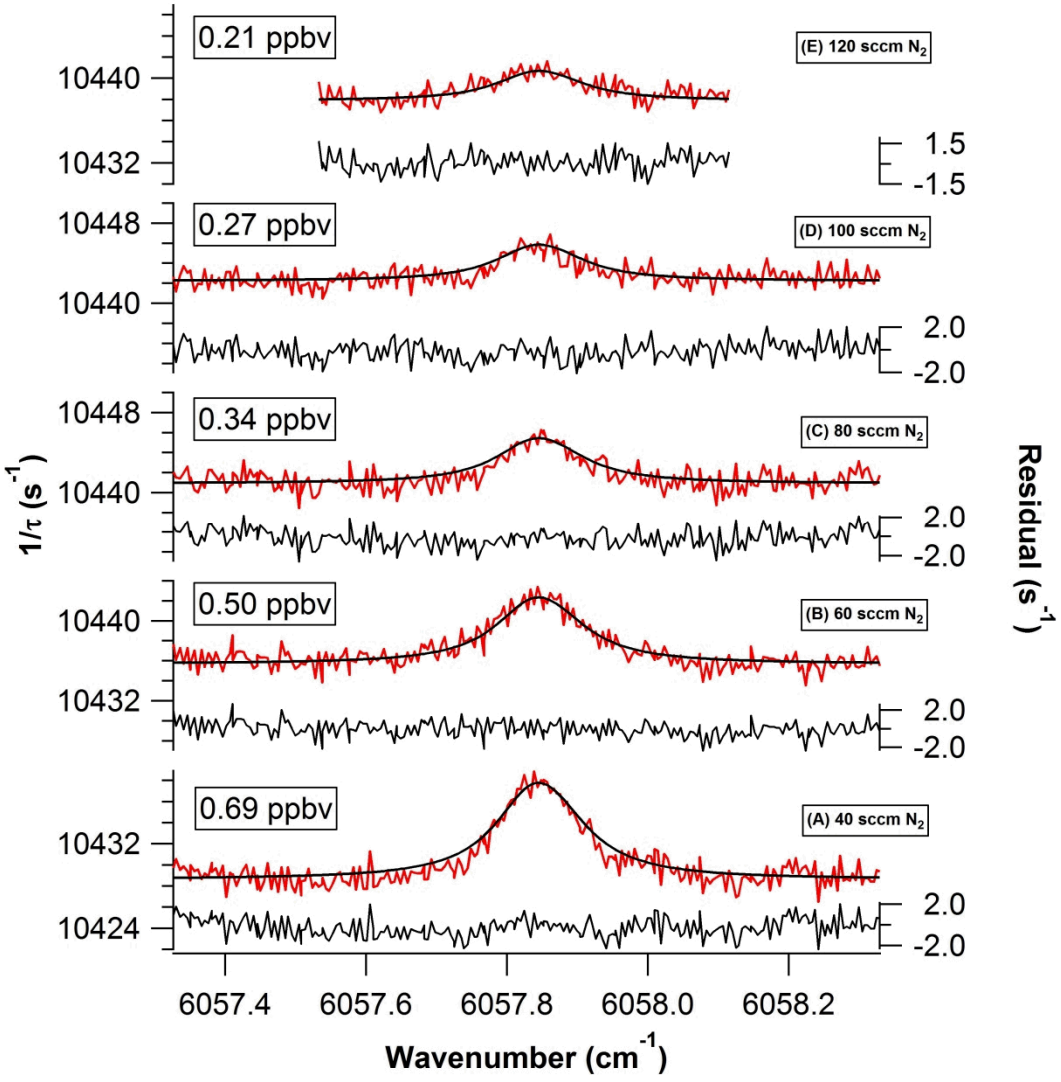

80 times spectrum averaging

1σ detection limit:

63 pptv

760 Torr N_2 buffer gas

HITRAN Database 2000; H. Huang and K. K. Lehmann, ***Applied Optics***, **49** 1378 (2010); Formisano *et al*., ***Science***, **306**, 1758 (2004)

Single Shot Sensitivity of CRDS

What is the ultimate sensitivity of Cavity Ring-Down Spectroscopy?

Detector Noise + Shot Noise

$$\sigma^2(t) = \frac{P_N^2}{2} + \frac{h\nu}{Q} A e^{-kt}$$

Detector Noise Limit

$$\sigma_k^2 = 8k^3 \Delta t \left(\frac{\sigma}{A}\right)^2 = 4k^3 \left(\frac{P_N}{A}\right)^2$$

$\tau = 100\mu s \quad \Delta t = 1\mu s \quad A/\sigma = 1000$

$\sigma_k = 2.8 s^{-1} \quad \alpha_{\min} = 9.4 \times 10^{-11} \text{cm}^{-1}$

Shot Noise Limit

$$\sigma_k^2 = k^3 \left(\frac{h\nu}{QA}\right)$$

$\tau = 100\mu s \quad Q = 0.64 \quad A = 1\mu\text{W} \quad \lambda = 1.65\mu\text{m}$

$\sigma_k = 0.43 s^{-1} \quad \alpha_{\min} = 1.4 \times 10^{-11} \text{cm}^{-1}$

Reached a sensitivity of 2.8 x 10^{-11} cm^{-1} in methane detection

K. K. Lehmann and H. Huang, ***Frontiers of Molecular Spectroscopy***, Chapter 18, Elsevier 2008

What is the sensitivity of CRDS in unit bandwidth?

Larger triggering threshold and **longer fitting time window** reduce the error of measured **decay rate *k***, but will decrease the **ring-down event rate** in a fixed time period.

This **tradeoff** between above factors gives the **highest sensitivity**.

Shot noise limited, $\Delta\nu_L >> \Delta\nu_c$:

$$P_{th} = 2.47P_0 \quad \langle \Delta t_{trig} \rangle = 6.01\tau$$
$$N\Delta t = 5.67\tau \quad \text{RD rate} = 0.086k$$

$$\alpha_{min} = 2.31 \cdot \frac{1-R}{L}\sqrt{\frac{h\nu}{QP_0}}$$

$$P_0 = 1\mu\text{W} \quad \lambda = 1.65\mu\text{m} \quad Q = 0.64 \quad \tau = 100\mu s$$
$$0.086k = 860\text{Hz} \quad \alpha_{min} = 3.3\times10^{-13}\text{cm}^{-1}/\text{Hz}^{1/2}$$

We have realized a sensitivity of 7.9 x 10^{-12} cm^{-1} $Hz^{-1/2}$ by a cheap setup, only 24 times worse than the optimized shot noise limit.

H. Huang and K. K. Lehmann, ***Journal of Physical Chemistry A***, **117**, 13399 (2013)

NICE-OHMS

Noise-Immune Cavity-Enhanced Optical-Heterodyne Molecular Spectroscopy

Hall *et al.* combined **frequency modulation** with **high finesse cavity**

J. Ye, L-S Ma, J.L. Hall, ***JOSA B* 15**, 6 (1998)

L-S Ma, J. Ye, P. Dube, J.L. Hall, ***JOSA B* 16**, 2255 (1999)

$$\alpha_{\min} = \frac{1-R}{L}\sqrt{\frac{h\nu}{QP_0}}\frac{1}{J_0(\beta)J_1(\beta)} \xrightarrow{\beta=0.5} 4.4\cdot\frac{1-R}{L}\sqrt{\frac{h\nu}{QP_0}}$$

Achieved a sensitivity of **1.0 x 10^{-14} cm^{-1} / $Hz^{1/2}$**, highest reported to date

This sensitivity was realized with a unique **intensity stabilized, sub-Hz linewidth** laser, with ***P_0* ~ mW**.

COMBUSTION RESEARCH FACILITY

Sensitive Detection: Crucial Intermediates Monitoring in Fuel Oxidation Chemistry

OH, RO_2, HO_2, QOOH, and CH_2O

ethane, propane, *n*-butane

ethanol, 1-butanol, diisopropyl ketone

Hydrocarbon Autoignition Chemistry is fundamental to new clean efficient combustion strategies.

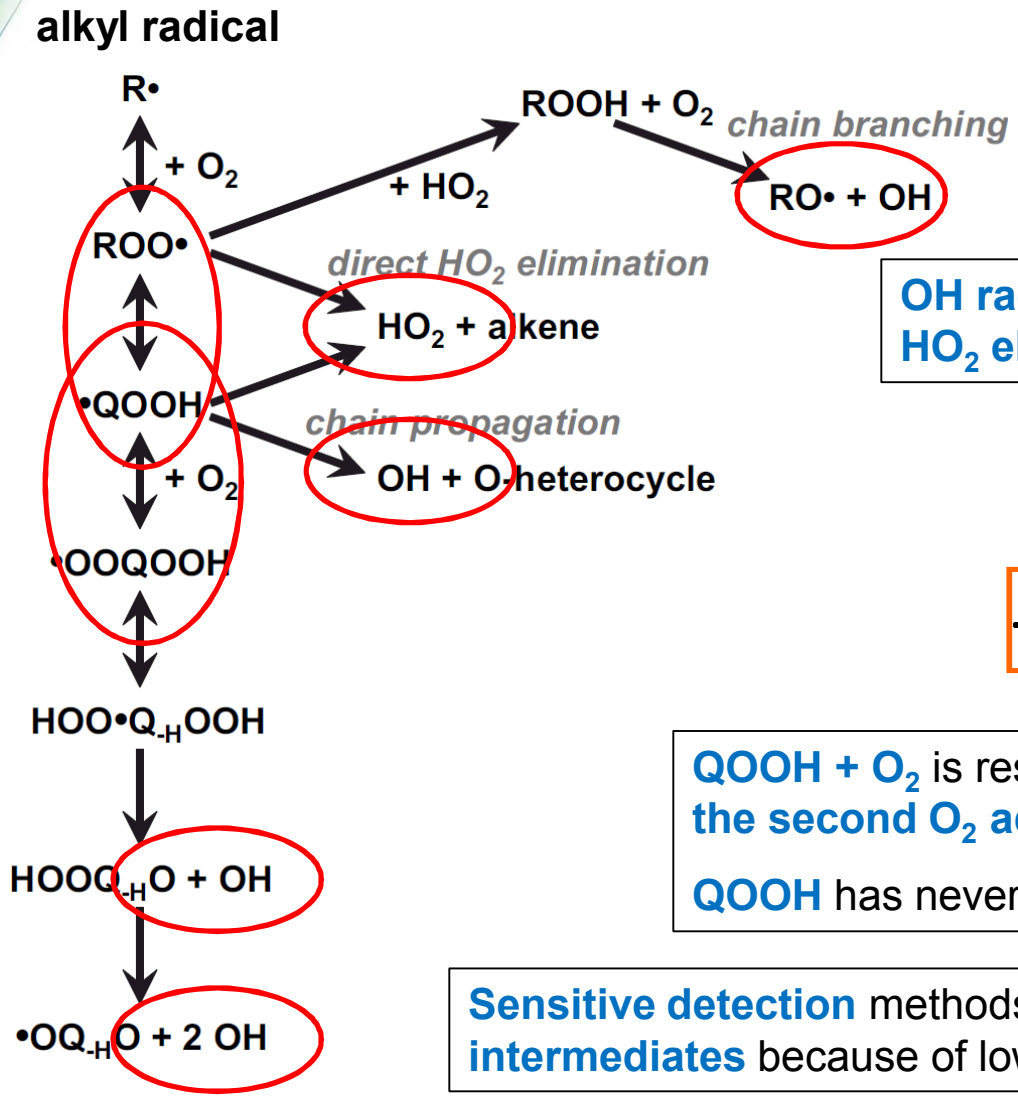

The **ignition phasing** in an **HCCI engine**, in principle, is determined by **LT autoignition chemistry**.

OH radical is the major chain propagator and **HO_2 elimination** is a chain-terminating step.

ROO
alkylperoxy

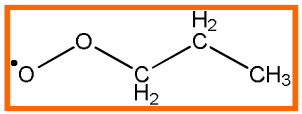

QOOH
hydroperoxyalkyl

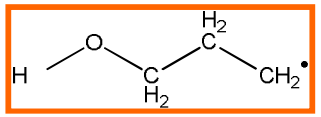

$QOOH + O_2$ is responsible for **chain branching** through **the second O_2 addition**.

QOOH has never been detected **directly** by any means.

Sensitive detection methods are necessary in monitoring **reactive intermediates** because of low concentrations.

Zádor, J.; Taatjes, C. A.; Fernandes, R. X. *PECS* **2011**, *37*, 341.

Herriott Cell Laminar Flow Reactor in Laser Chemistry Lab at CRF Sandia

Laser-photolysis **Cl-initiated** oxidation of fuels in a multi-pass reactor

355nm Cl_2

266nm $(COCl)_2$

Absorption length **10 ~ 20 m**

Time resolution **~1μs**

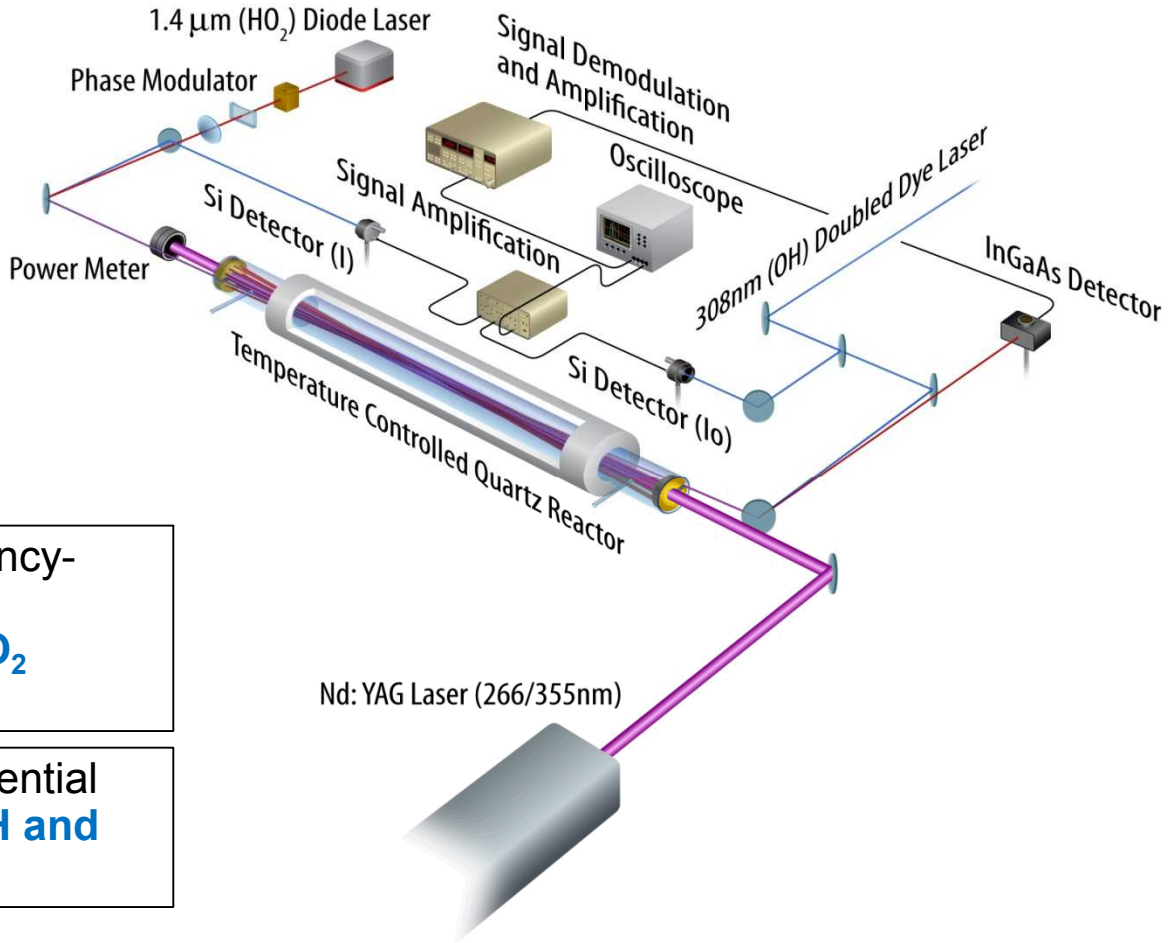

Infrared (**1509nm**) frequency-modulation or differential absorption detection of **HO_2 radicals**

Ultraviolet (**308nm**) differential absorption detection of **OH and ROO radicals**

E. P. Clifford et al. *JPCA* **104** (2000) 11549

Absorption Features near 308nm

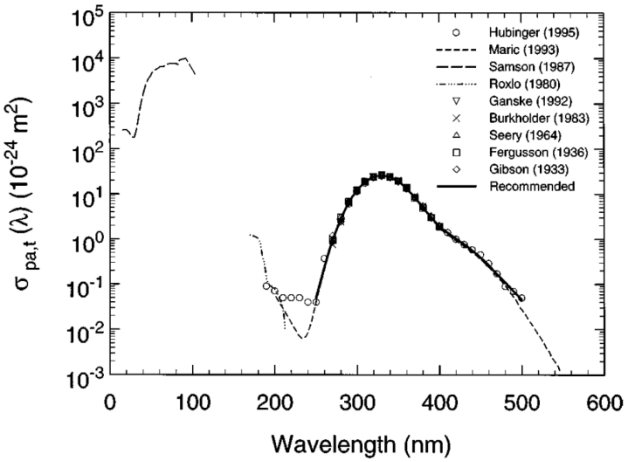

Cl_2: **1.7 × 10^{-19} cm^{-2}** at 355nm

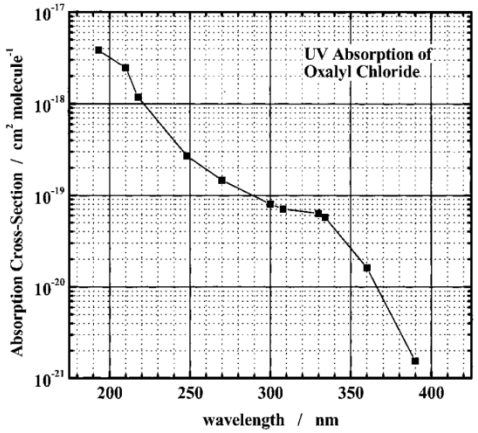

$(COCl)_2$: **1.6 × 10^{-19} cm^{-2}** at 266nm

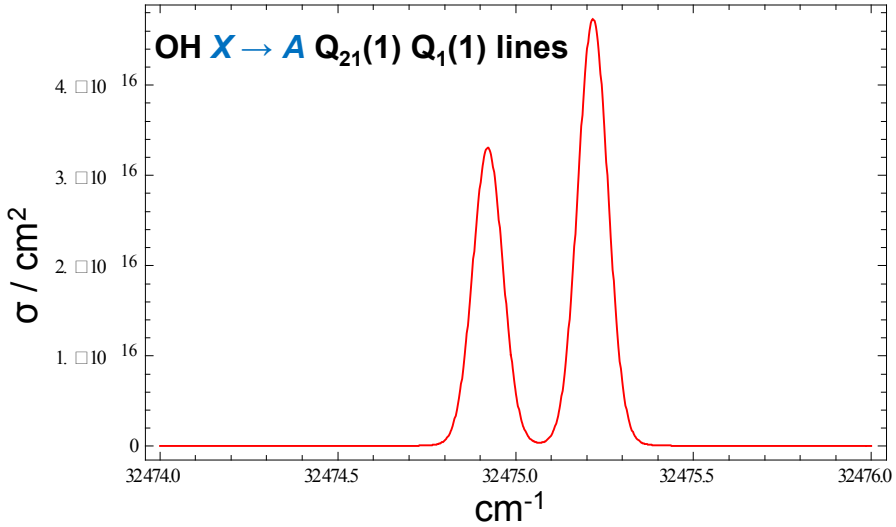

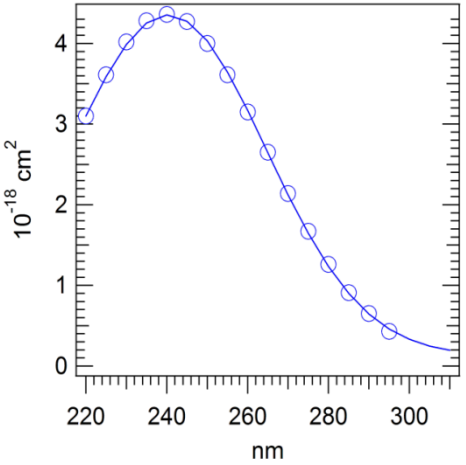

$C_2H_5O_2$: **2 × 10^{-19} cm^{-2}** at 308nm

JPCRD **28** (1999) 131; JPCA **105** (2001) 97; *J Geophys Res* **106** (2001) 12157; *J Geophys Res* **100** (1995) 7397; HITRAN Database 2000

We can detect both OH and ROO.

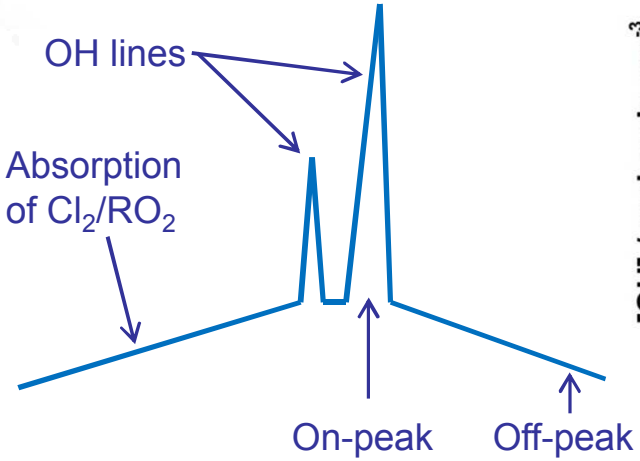

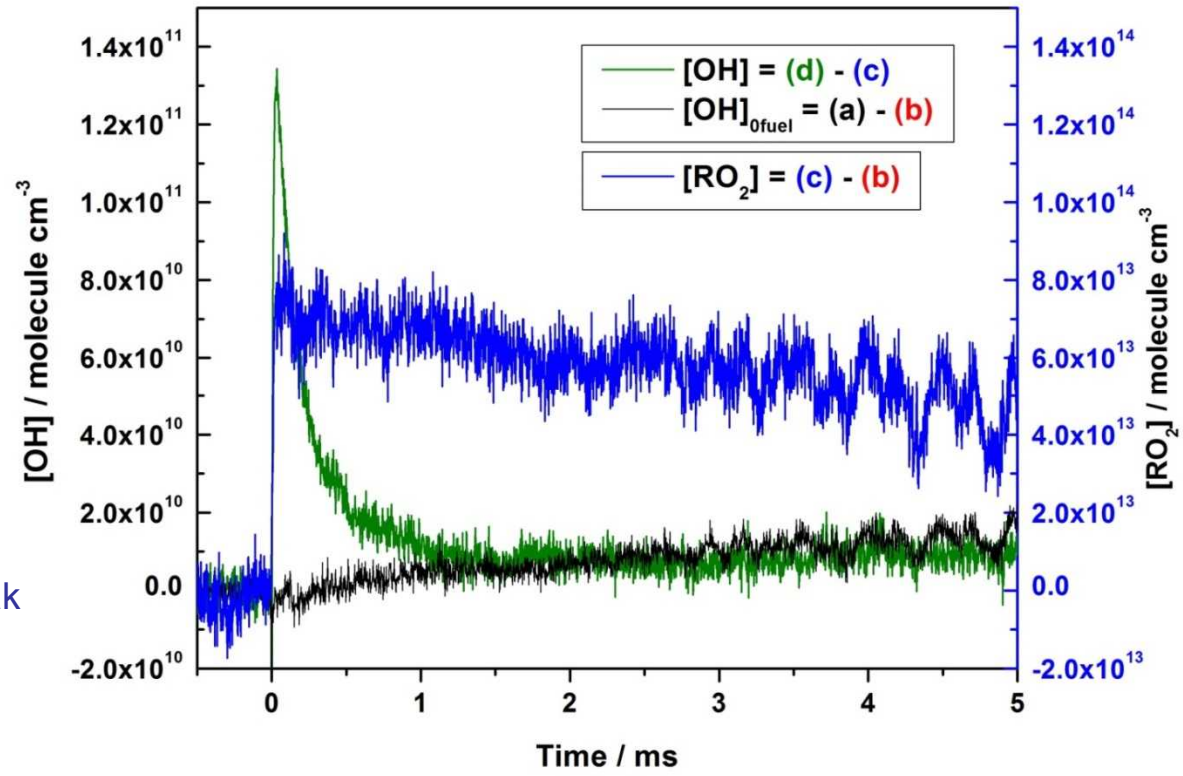

(a) no fuel, on-peak (b) no fuel, off-peak

(c) w. fuel, off-peak (d) w. fuel, on-peak

Thermal lensing noise is greatly removed by this subtraction.

[total] ~10^{17} cm^{-3}, $[Cl]_0$ ~10^{13} cm^{-3}, [OH] detection limit ~10^{10} cm^{-3}

OH and RO_2 in ethyl + O_2 system 660-740 K, 30 Torr, w. Cl_2

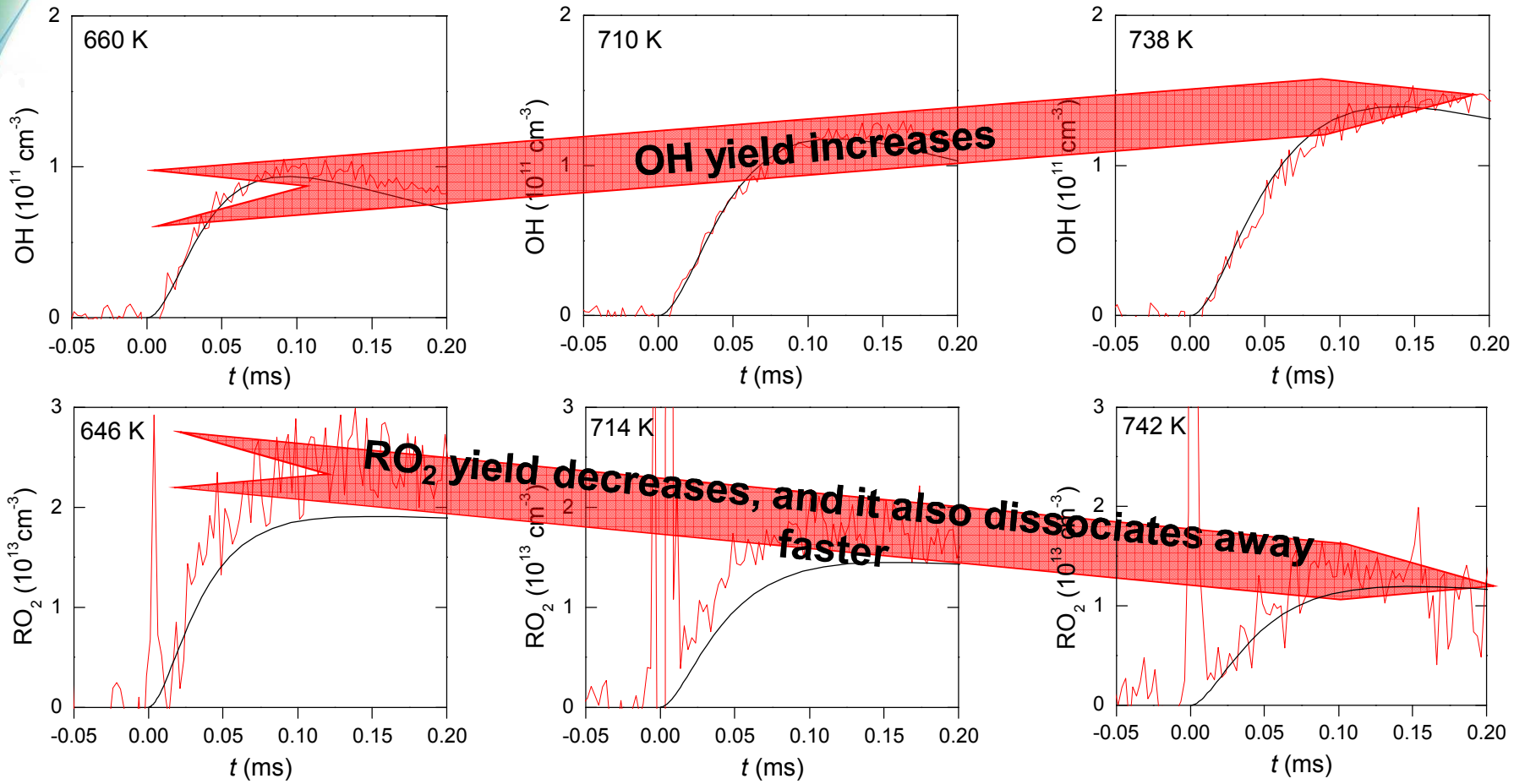

Measured and calculated OH absolute concentrations agree very well in a time window of 200 μs.

Data unpublished

RO_2 detection clarifies effects of 2^{ndary} chemistry.

Constraining RO_2 to its measured values and adding $RO_2 + HO_2 \rightarrow OH$ eliminates almost all discrepancies on the whole 5 ms timescale.

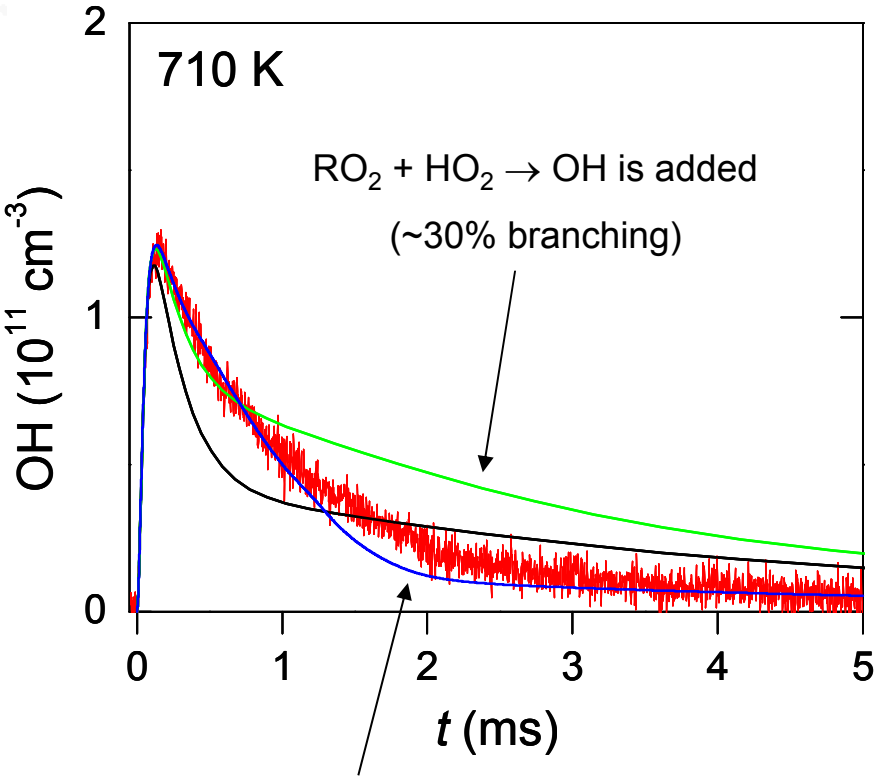

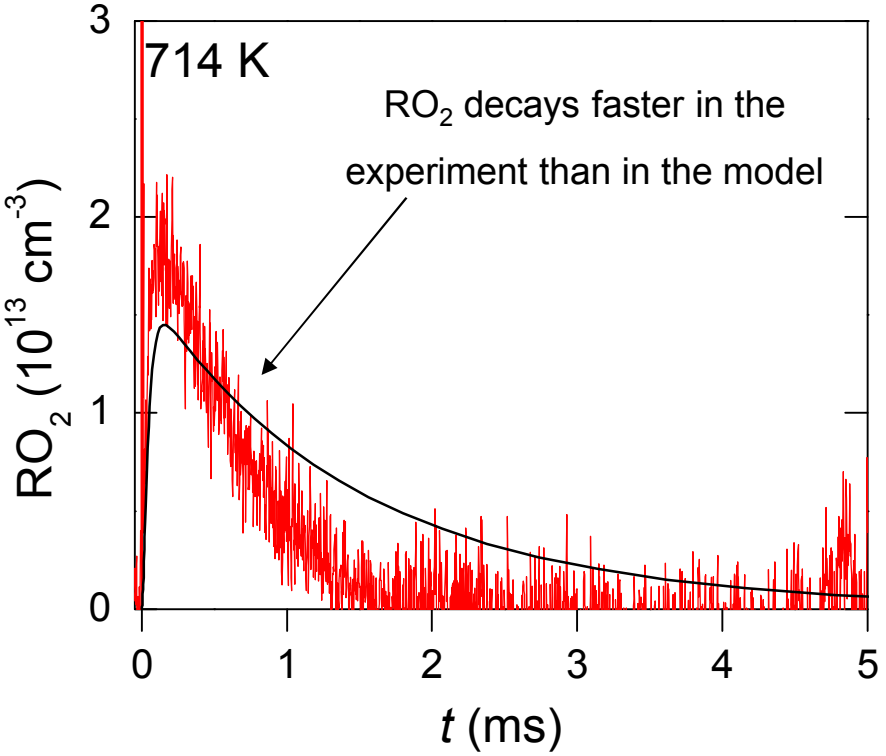

Data unpublished

Results for the propyl + O_2 system 426-697 K, 10 Torr, w. $(COCl)_2$

~730K OH yield from ethyl + O_2

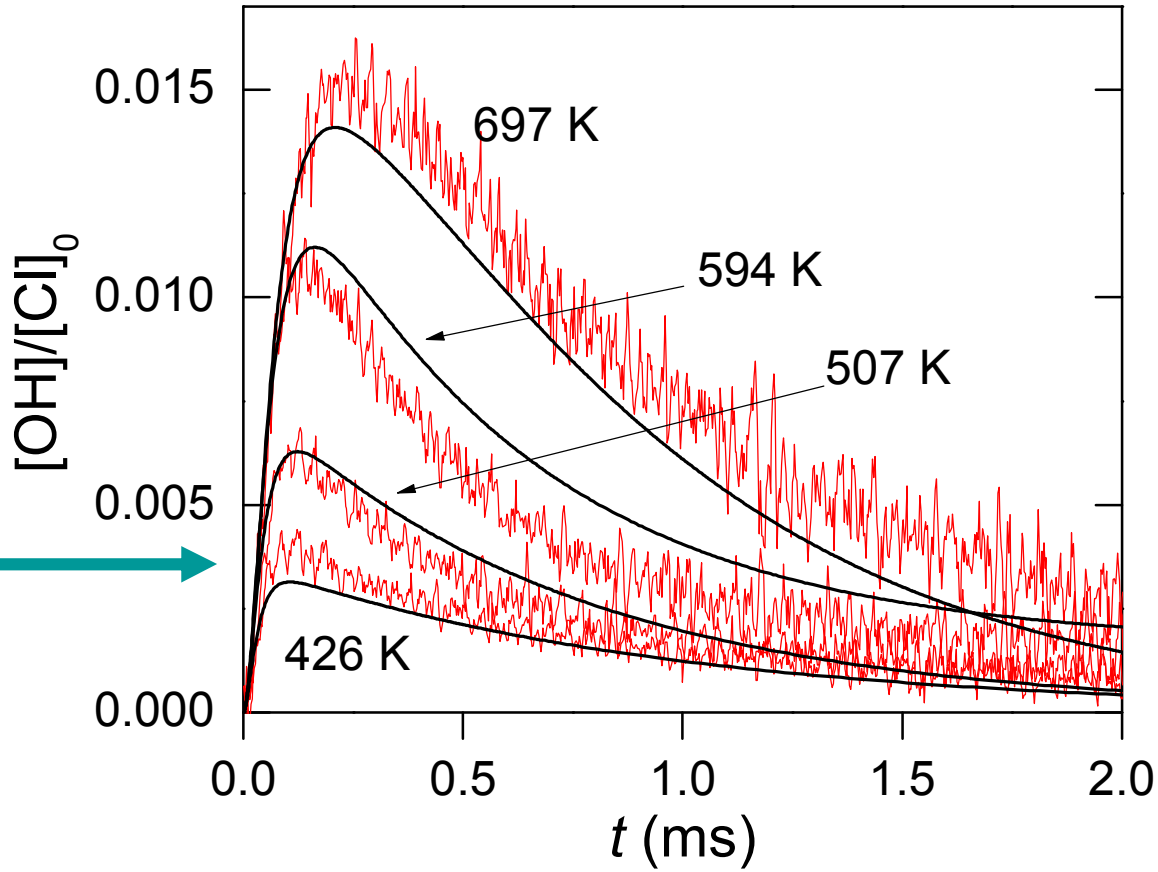

The propyl radical produces more OH, therefore, secondary chemistry is less important, even at longer times.

At 10 Torr, less RO_2 is stabilized.

Huang, H.; Merthe, D.; Zádor, J.; Jusinski, L. E.; Taatjes, C. A. *Proc. Combust. Inst.* **2010**, *33*, 293.

Related barrier heights on the ethyl + O_2 and propyl + O_2 potential energy surfaces

- Previous HO_2 measurements (DeSain et al.)
- Current OH measurements

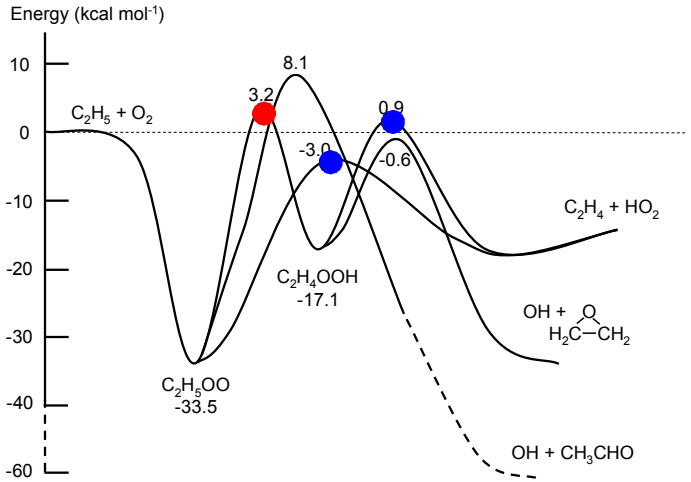

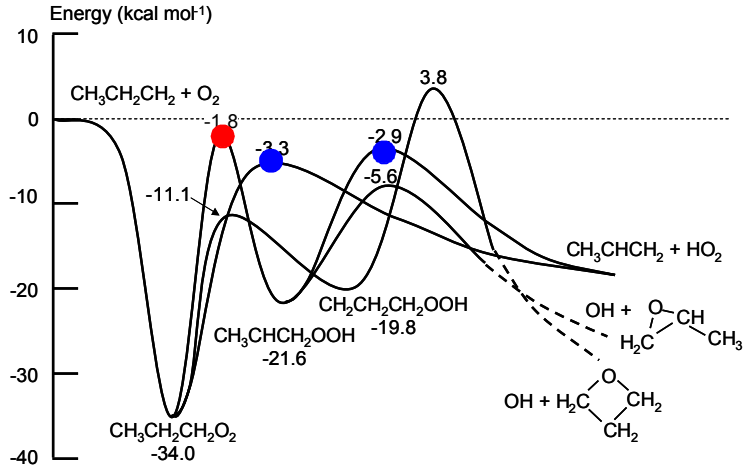

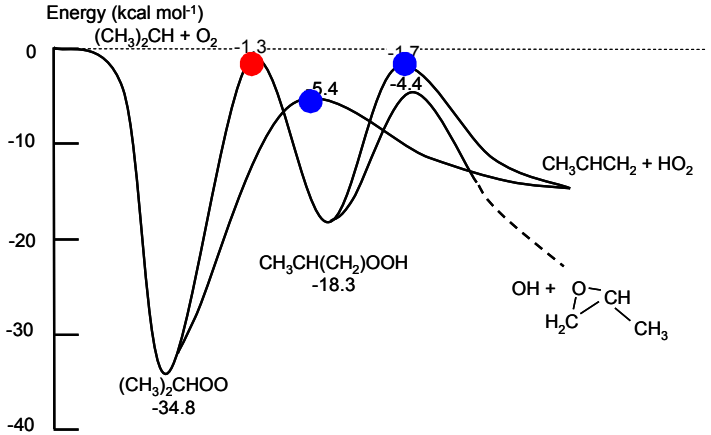

J. D. DeSain, S. J. Klippenstein, J. A. Miller, and C. A. Taatjes, *JPCA* **2003**, *107*, 4415-4427

Possible issues of OH detection at 308nm

Measure **OH** with a cw **IR** laser

CW 308nm probe laser dissociates **Cl_2 / $(COCl)_2$** continuously, generating a background of reactions along the probe path before the **355nm / 266nm** photolysis pulse arrival.

308nm probe laser dissociates **RO_2** and **OOQOOH** radicals.

Some precursors, e.g. *tert*-butyl hydroperoxide **(TBHP)**, absorb at **uv** region.

OH fundamental transition lines

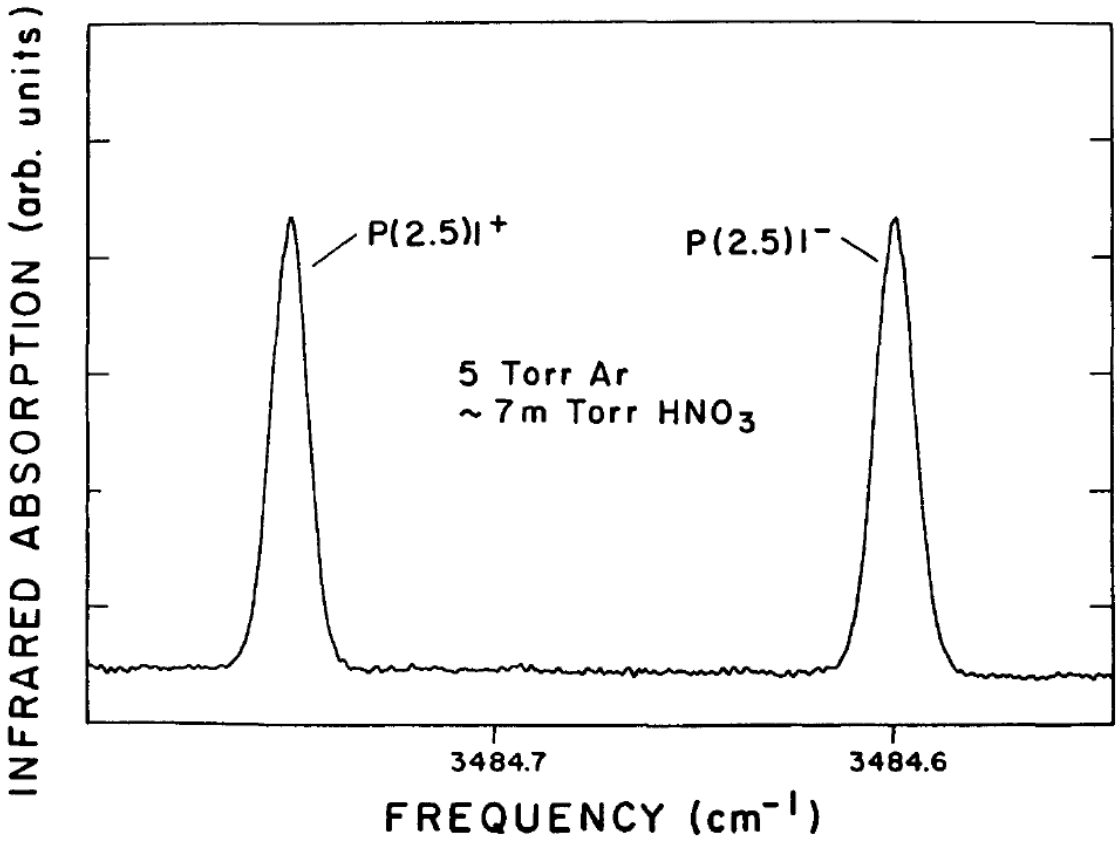

Cross section σ ~10^{-18} cm^2, [OH] detection limit ~10^{11} cm^{-3}

Broad weak absorption features exist but can be subtracted.

D. D. Nelson, Jr., A. Schiffman, and D. J. Nesbitt, *JCP* **90** (1989) 5455; HITRAN Database 2000

Making enough QOOH radicals!

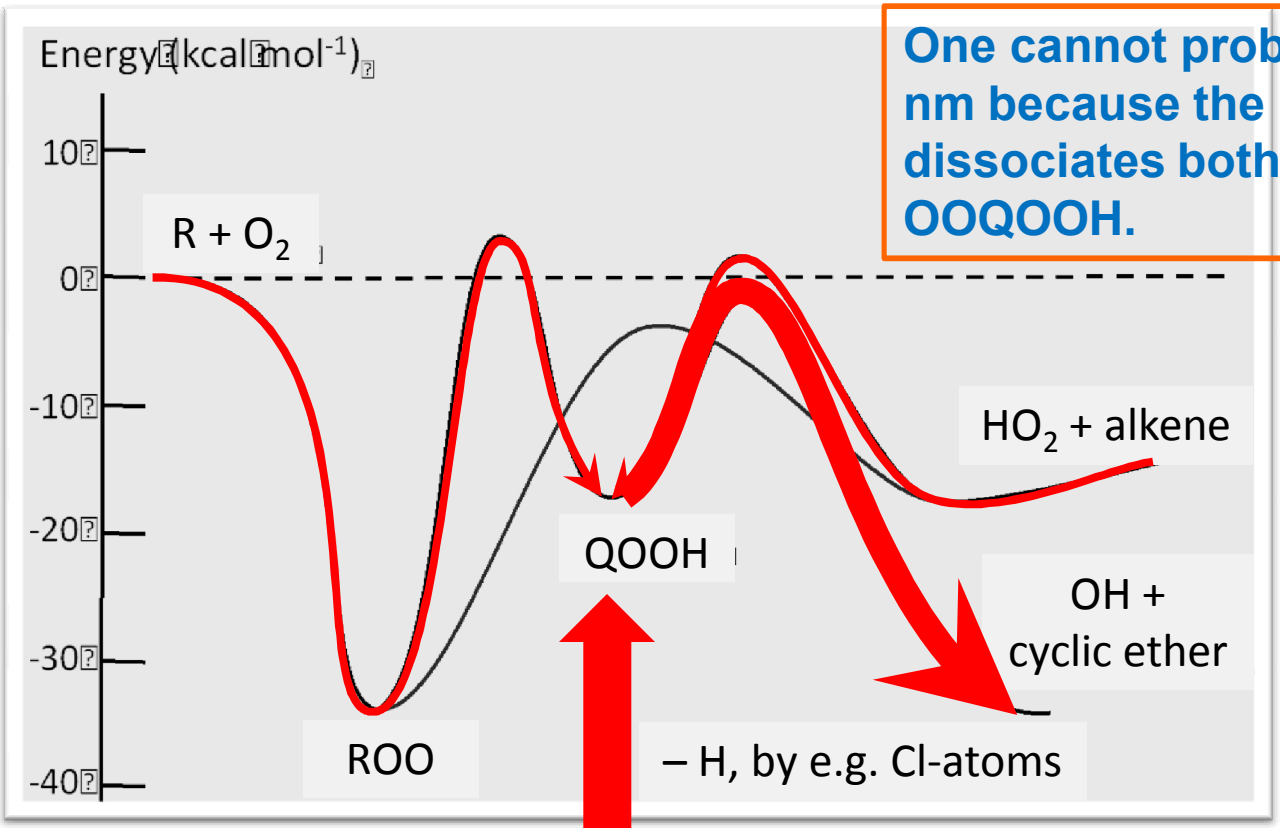

One cannot probe OH at 308 nm because the probe laser dissociates both TBHP and OOQOOH.

Recipes to make QOOH radicals:

1. from R + O_2 or from ROO
2. from HO_2 + alkene
3. ?

ROOH

tert-butyl hydroperoxide

TBHP generates only one type QOOH.

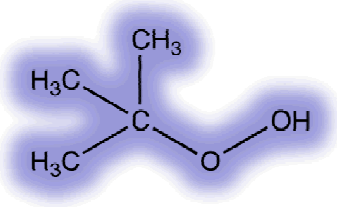

Zador, Huang, Welz, Zetterberg, Osborn and Taatjes, *PCCP,* 2013, **15**, 10753--10760

With OxCl and at 300K the chemical mechanism has been greatly simplified.

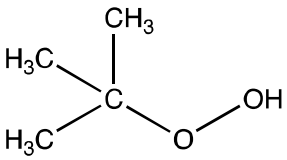

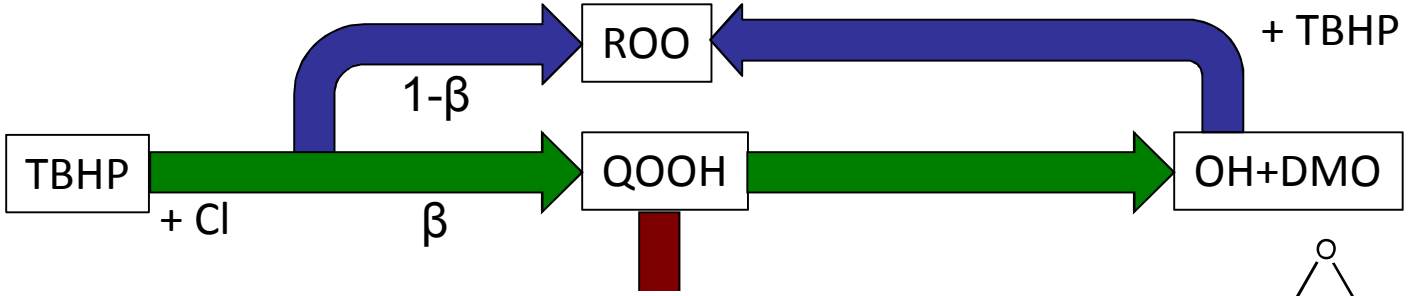

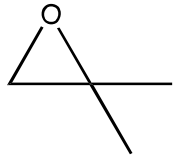

$(CH_3)_3COOH$ (*tert*-butyl hydroperoxide): OH reaction rate coefficients between 206 and 375 K and the OH photolysis quantum yield at 248 nm†

Munkhbayar Baasandorj,[ab] Dimitrios K. Papanastasiou,[ab] Ranajit K. Talukdar,[ab] Alam S. Hasson[c] and James B. Burkholder*[a]

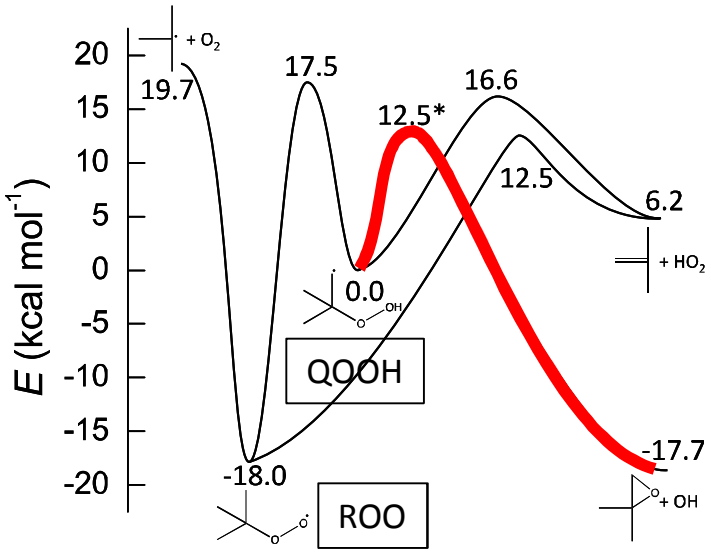

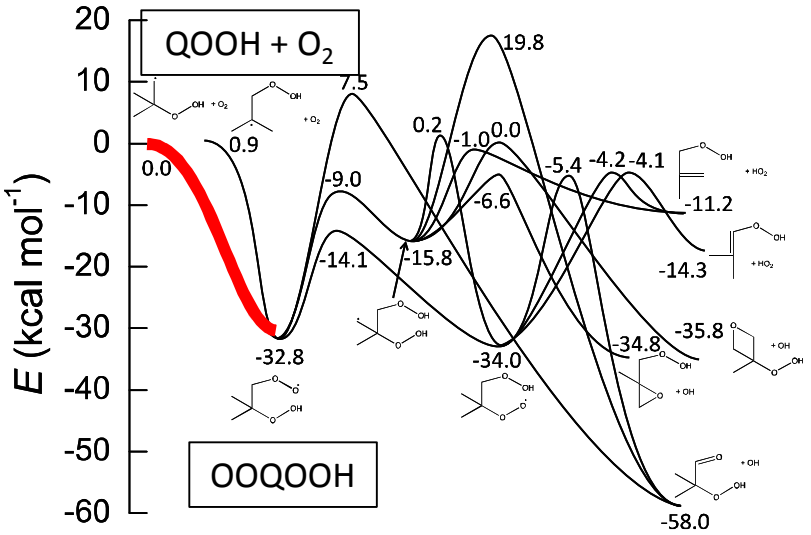

Zador, Huang, Welz, Zetterberg, Osborn and Taatjes, *PCCP,* 2013, **15**, 10753--10760

Direct determination of QOOH decomposition and QOOH + O_2 rate coefficients

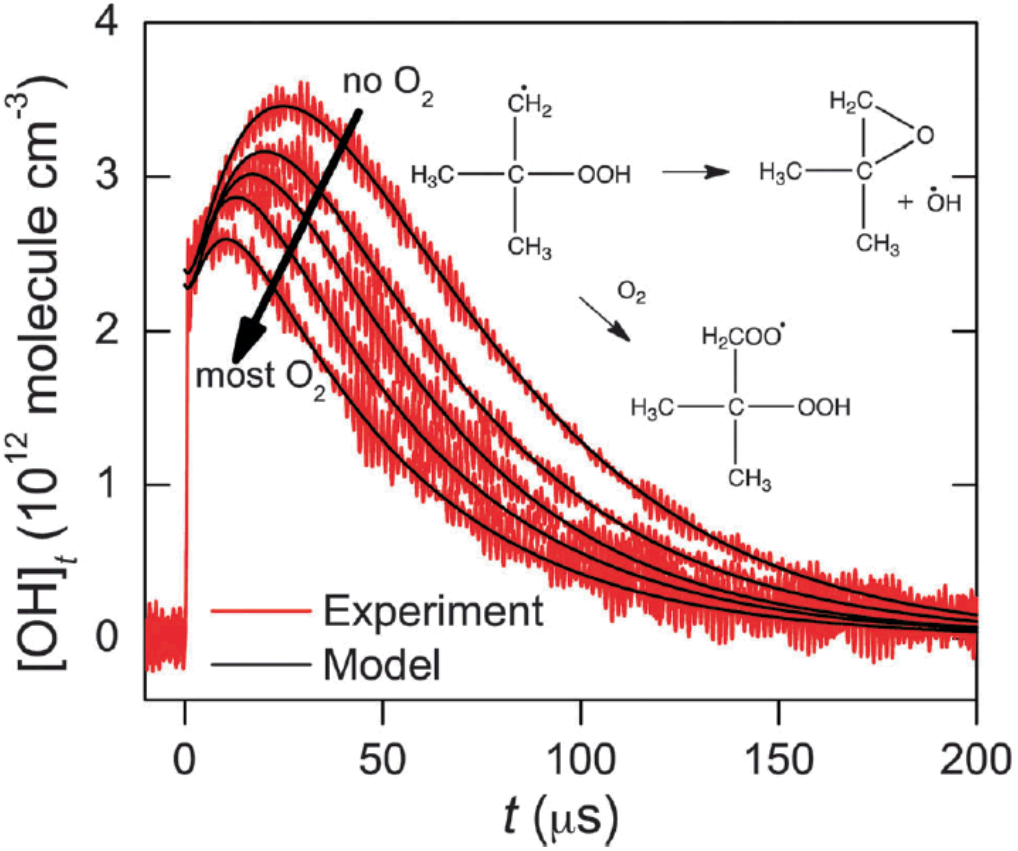

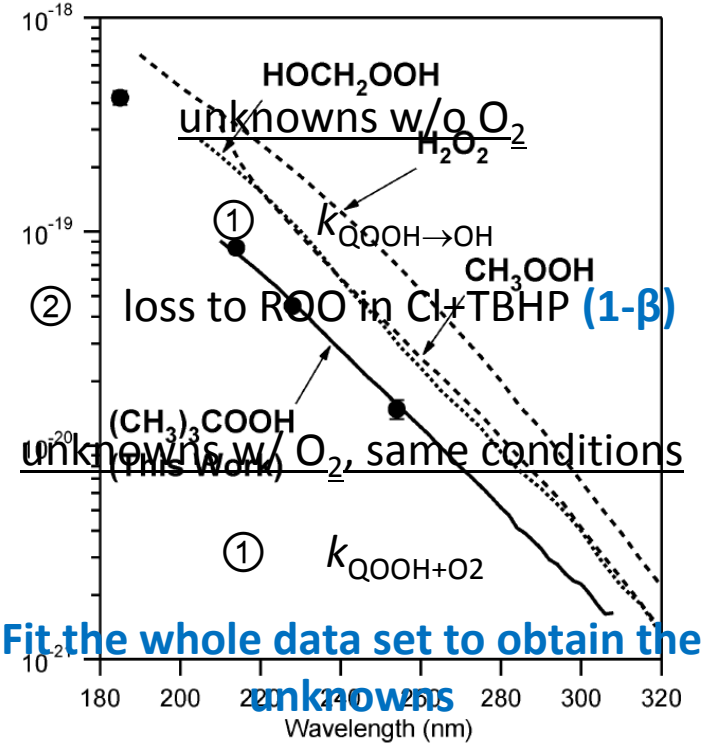

Fit the whole data set to obtain the unknowns

Baasandorj *et al.*, *PCCP*, 2010, **12**, 12101–12111

Competition between **QOOH dissociation** and **addition of O_2**

Similar results using **Cl_2** except initial **OH** concentration and chain chlorination

Zador, Huang, Welz, Zetterberg, Osborn and Taatjes, *PCCP,* 2013, **15**, 10753--10760

Yield of DMO (m/z=72) vs. O_2 gives $k_{QOOH+O2}$ at 4 Torr.

$$\frac{[DMO]_\infty^0 - [DMO]_\infty}{[DMO]_\infty} = \frac{k_{QOOH+O2}}{k_{QOOH\rightarrow OH} + L_{QOOH}}[O_2]$$

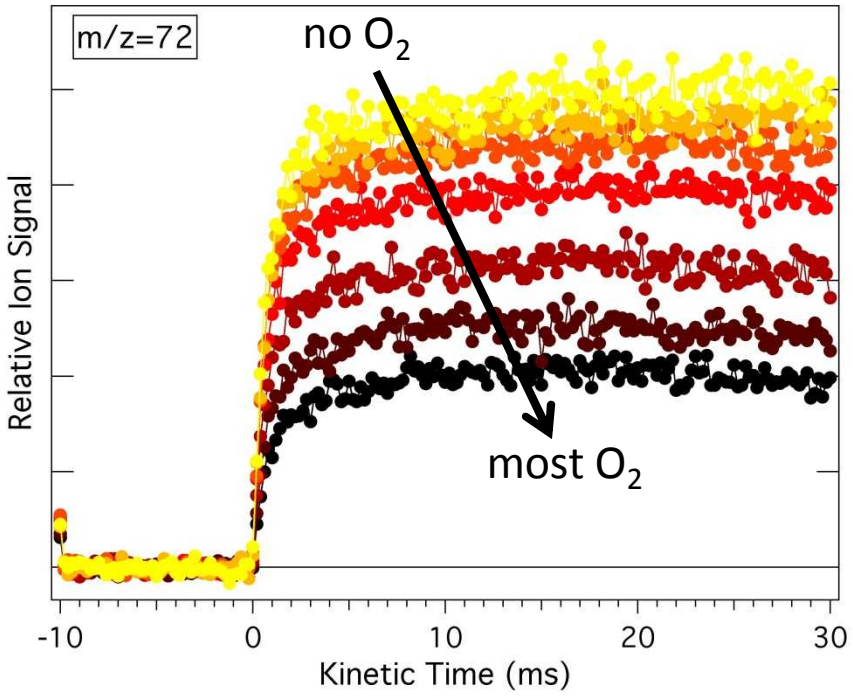

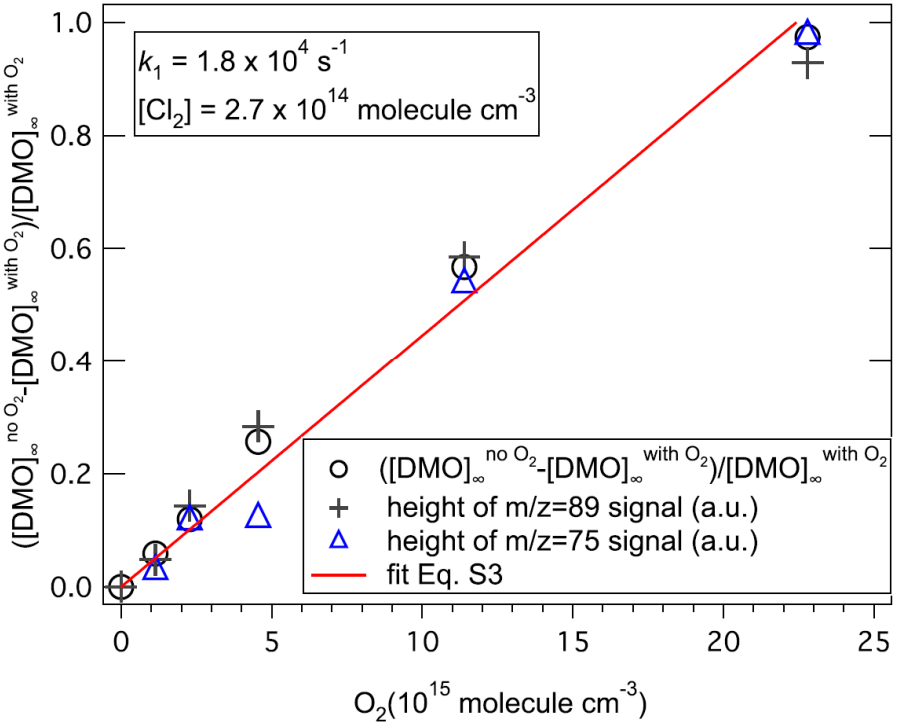

DMO: dimethyloxirane

Zador, Huang, Welz, Zetterberg, Osborn and Taatjes, *PCCP,* 2013, **15**, 10753--10760

OH measurement determines both decomposition and 2nd O_2 addition rate coefficients of QOOH.

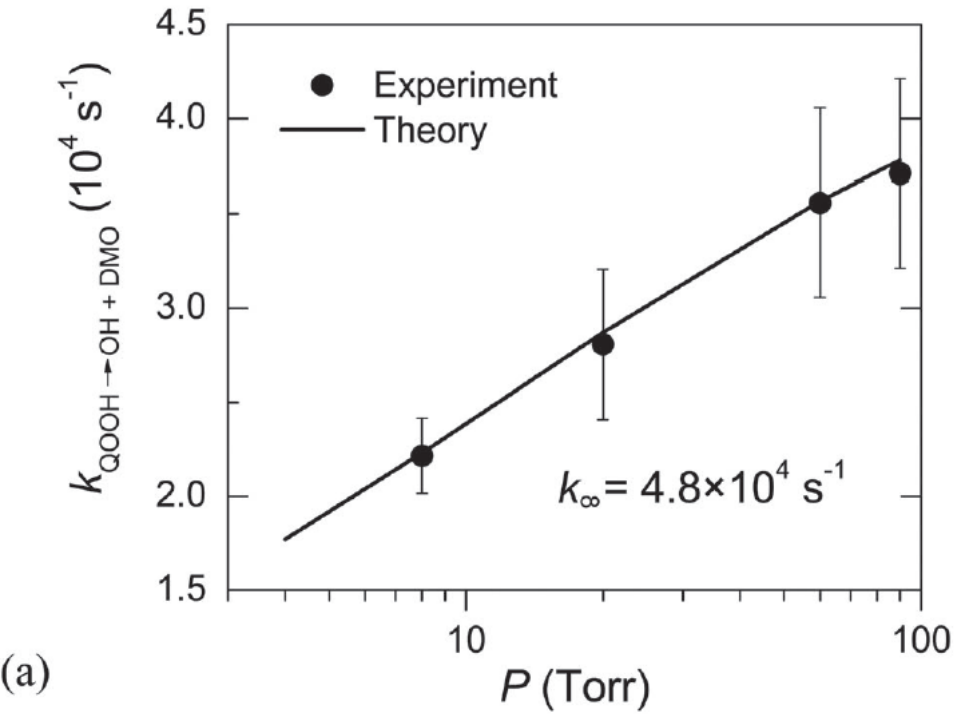

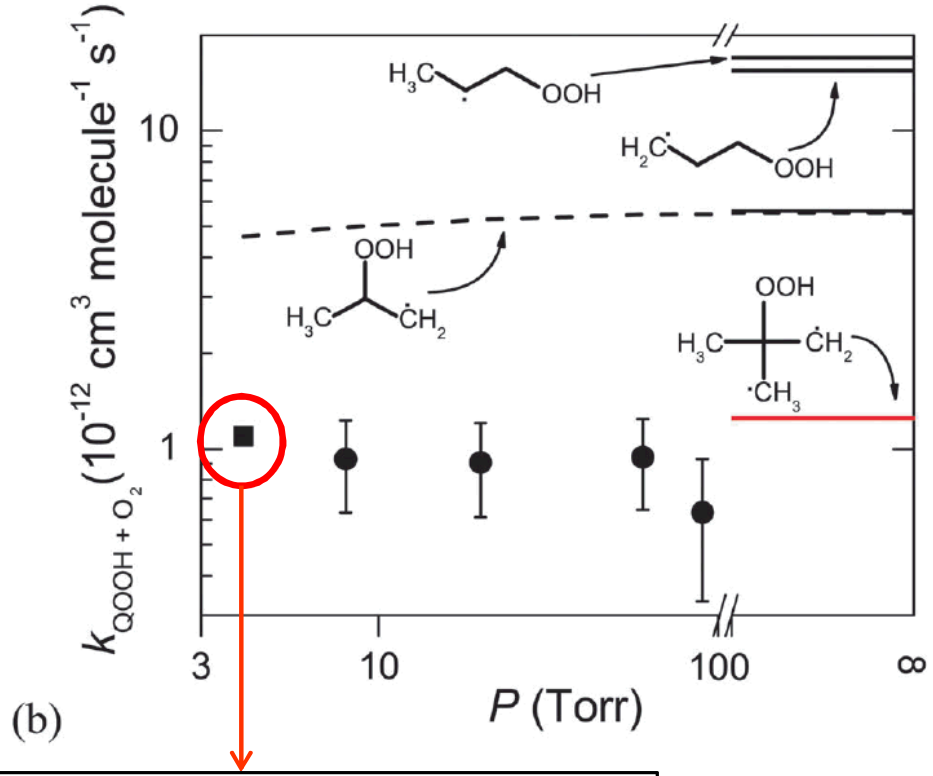

Multiplexed Photo-Ionization Mass Spectrometry **(MPIMS)** at ALS

Zador, Huang, Welz, Zetterberg, Osborn and Taatjes, *PCCP,* 2013, **15**, 10753; Goldsmith, Green and Klippenstein, JPCA, 2012, **116**, 3325

Conclusions #1

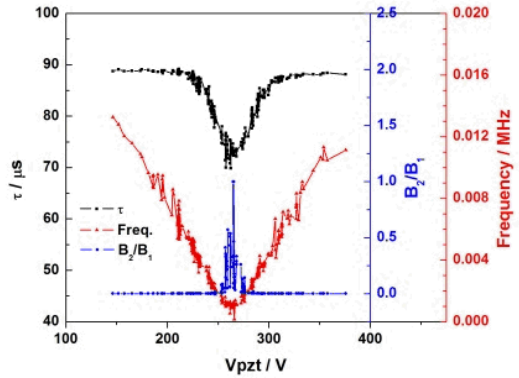

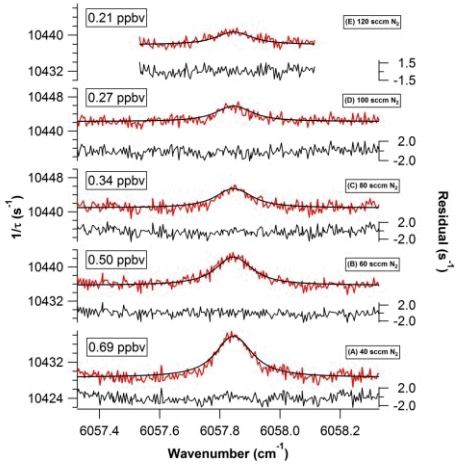

$$\alpha_{\min} = 2.31 \cdot \frac{1-R}{L} \sqrt{\frac{h\nu}{QP_0}}$$

High order transverse mode excitation can cause mode beating in ring-down signal, which deteriorates the sensitivity of CRDS severely.

We have reached a detection limit of CH_4 of 63 pptv in N_2 at 760 Torr. Our short term sensitivity is 7.9 x 10^{-12} cm^{-1} $Hz^{-1/2}$, 24 times worse than the optimum shot noise limit under similar conditions, 3.3 x 10^{-13} cm^{-1} $Hz^{-1/2}$.

Both CRDS method and NICE-OHMS are ultimately shot noise limited, with similar final sensitivities. But CRDS is a much simpler method.

Conclusions #2

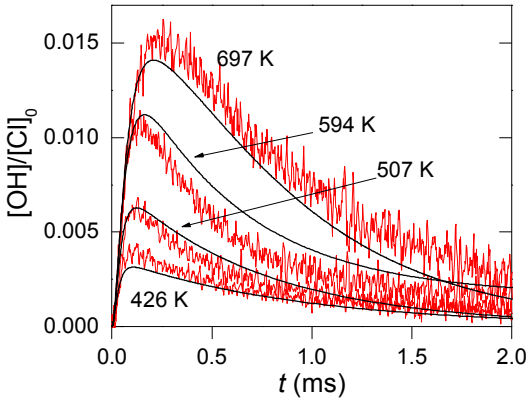

OH and ROO detection at 308nm has been applied to study the chemical kinetics of ethyl / propyl + O_2 systems. More sensitive measurements, e.g. in the IR region are needed to reduce probe interference.

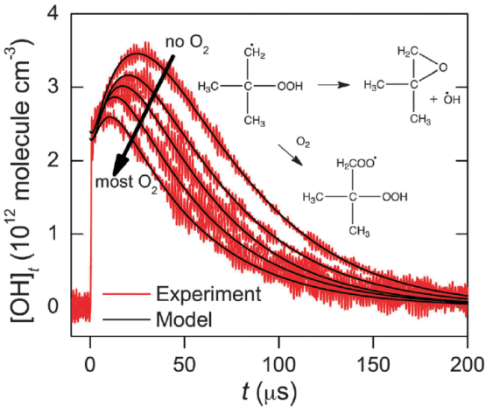

A new way to produce enough QOOH from alkyl hydroperoxide + Cl reation

Successfully measured the decomposition and 2nd O_2 addition rates of one QOOH, supported by high level quantum chemistry calculations.

Next: direct observation of chain branching at higher temperatures

Thank you!


CRF

For **Cl_2**, in **1 ms**, the background **[Cl]** by the probe laser is estimated to be less than **10%** of **[Cl]** by the photolysis pulse. For **$(COCl)_2$**, the same number is **5%**.

For ethylperoxy (**C_2H_5OO**), the dissociated **$[RO_2]$** by the 308nm probe laser in **1 ms** is less than **10%** of peak **$[RO_2] \sim [Cl]_0$**.

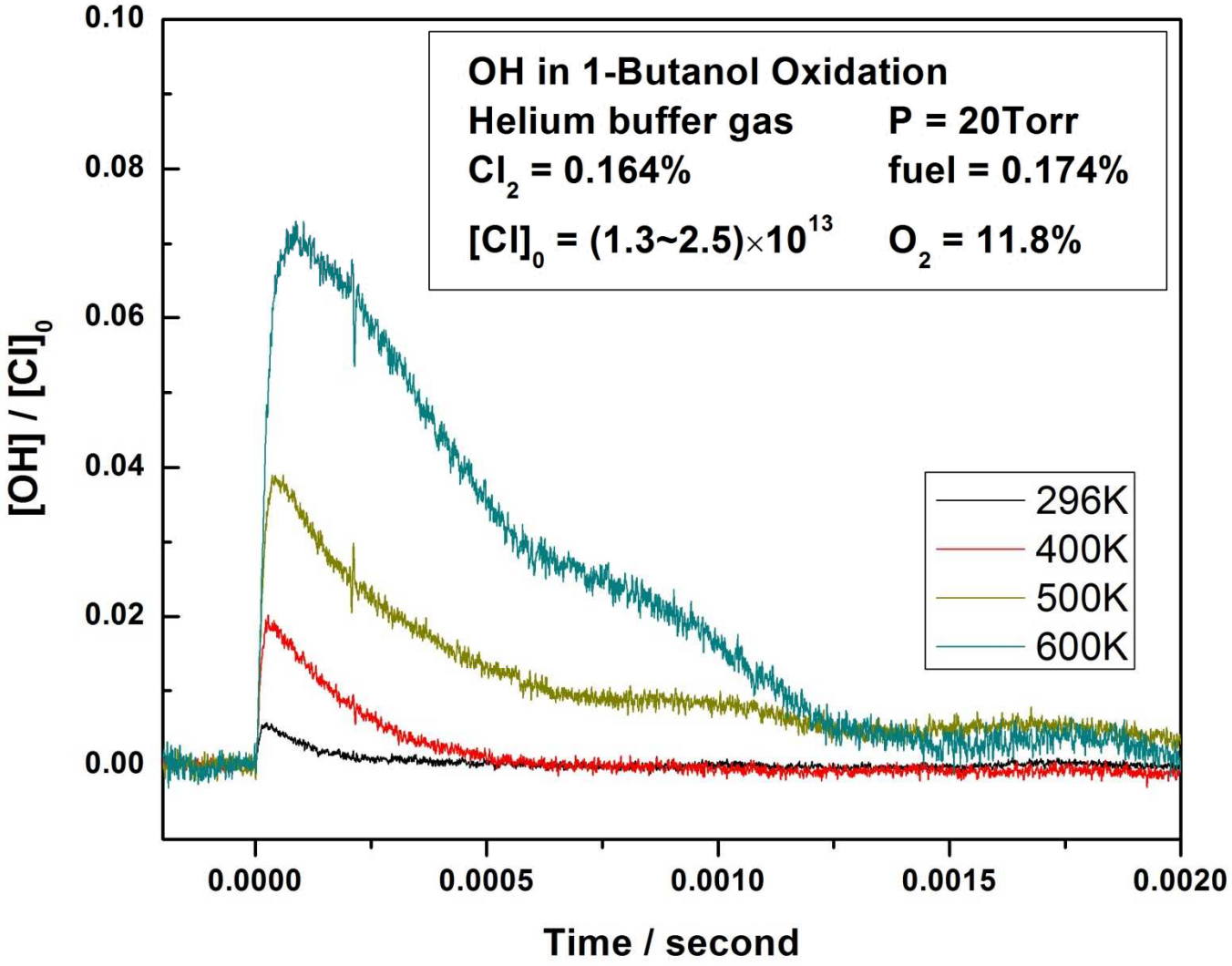
OH in 1-Butanol Oxidation
Helium buffer gas
P = 20Torr
Cl2 = 0.164%
fuel = 0.174%
[Cl]0 = (1.3~2.5)×10^13
O2 = 11.8%
296K
400K
500K
600K
[OH] / [Cl]0
Time / second
0.10
0.08
0.06
0.04
0.02
0.00
0.0000
0.0005
0.0010
0.0015
0.0020

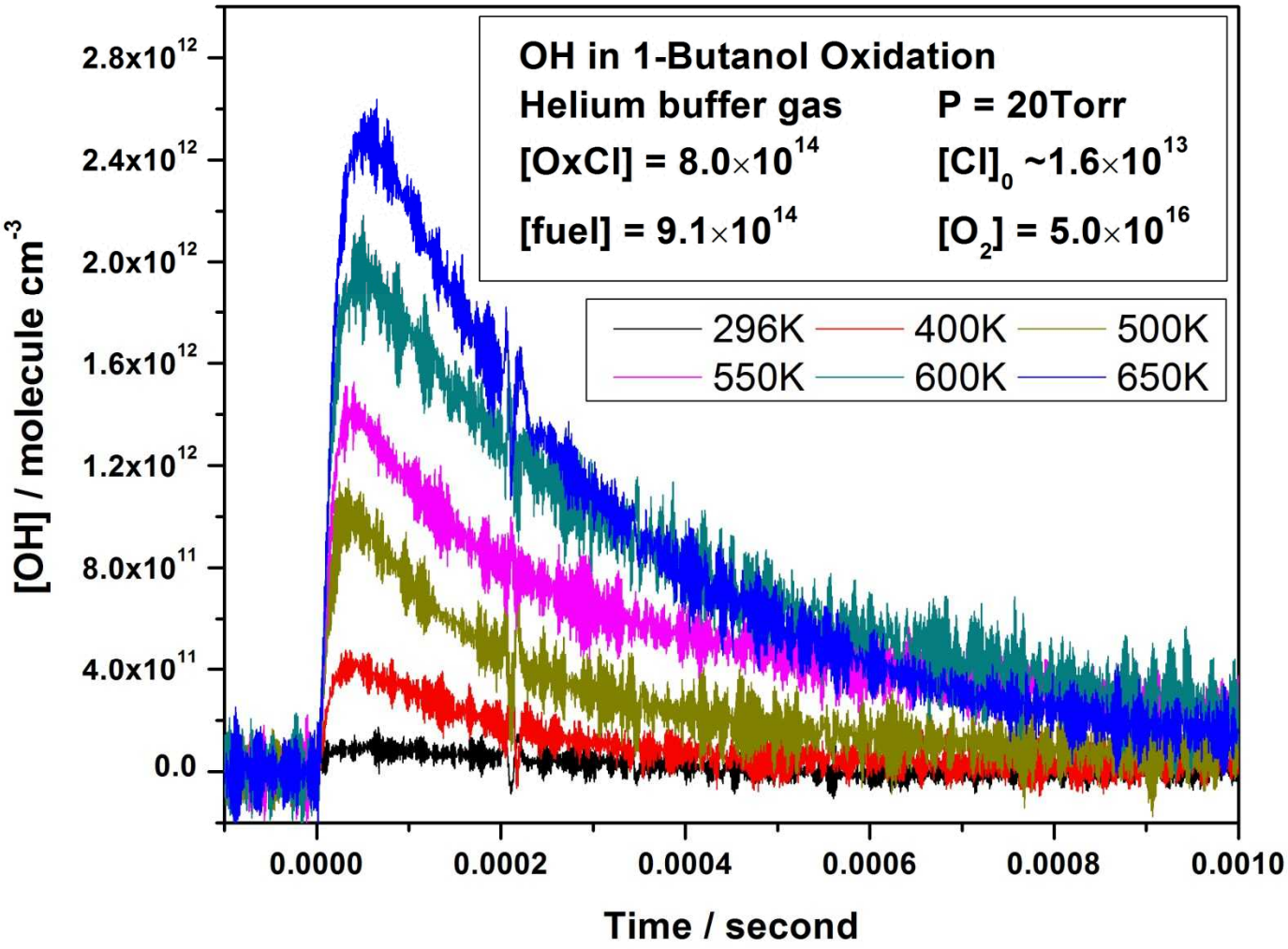
OH in 1-Butanol Oxidation
Helium buffer gas
P = 20Torr
[OxCl] = 8.0×10^14
[Cl]0 ~1.6×10^13
[fuel] = 9.1×10^14
[O2] = 5.0×10^16
296K
400K
500K
550K
600K
650K
[OH] / molecule cm^-3
2.8x10^12
2.4x10^12
2.0x10^12
1.6x10^12
1.2x10^12
8.0x10^11
4.0x10^11
0.0
0.0000
0.0002
0.0004
0.0006
0.0008
0.0010
Time / second

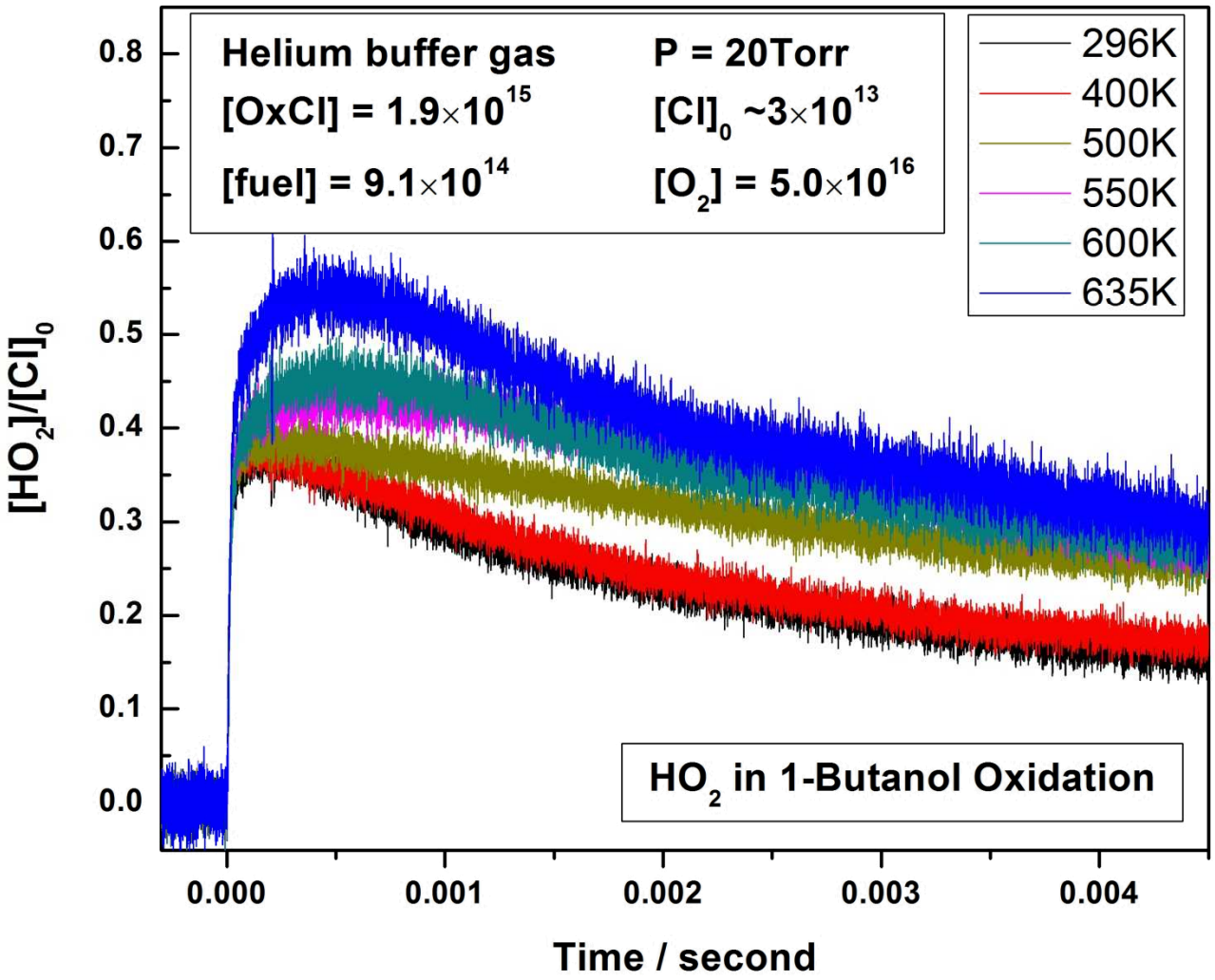
Helium buffer gas
P = 20Torr
[OxCl] = 1.9×10^15
[Cl]0 ~3×10^13
[fuel] = 9.1×10^14
[O2] = 5.0×10^16
296K
400K
500K
550K
600K
635K
HO2 in 1-Butanol Oxidation
[HO2]/[Cl]0
0.0
0.1
0.2
0.3
0.4
0.5
0.6
0.7
0.8
0.000
0.001
0.002
0.003
0.004
Time / second

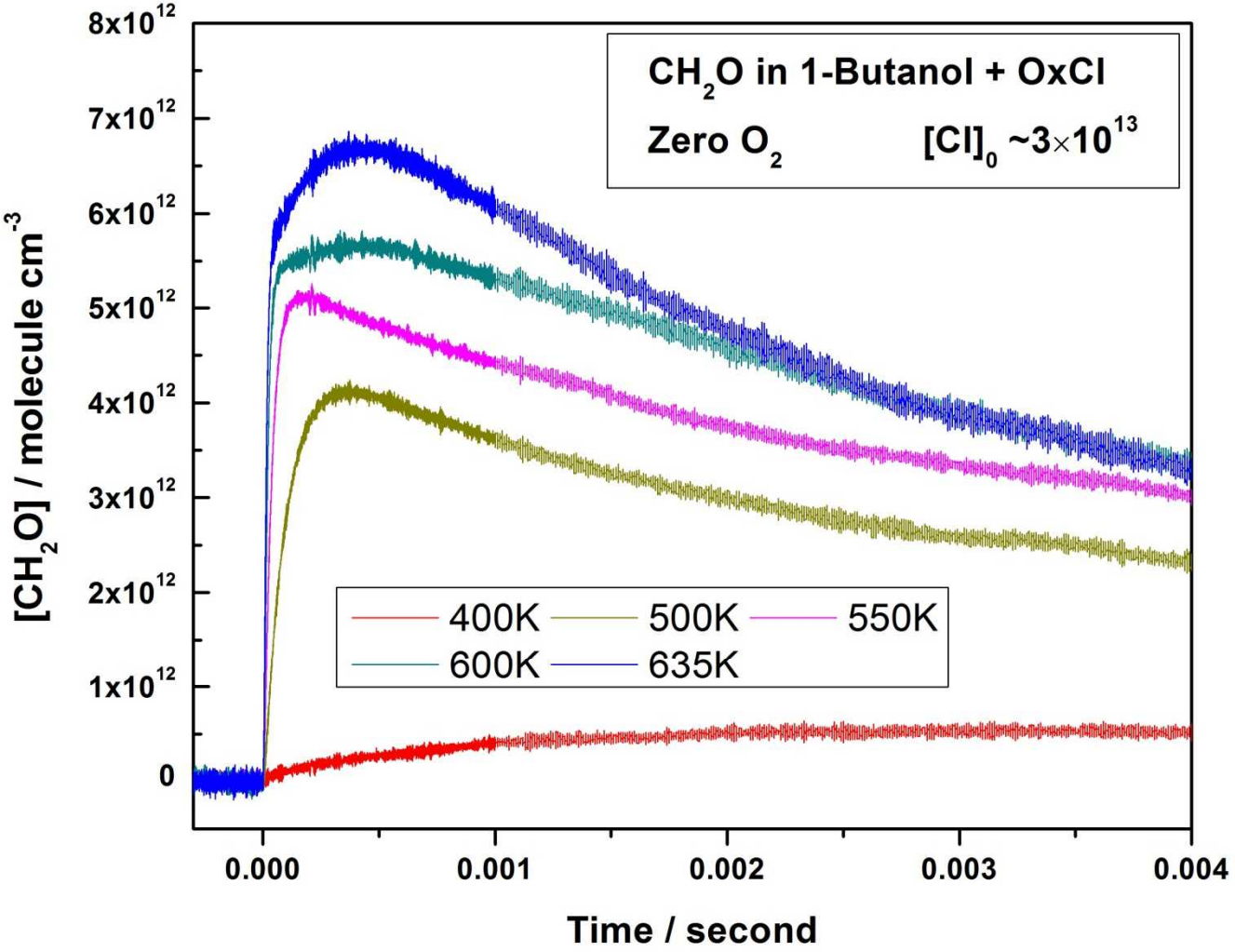
CH2O in 1-Butanol + OxCl
Zero O2
[Cl]0 ~3×10^13
400K
500K
550K
600K
635K
[CH2O] / molecule cm-3
8x10^12
7x10^12
6x10^12
5x10^12
4x10^12
3x10^12
2x10^12
1x10^12
0
0.000
0.001
0.002
0.003
0.004
Time / second

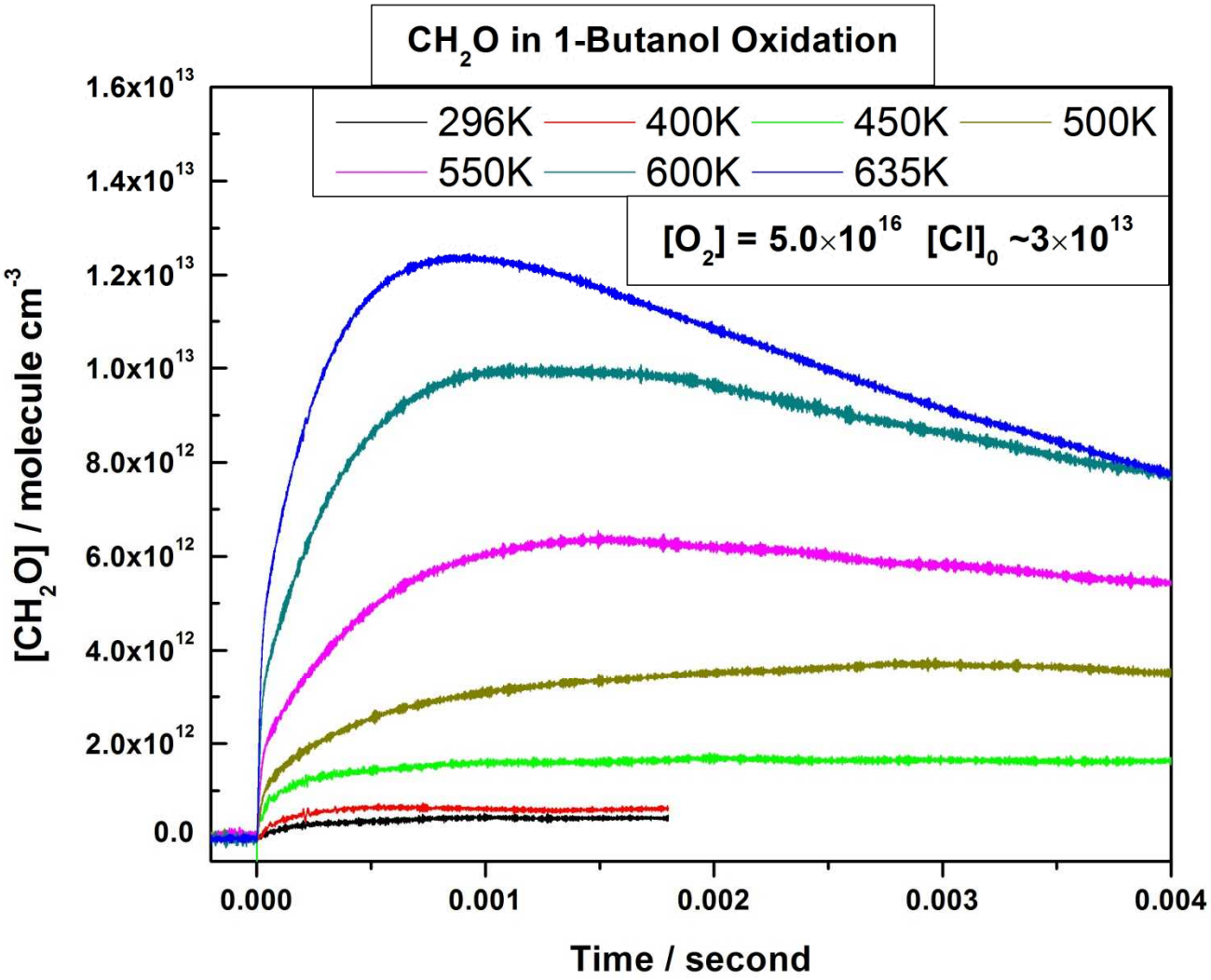
CH2O in 1-Butanol Oxidation
296K
400K
450K
500K
550K
600K
635K
[O2] = 5.0×10^16 [Cl]0 ~3×10^13
[CH2O] / molecule cm-3
1.6x10^13
1.4x10^13
1.2x10^13
1.0x10^13
8.0x10^12
6.0x10^12
4.0x10^12
2.0x10^12
0.0
0.000
0.001
0.002
0.003
0.004
Time / second

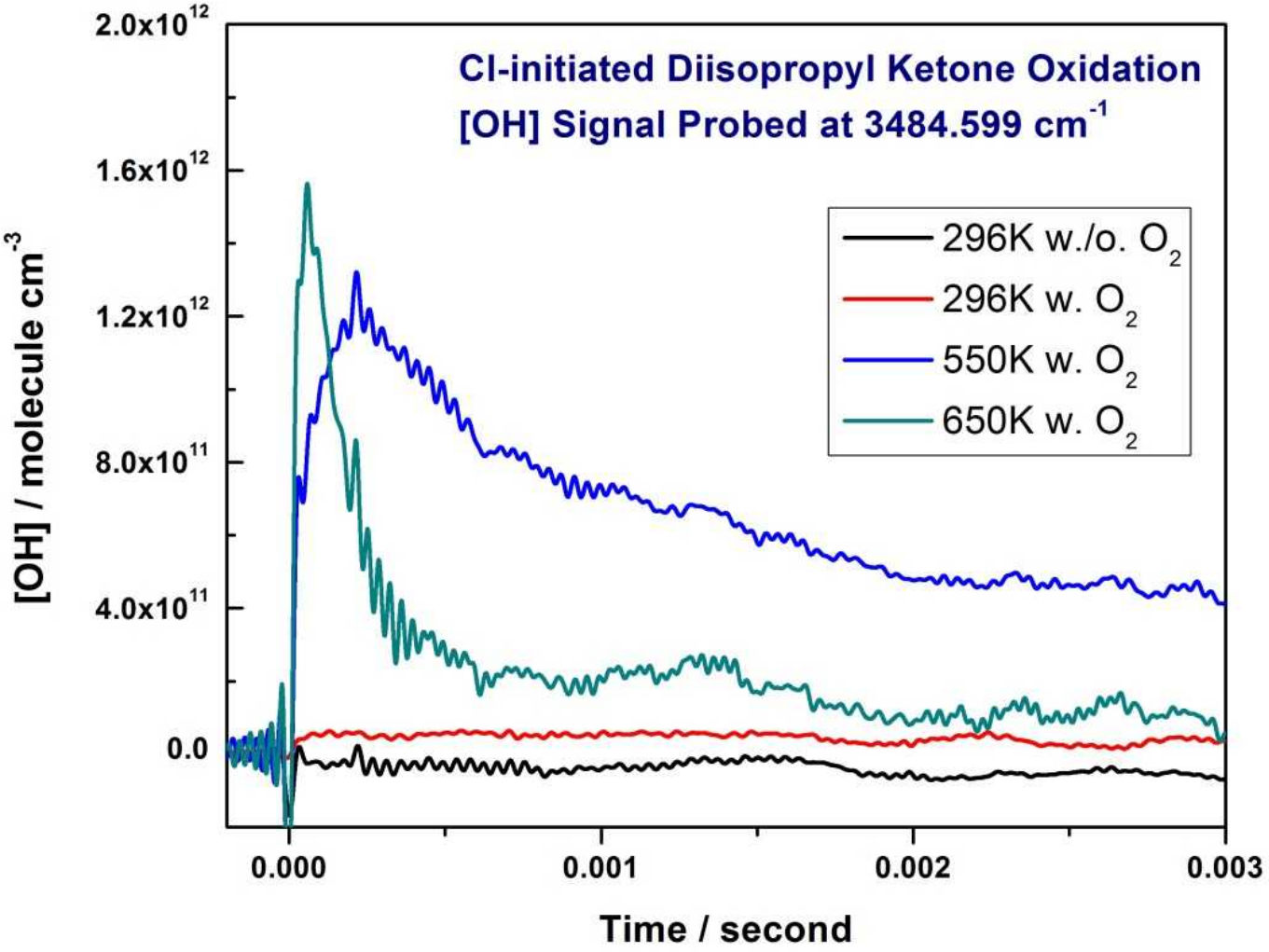
Cl-initiated Diisopropyl Ketone Oxidation
[OH] Signal Probed at 3484.599 cm-1
296K w./o. O2
296K w. O2
550K w. O2
650K w. O2
[OH] / molecule cm-3
2.0x10^12
1.6x10^12
1.2x10^12
8.0x10^11
4.0x10^11
0.0
0.000
0.001
0.002
0.003
Time / second

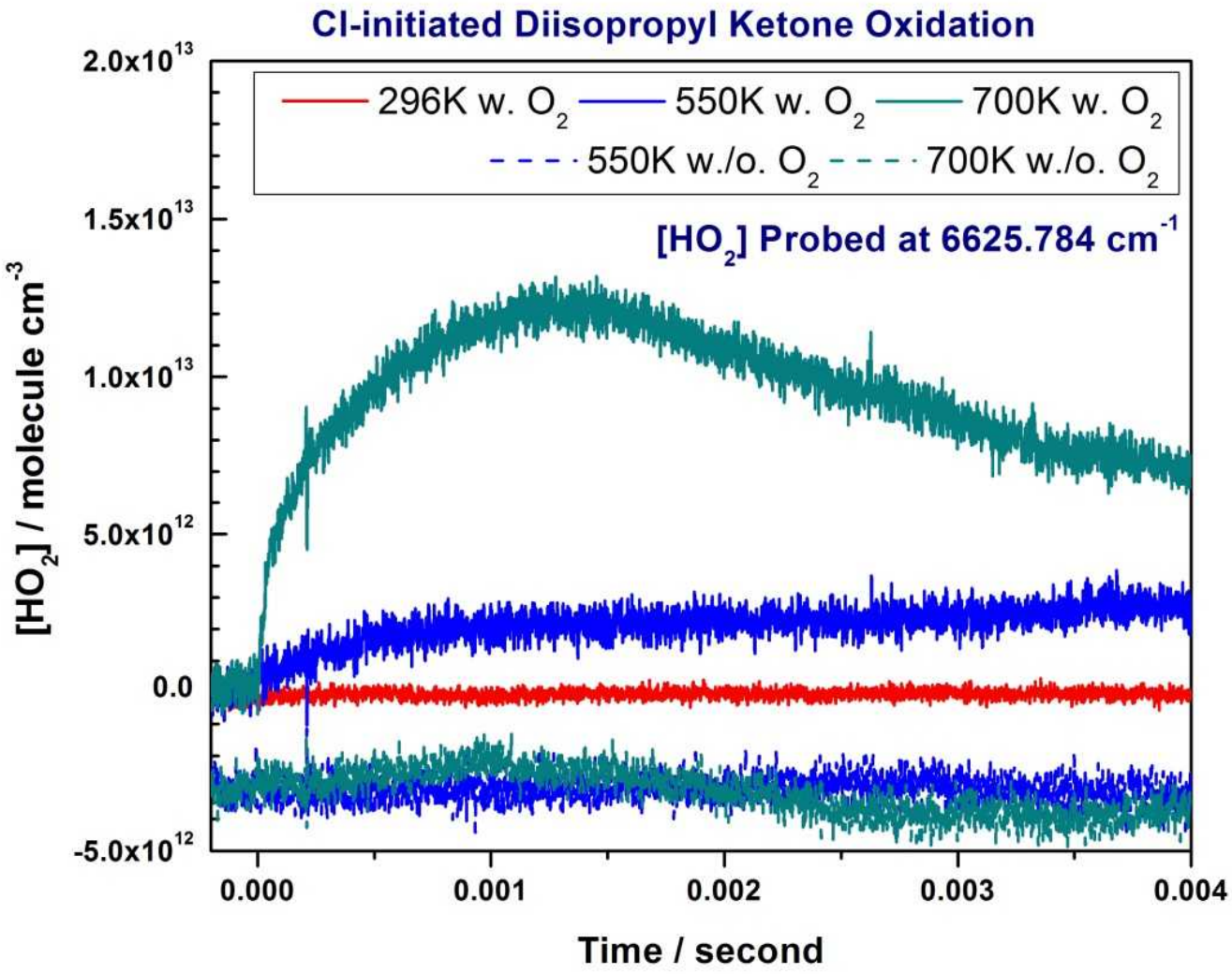
Cl-initiated Diisopropyl Ketone Oxidation
296K w. O2
550K w. O2
700K w. O2
550K w./o. O2
700K w./o. O2
[HO2] Probed at 6625.784 cm-1
[HO2] / molecule cm-3
2.0x10^13
1.5x10^13
1.0x10^13
5.0x10^12
0.0
-5.0x10^12
0.000
0.001
0.002
0.003
0.004
Time / second

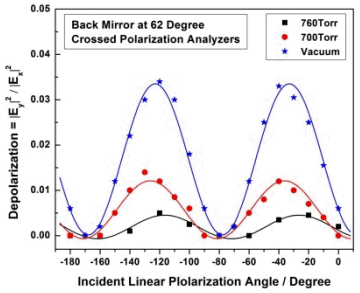

Supermirrors have both residual and strain induced linear birefringence, and polarization dependent loss (linear dichroism). Mismatched polarization analysis in detection can generate mode beating in ring-down signal, killing the sensitivity.

High order transverse mode excitation can be easily suppressed by a small size intracavity aperture.

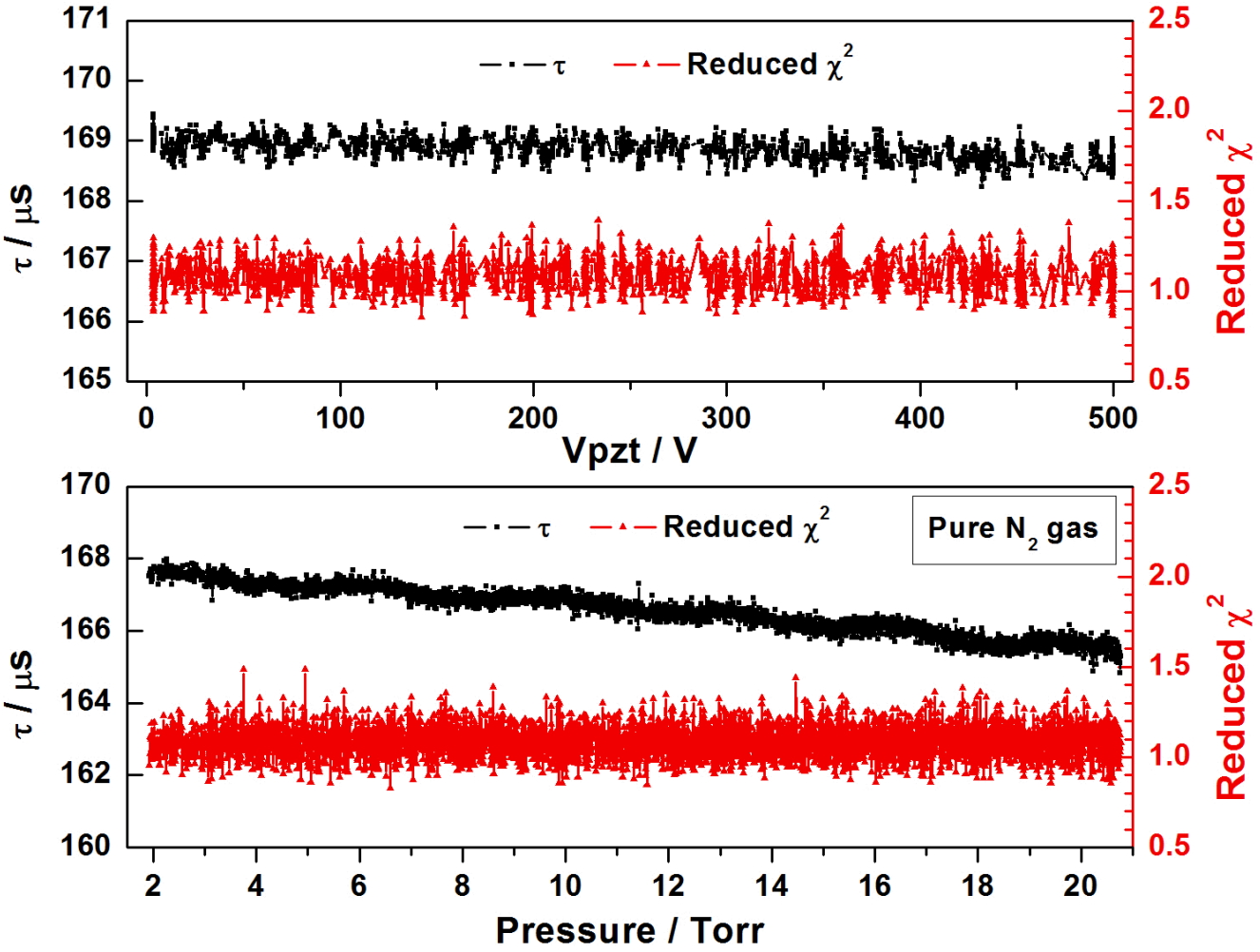

TEM_{00} mode size is **0.526mm** at the intracavity aperture of **4mm** diameter.

Linewidth of DFB Laser

Self homodyne measurement: delay time 11.4μs

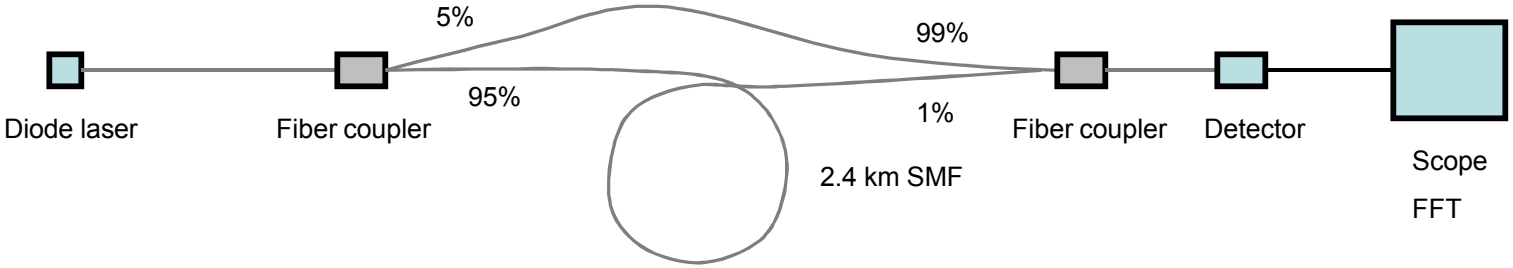

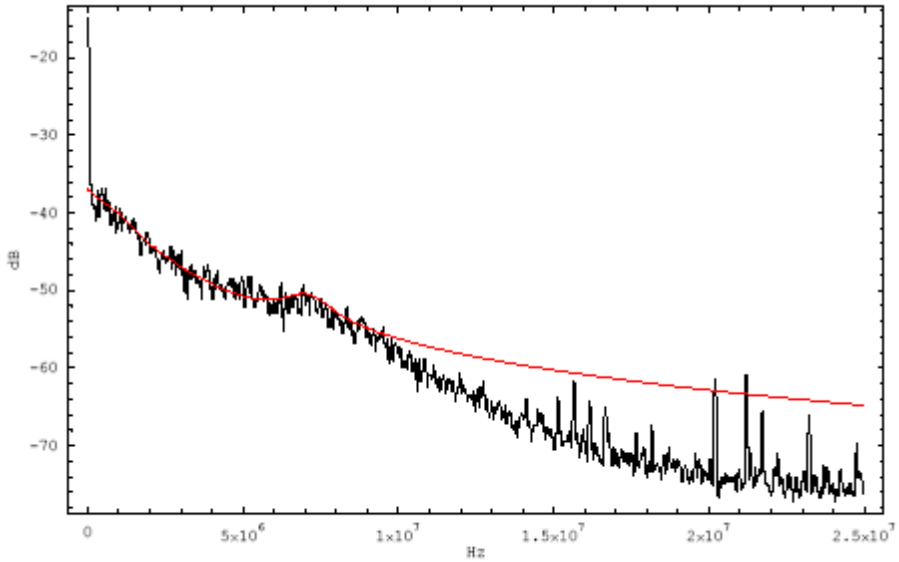

$$\Delta\nu_L \approx 1\,MHz$$

Mode Splitting of $TEM_{10/01}$

$$y(t) = A + B_1 \exp(-k_1 t) + B_2 \exp(-k_2 t) + B_3 \exp(-\frac{k_1 t}{2}) \exp(-\frac{k_2 t}{2}) \cos(2\pi \cdot \Delta\nu \cdot t + \Delta\varphi)$$

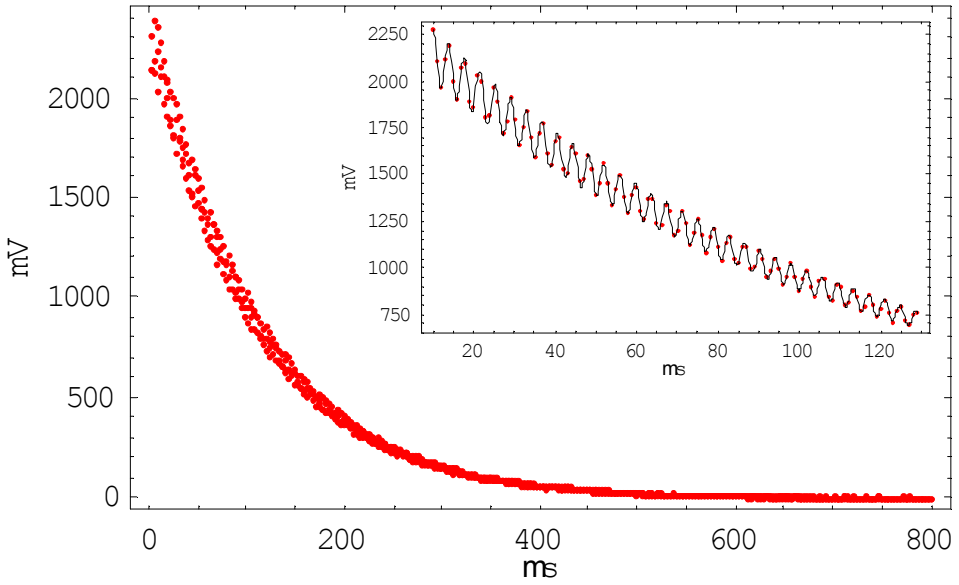

$A = -2.60\ mV$

$B_1 = 1518.66\ mV$

$B_2 = 830.02\ mV$

$B_3 = 152.22\ mV$

$\tau_1 = 1/k_1 = 104.72\ \mu s$

$\tau_2 = 1/k_2 = 119.05\ \mu s$

$\Delta\nu = 261.25\ kHz$

$\Delta\varphi = 2.46$

$\chi^2 = 1.017$

- The TEM_{10} and TEM_{01} modes are no longer orthogonal with each other ($B_3 > 0$). Possible reasons include spatial anisotropy of supermirrors or nonuniform quantum efficiency of the detector.
- A small difference of 0.26% between the radius of curvature of the mirror in x direction and that in y direction will generate this splitting.

Fabre C. *et al.*, ***Optics Letters*** **11** 365 (1986)

Effect of Ambient Pressure Change

- **A**: lab pressure change; **B**: τ by laser #1; **C**: τ by laser #2
- Differential measurement
- **τ is strongly correlated with the change of pressure difference between inside and outside of the ring-down cell.**

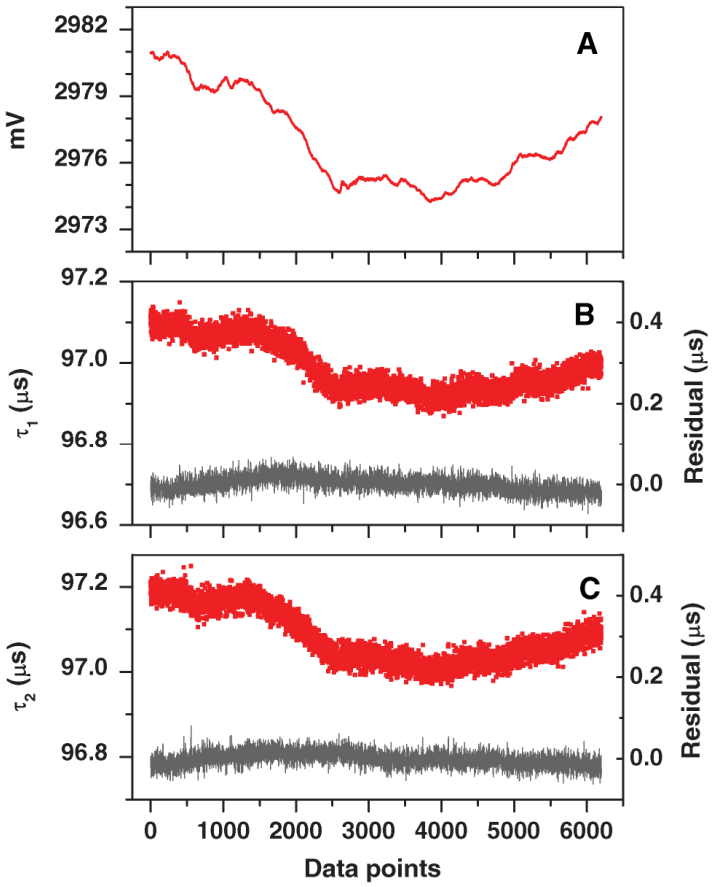

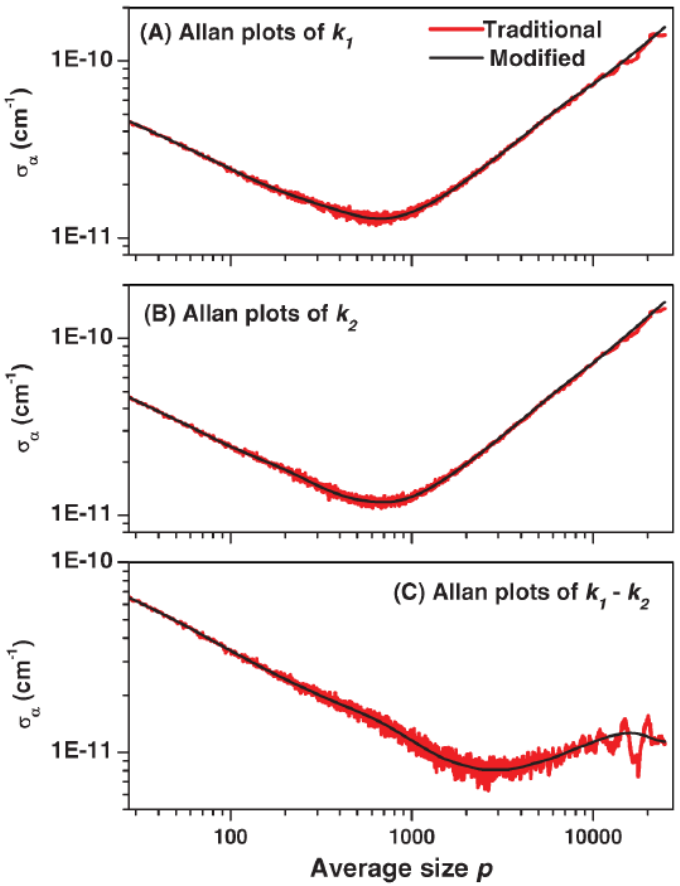

SOA as Light Modulator

Semiconductor Optical Amplifier (SOA):

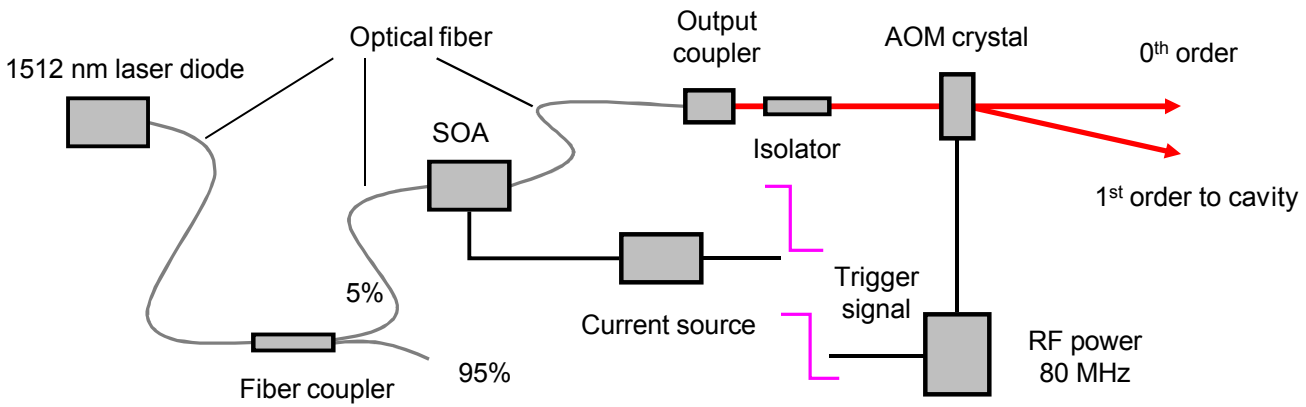

- Highest extinction ratio (> 80 dB) when used as light modulator
- Fast speed: ns or sub ns
- Broadband gain media: ~70 nm
- Optical fiber connected, no extra alignment needed when λ tuning

M. J. Connelly, ***Semiconductor Optical Amplifier***, Kluwer, Boston, 2002.

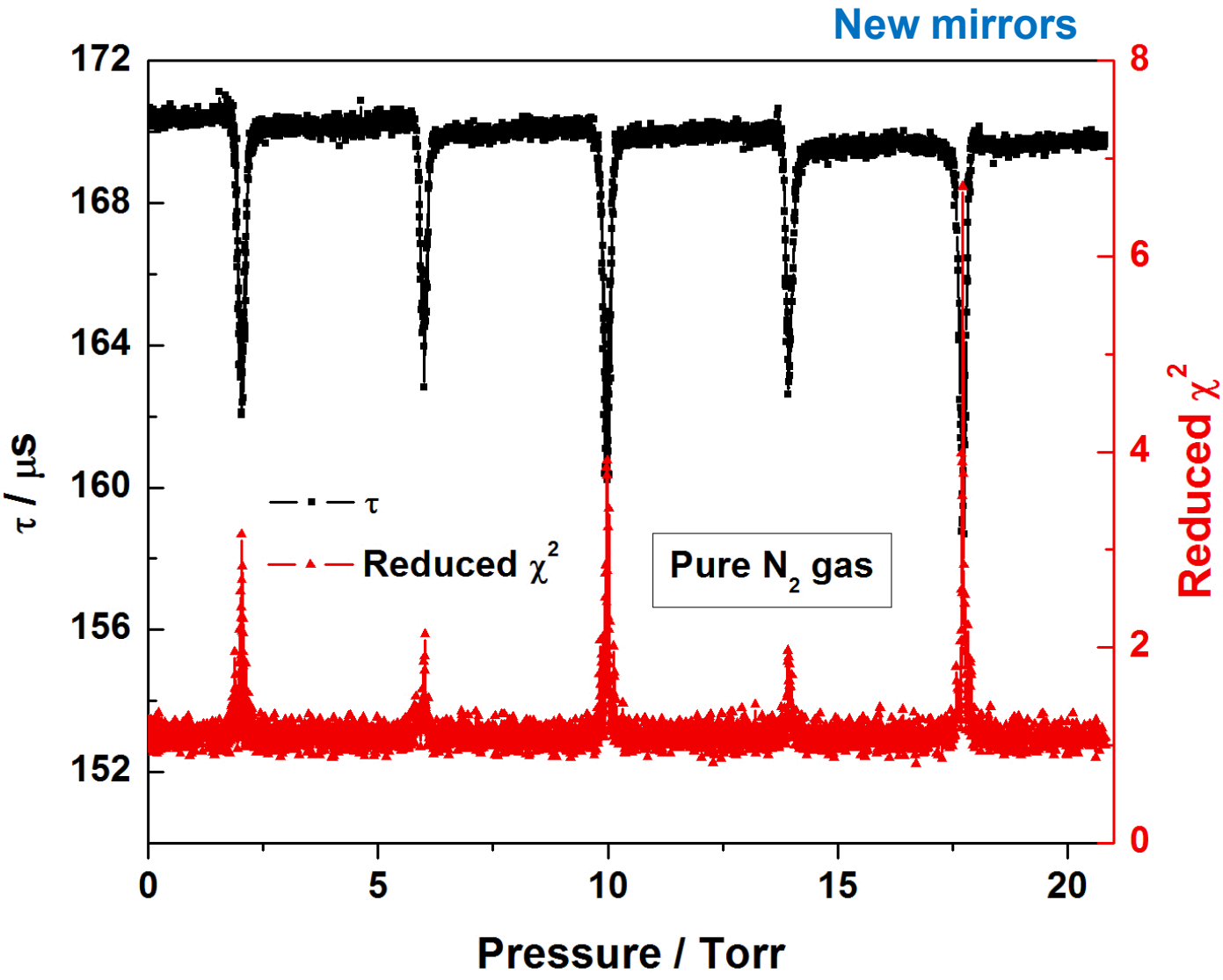
New mirrors
172
168
164
160
156
152
τ / μs
0
5
10
15
20
Pressure / Torr
8
6
4
2
0
Reduced χ²
τ
Reduced χ²
Pure N₂ gas

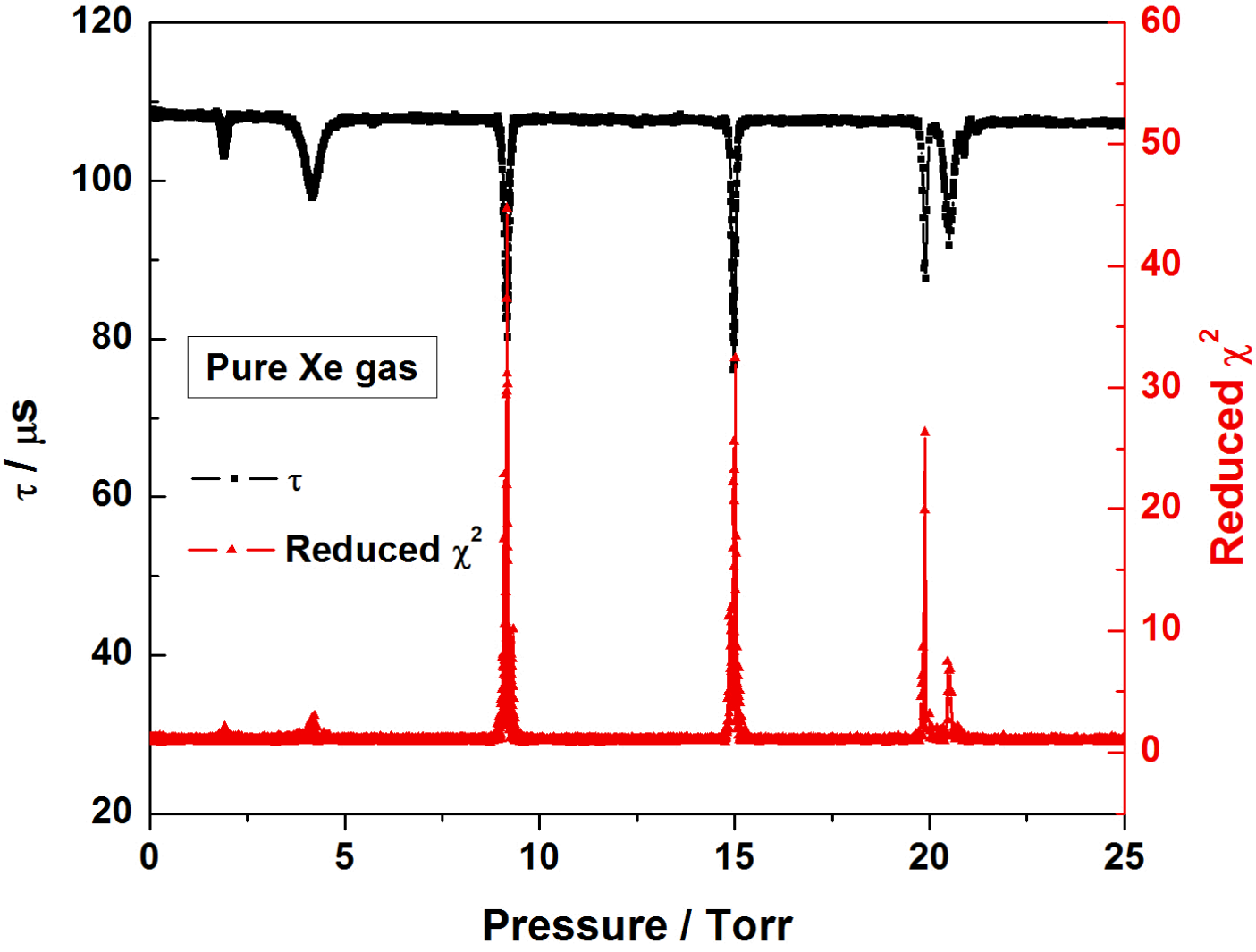
120
100
80
60
40
20
τ / μs
60
50
40
30
20
10
0
Reduced χ²
0
5
10
15
20
25
Pressure / Torr
Pure Xe gas
τ
Reduced χ²

Resonance by tuning!

- Xenon: 81% scan from refractive index increase with pressure
- Cavity length change ~ 0.1μm/Torr, Δν tuning rate **30.7 kHz/torr**

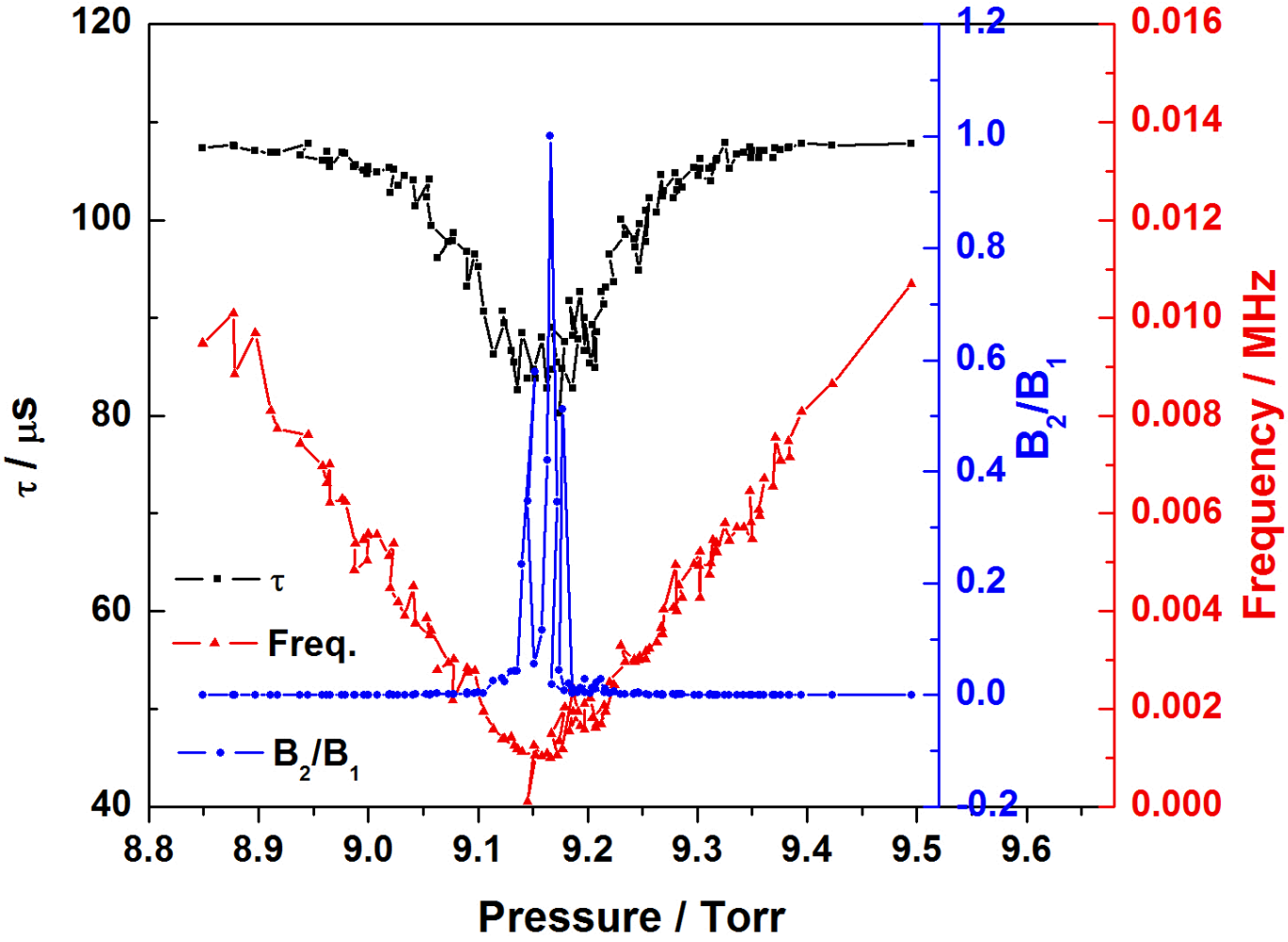

Optimal Least Squares Fit (LSF)

$$\vec{y} = \{y_i\} \qquad i = 0, \ldots, N-1 \qquad \Delta t$$

$$y(t) = F(t) + \varepsilon(t) = Ae^{-kt} + B + \varepsilon(t) \qquad \langle \varepsilon(t) \rangle = 0$$

$$\chi^2(A,B,k) = (\vec{y} - \vec{F})^{\mathrm{T}} \cdot \widetilde{W} \cdot (\vec{y} - \vec{F}) \qquad \vec{F} = \{F_i\} = \{Ae^{-ki\Delta t} + B\}$$

$$(\vec{y} - \vec{F}(A,B,k))^{\mathrm{T}} \cdot \widetilde{W} \cdot \nabla F = \vec{0}^{\mathrm{T}} \qquad \nabla F_{ij} = \left(\frac{\partial F_i}{\partial p_j} \right) \qquad \vec{p} = \{A,B,k\}^{\mathrm{T}}$$

$$\widetilde{\alpha} = \nabla F^{\mathrm{T}} \cdot \widetilde{W} \cdot \nabla F \qquad \widetilde{c} = \widetilde{\alpha}^{-1}$$

$$\vec{\beta} = \nabla F^{\mathrm{T}} \cdot \widetilde{W} \cdot (\vec{y} - \vec{F}) \qquad \delta \vec{p} = \widetilde{c} \cdot \vec{\beta}$$

The diagonal elements of **covariance matrix *c*** are the variances of the fit parameters ***A***, ***B***, and ***k***.

If exponential decay is sampled evenly in time, the **curvature matrix α** and the **vector β** can be written down in closed form expressions for either **detector noise limited (DNL)** or **shot noise limited (SNL)** signal.

K. K. Lehmann and H. Huang, ***Frontiers of Molecular Spectroscopy***, Chapter 18, Elsevier 2008

α and β of DNL Case

$$\alpha_{B,B} = \frac{N}{\sigma^2}$$

$$\alpha_{B,A} = \left(\frac{1-a^N}{1-a}\right)\frac{1}{\sigma^2}$$

$$\alpha_{B,k} = -A\Delta t\left(\frac{a(1-a^N)}{(1-a)^2} - \frac{Na^N}{1-a}\right)\frac{1}{\sigma^2}$$

$$\alpha_{A,A} = \left(\frac{1-a^{2N}}{1-a^2}\right)\frac{1}{\sigma^2}$$

$$\alpha_{A,k} = -A\Delta t\left(\frac{a^2(1-a^{2N})}{(1-a^2)^2} - \frac{Na^{2N}}{1-a^2}\right)\frac{1}{\sigma^2}$$

$$\alpha_{k,k} = (A\Delta t)^2\left(\frac{2a^4(1-a^{2N})}{(1-a^2)^3} + \frac{a^2-(2N+1)a^{2N+2}}{(1-a^2)^2} - \frac{N^2a^{2N}}{1-a^2}\right)\frac{1}{\sigma^2} \quad (23)$$

$$a = \exp(-k\Delta t)$$

Detector noise **σ**

$$\beta_B = \left(\sum_i y_i - A\left(\frac{1-a^N}{1-a}\right) - BN\right)\frac{1}{\sigma^2}$$

$$\beta_A = \left(\sum_i y_i a^i - A\left(\frac{1-a^{2N}}{1-a^2}\right) - B\left(\frac{1-a^N}{1-a}\right)\right)\frac{1}{\sigma^2} \quad (24)$$

$$\beta_k = -A\Delta t\left(\sum_i y_i i a^i - A\left(\frac{a^2(1-a^{2N})}{(1-a^2)^2} - \frac{Na^{2N}}{1-a^2}\right) - B\left(\frac{a(1-a^N)}{(1-a)^2} - \frac{Na^N}{1-a}\right)\right)\frac{1}{\sigma^2}.$$

Each cycle of iteration:

3*N* multiplications

3*N* additions

Substantially more efficient than a general purpose fitting package

K. K. Lehmann and H. Huang, ***Frontiers of Molecular Spectroscopy***, Chapter 18, Elsevier 2008

Cavity Excited by a Noisy Laser

Lorentzian lineshape of a CW diode laser can be understood by a model of **random walk of its field phase**, with $D = \pi \Delta \nu_L$ the phase diffusion constant.

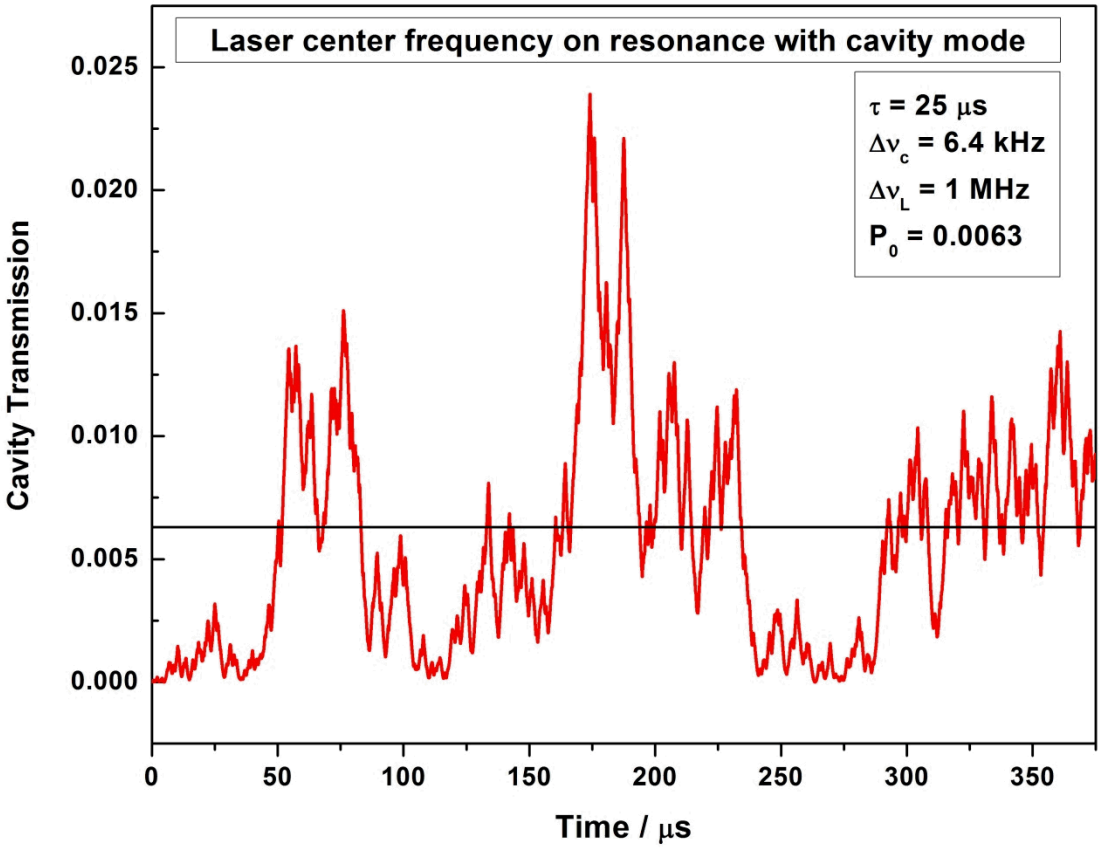

$$P_0 = \left(\frac{T}{1-R}\right)^2 \frac{\Delta\nu_c}{\Delta\nu_c + \Delta\nu_L} P_{\text{in}}$$

$$\Delta\nu_c = 1/2\pi\tau$$

$$P_0 \approx (10^{-4} \sim 10^{-3}) P_{\text{in}}$$

C. H. Henry, ***IEEE J. Quantum Electronics***, **QE-18** 259 (1982)

CW-CRDS: Finite Extinction

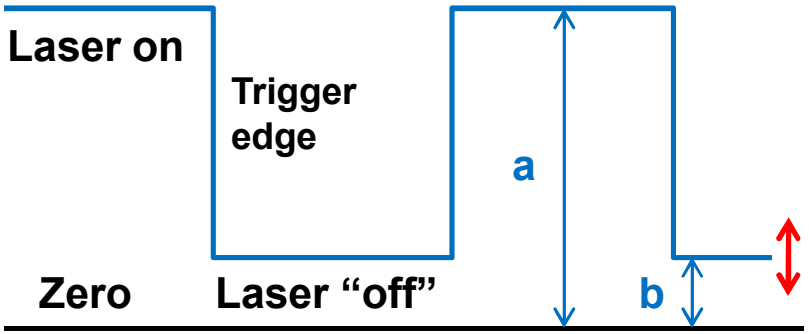

Extinction Ratio: $\varepsilon_r = b / a$

or in dB $= 10 \log(a / b)$

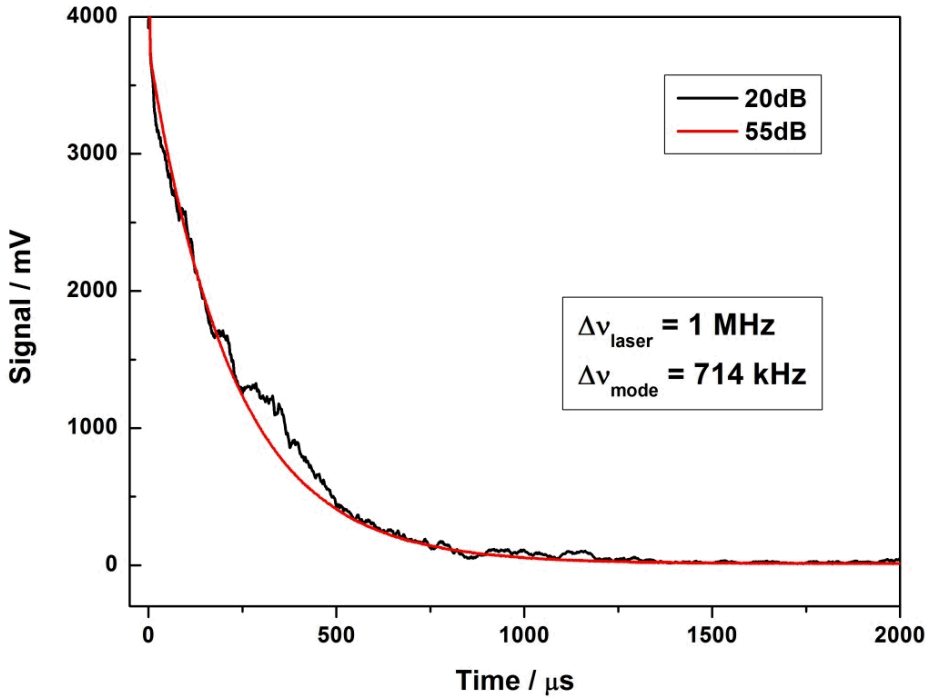

Noise linearly depends on the extinction ratio of light switch.

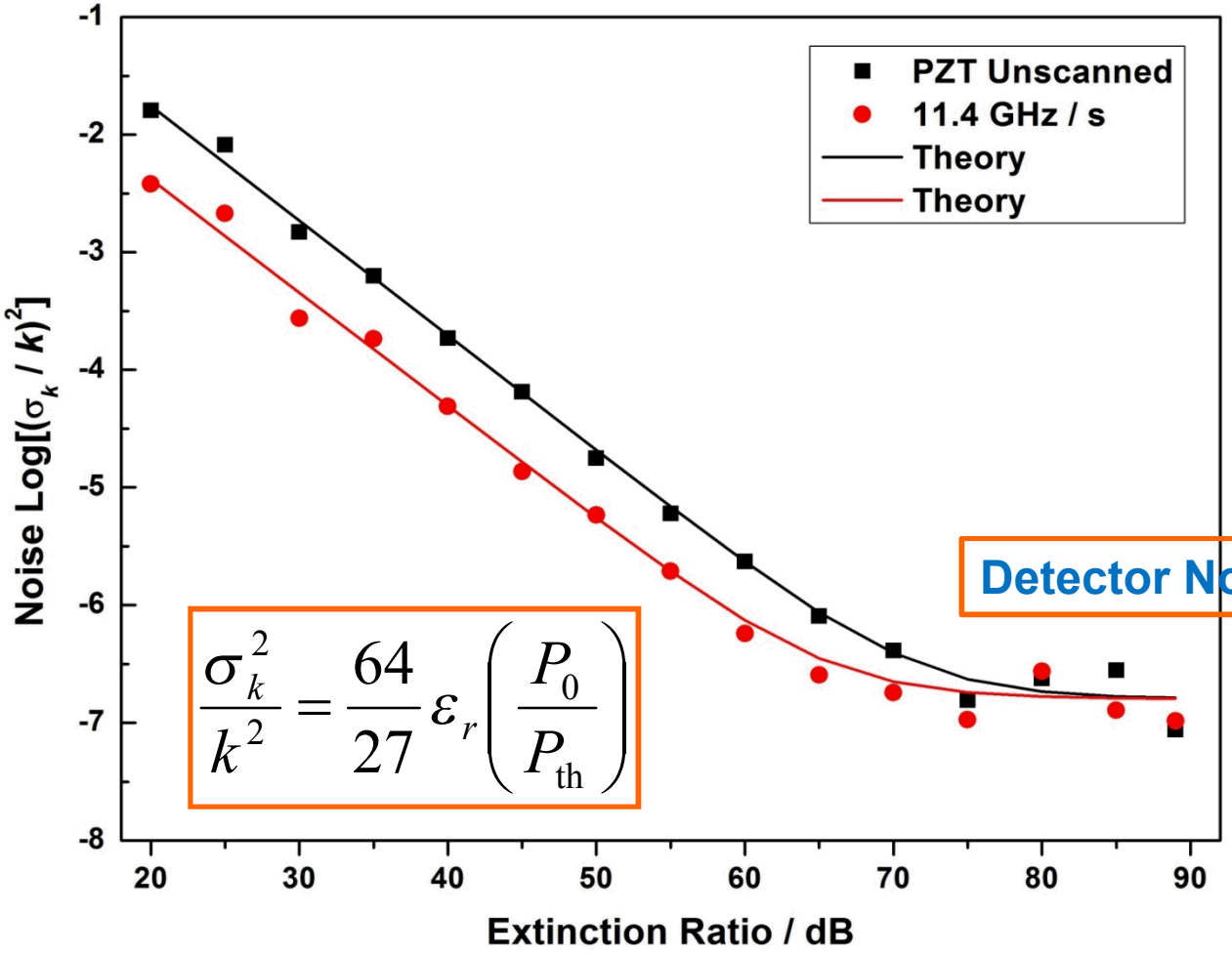

Detector Noise Limit

Semiconductor Optical Amplifier **(SOA)** is a perfect light switch for CW-CRDS.

Highest extinction ratio: **> 80 dB**, very fast speed: **~ ns**, and broadband gain: **~ 70 nm**

H. Huang and K. K. Lehmann, ***Chemical Physics Letters***, **463** 246 (2008)

H. Huang and K. K. Lehmann, ***Applied Physics B***, **94** 355 (2009)

Setup w. Polarization Control

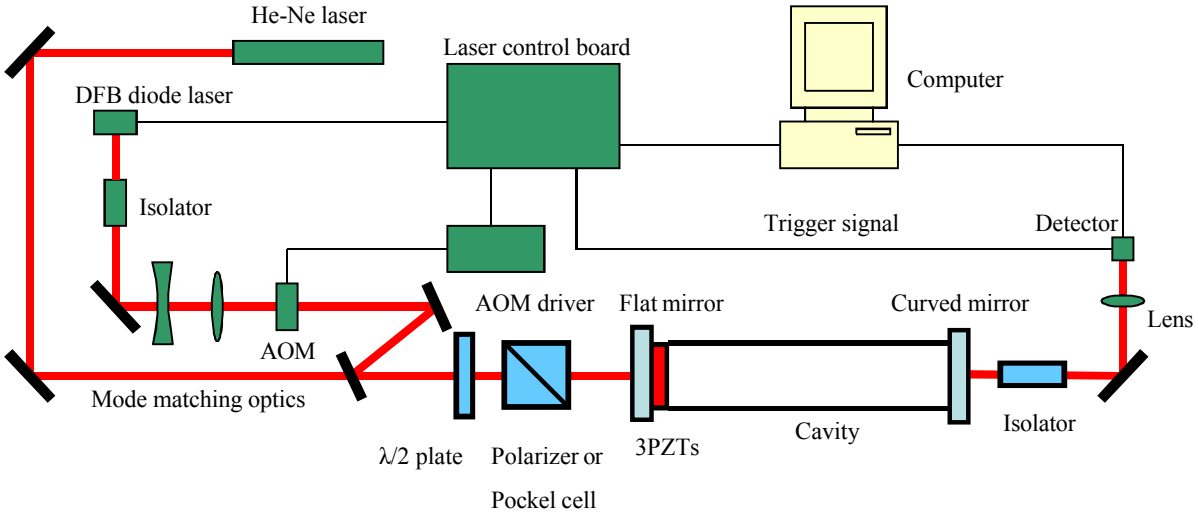

Intracavity Aperture

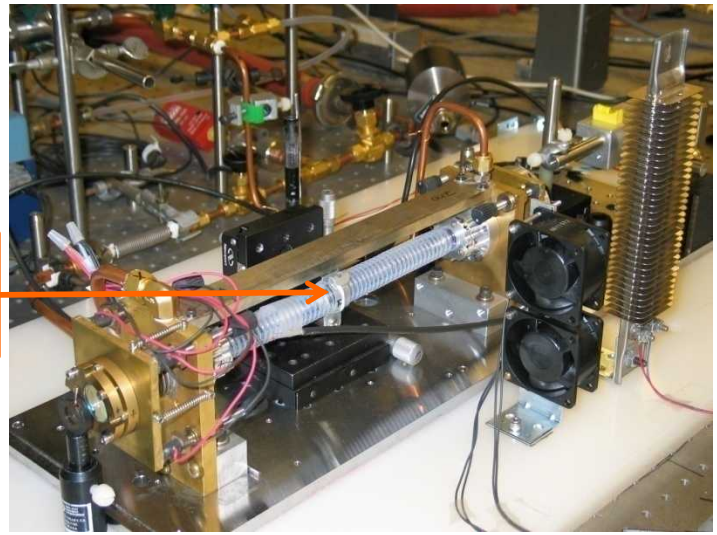

The two analyzer angles of lowest noise level of τ correspond to **two polarization eigenmodes** which are perpendicular with each other.

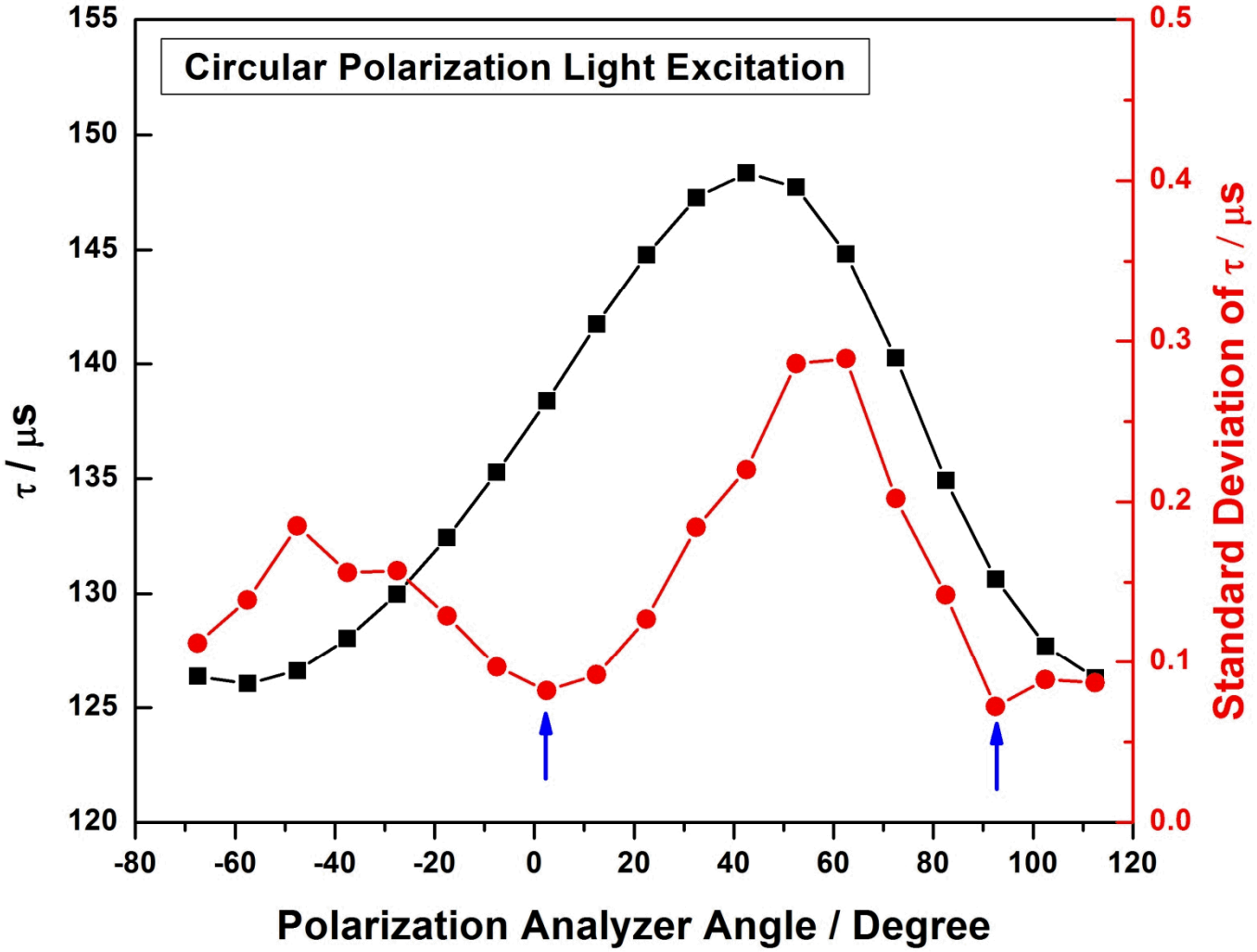

The two polarization eigenmodes rotate with back mirror orientation.

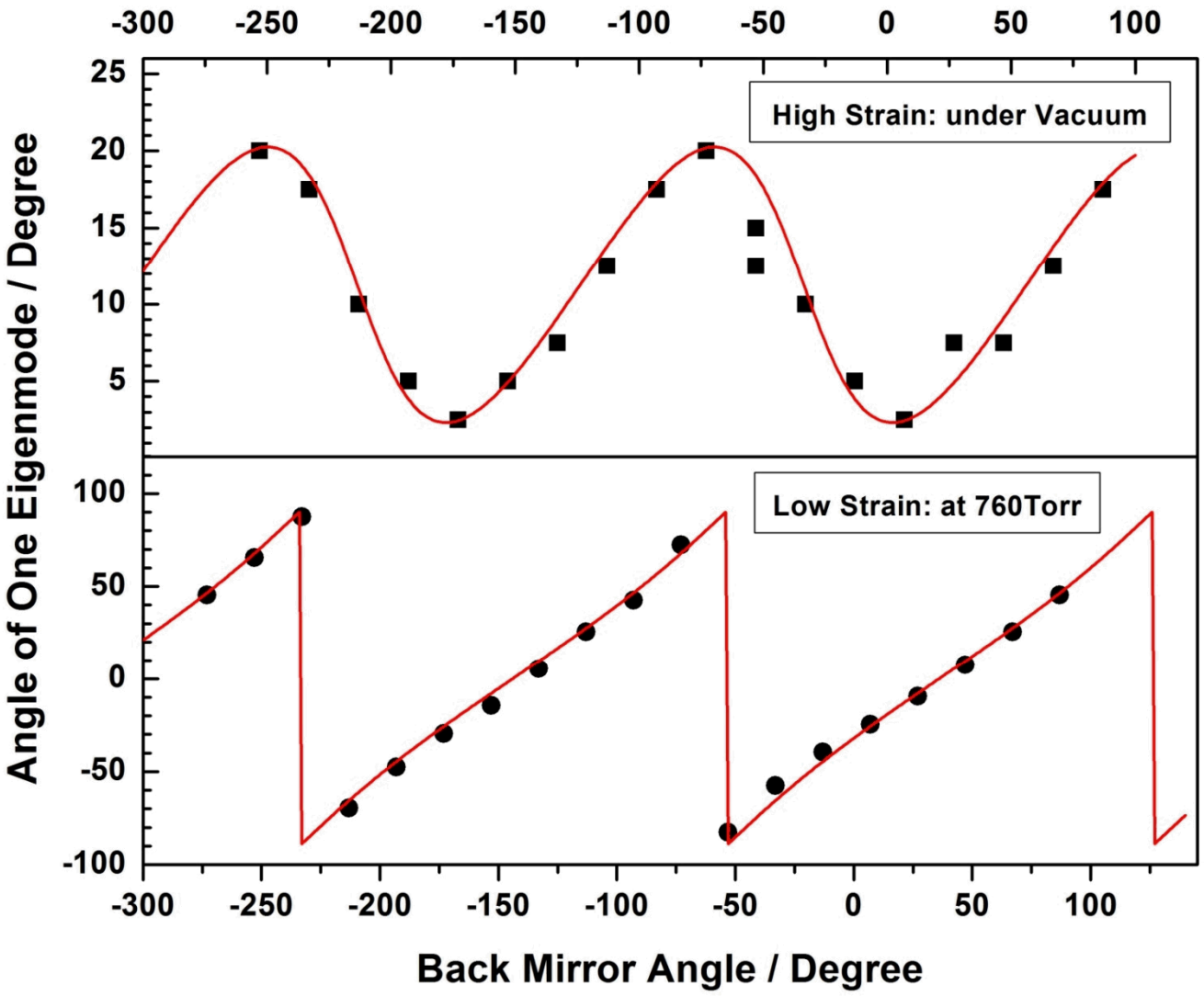

The reflectivity of cavity mirrors depends on the incident polarization angle (linear dichroism).

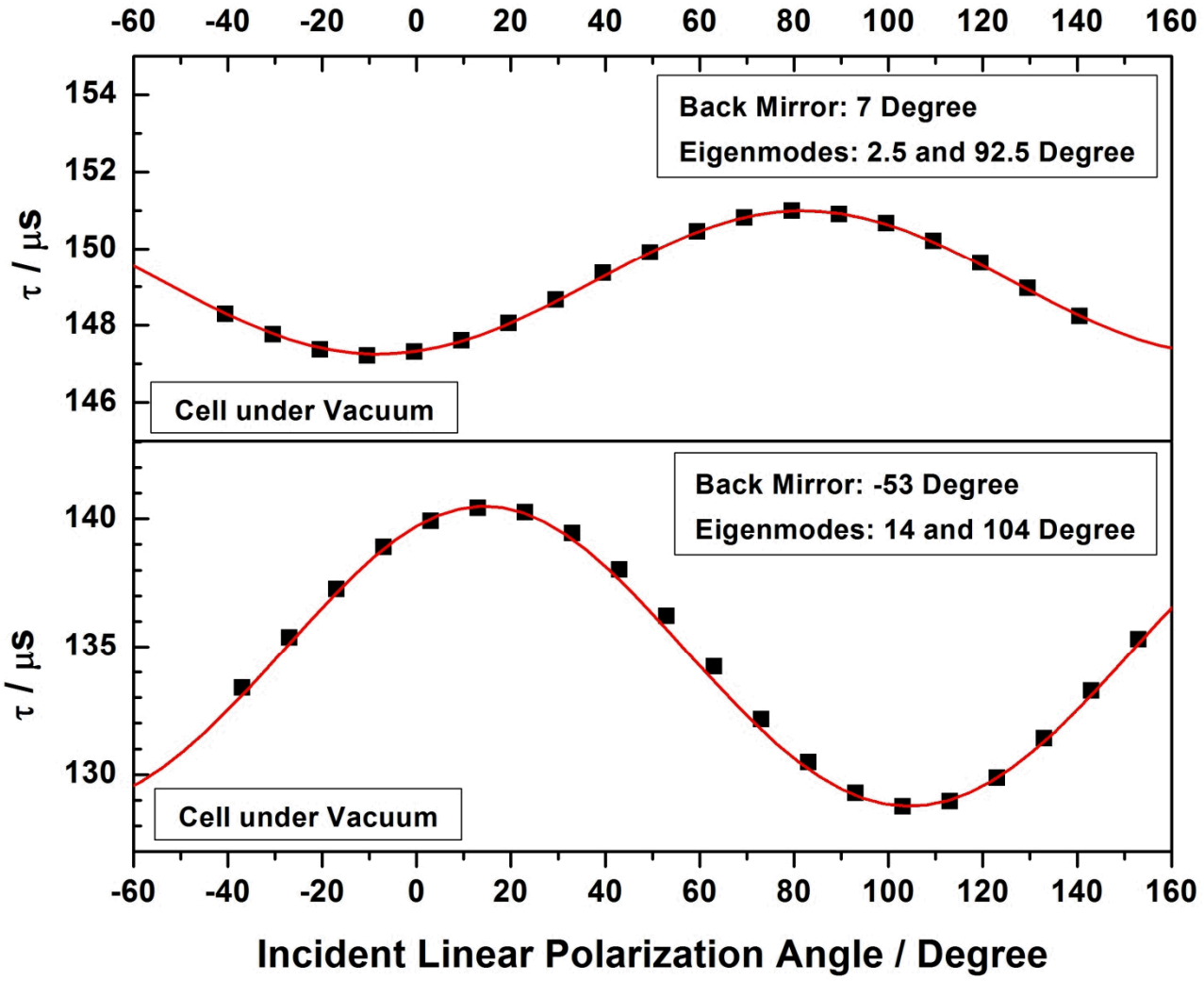

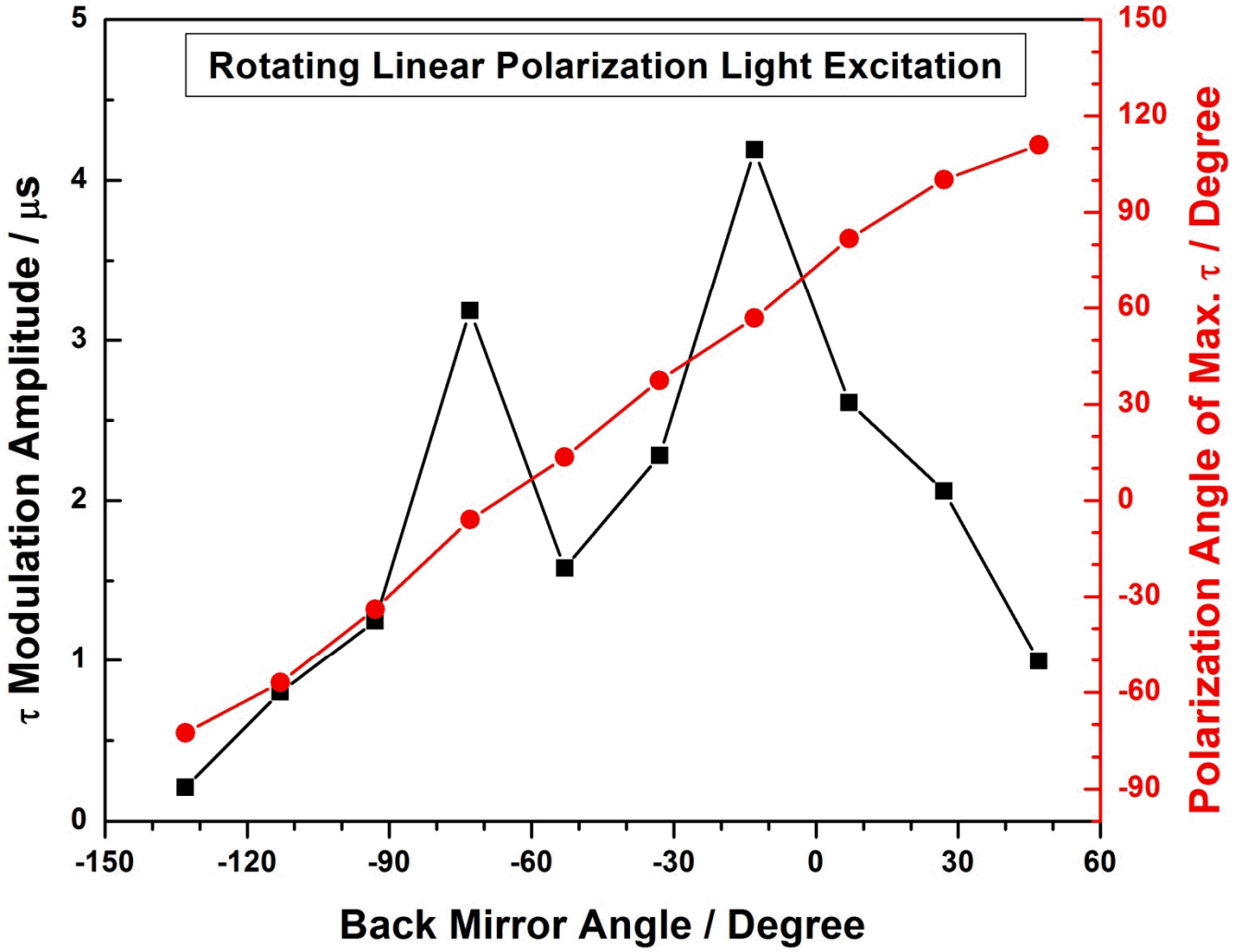

- τ strongly depends on local conditions (e.g. defects) of mirror surface.
- The incident laser polarization angle of **maximum τ** changes smoothly with **back mirror orientation angle**.

HR Coating as a Waveplate

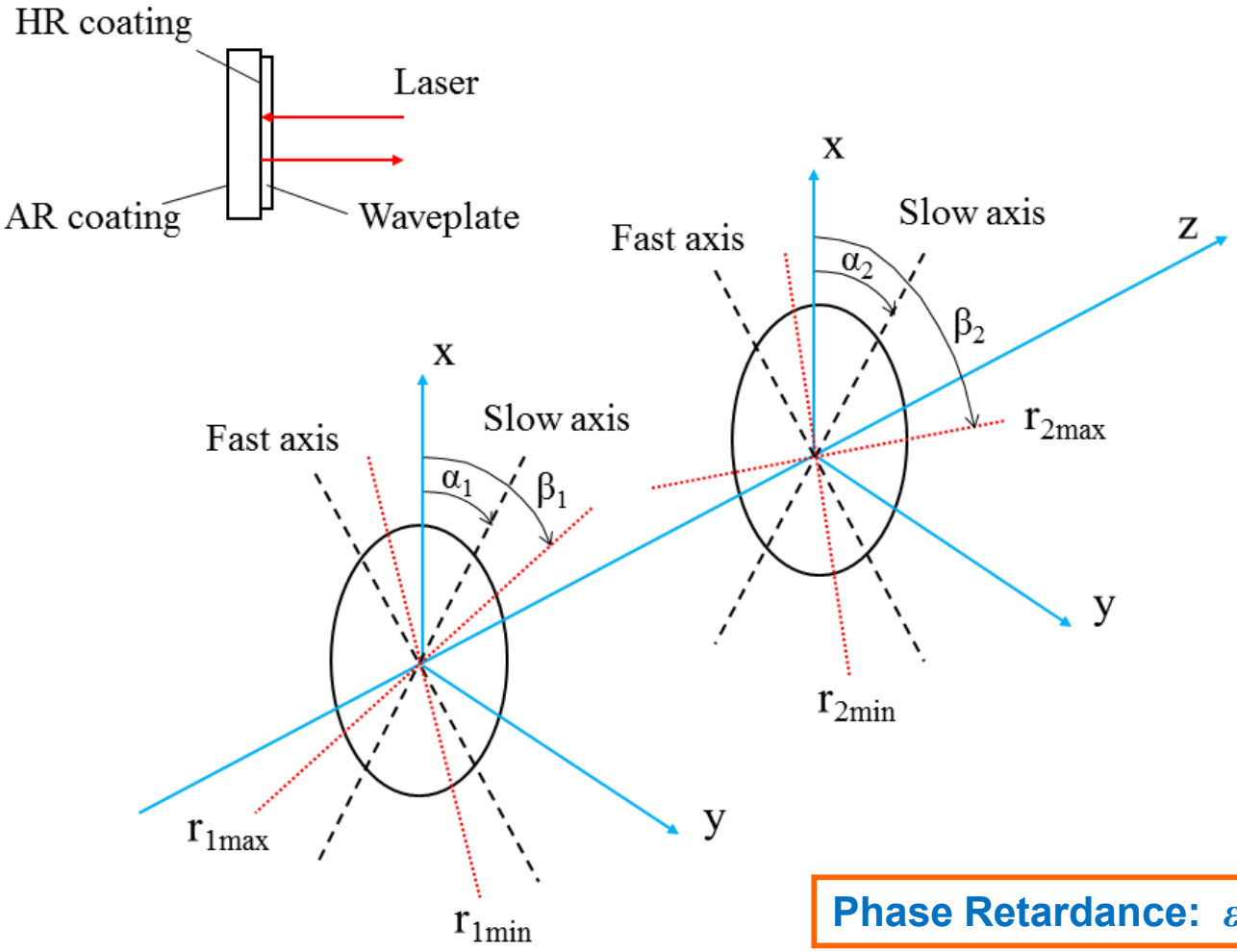

Phase Retardance: ε_1 and ε_2

D. Jacob, *et al*., ***Optics Letters*** **20**, 671–673 (1995) J. L. Hall, J. Ye, and L. Ma, ***Physical Review A*** **62**, 013815 (2000)

J. Morville and D. Romanini, ***Applied Physics B*** **74**, 495–501 (2002)

The Model

Reflection **Jones matrix**:

$$G_i = a_i R(-\beta_i)\cdot\begin{pmatrix}1+b_i & 0\\ 0 & 1-b_i\end{pmatrix}\cdot R(\beta_i),\quad with\quad a_i=\frac{r_{i\max}+r_{i\min}}{2},\ b_i=\frac{r_{i\max}-r_{i\min}}{r_{i\max}+r_{i\min}}$$

Waveplate transmission Jones matrix:

$$F_i = R(-\alpha_i)\cdot\begin{pmatrix}\exp(j\varepsilon_i/2) & 0\\ 0 & \exp(-j\varepsilon_i/2)\end{pmatrix}\cdot R(\alpha_i)$$

$$R(\theta)=\begin{pmatrix}\cos(\theta) & \sin(\theta)\\ -\sin(\theta) & \cos(\theta)\end{pmatrix}$$

Round trip Jones matrix with linear approximation:

$$M_i = F_i\cdot G_i\cdot F_i \qquad M = M_1\cdot M_2$$

$$M = a_1a_2\left[\begin{pmatrix}1 & 0\\ 0 & 1\end{pmatrix}+\begin{pmatrix}b\cos(2\beta)+j\varepsilon\cos(2\alpha) & b\sin(2\beta)+j\varepsilon\sin(2\alpha)\\ b\sin(2\beta)+j\varepsilon\sin(2\alpha) & -b\cos(2\beta)-j\varepsilon\cos(2\alpha)\end{pmatrix}\right]$$

Round trip values for linear dichroism and birefringence:

$$b^2 = b_1^2+b_2^2+2b_1b_2\cos(2(\beta_1-\beta_2))$$

$$\beta=\frac{\beta_1+\beta_2}{2}+\frac{1}{2}\tan^{-1}\left(\frac{b_1-b_2}{b_1+b_2}\tan(\beta_1-\beta_2)\right)$$

$$\varepsilon^2 = \varepsilon_1^2+\varepsilon_2^2+2\varepsilon_1\varepsilon_2\cos(2(\alpha_1-\alpha_2))$$

$$\alpha=\frac{\alpha_1+\alpha_2}{2}+\frac{1}{2}\tan^{-1}\left(\frac{\varepsilon_1-\varepsilon_2}{\varepsilon_1+\varepsilon_2}\tan(\alpha_1-\alpha_2)\right)$$

Round trip Jones matrix *M* no longer Hermitian

E. Hecht, ***Optics***, Addison-Wesley, 2002, 4th ed.

Two **almost linear** polarization eigenmodes but **no longer orthogonal**

$$\lambda_{1,2} = a_1 a_2 \left(1 \pm [b^2 - \varepsilon^2 + 2jb\varepsilon\cos(2(\beta-\alpha))]^{1/2}\right)$$

Frequency splitting between two polarization states of TEM_{00} mode

$$\delta\nu = \frac{\arg(\lambda_1) - \arg(\lambda_2)}{2\pi} FSR \approx \frac{FSR}{\pi}\mathrm{Im}\left([b^2 - \varepsilon^2 + 2jb\varepsilon\cos(2(\beta-\alpha))]^{1/2}\right)$$

$$\tau \approx 130\mu s, \tau_{\max} - \tau_{\min} = 5\mu s, \varepsilon_i \approx 10^{-6}, b_i \approx 10^{-8}, \delta\nu \approx 0.1kHz$$

Two eigenmodes have **different time constants**.

$$\tau_i = \frac{-t_r}{2\ln(|\lambda_i|)}$$

If weak depolarization, τ is a **sine** of incident polarization angle.

$$With \quad \varepsilon \cdot FSR \cdot \tau << 1 \quad and \quad b \cdot FSR \cdot \tau << 1$$

$$u = \begin{bmatrix}\cos(\theta)\\ \sin(\theta)\end{bmatrix} \quad u' = M \cdot u = M \cdot \begin{bmatrix}\cos(\theta)\\ \sin(\theta)\end{bmatrix} \quad \tau(\theta) \approx \frac{-t_r}{2\ln(|u'|)}$$

The relative phase retardance determines the rotation behavior of two polarization eigenmodes.

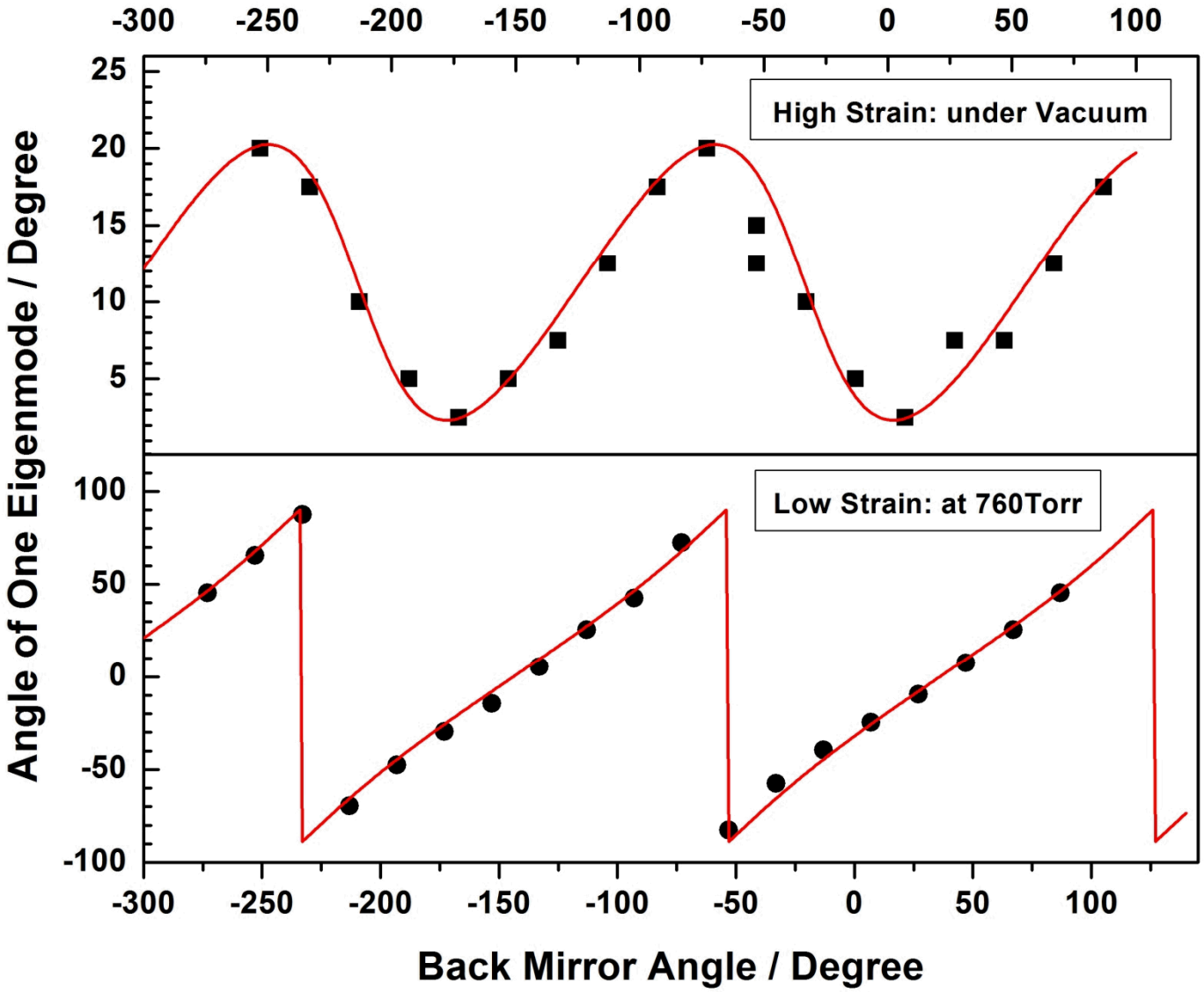

Back mirror at **56** degree, both slow (fast) axes parallel

$$\varepsilon_1 \approx 3.3\varepsilon_2$$
$$b << \varepsilon$$

Back mirror at **36** degree, its slow (fast) axis along **0** degree

$$6\varepsilon_1 \approx \varepsilon_2$$
$$b << \varepsilon$$

Under weak depolarization conditions, the decay time constant τ is a sine of incident polarization angle.

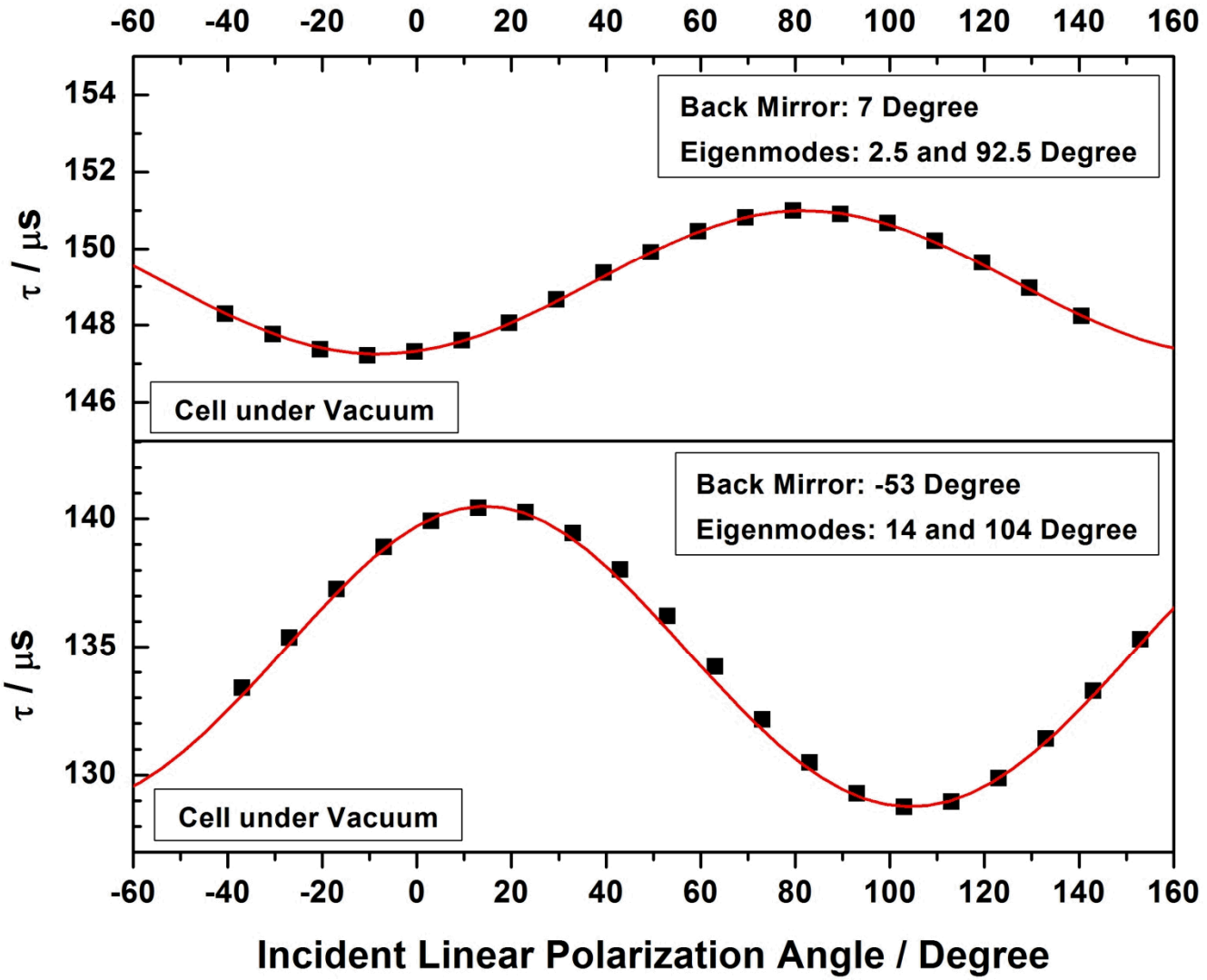

The polarization angle of maximum τ corresponds to the parameter β in the model.

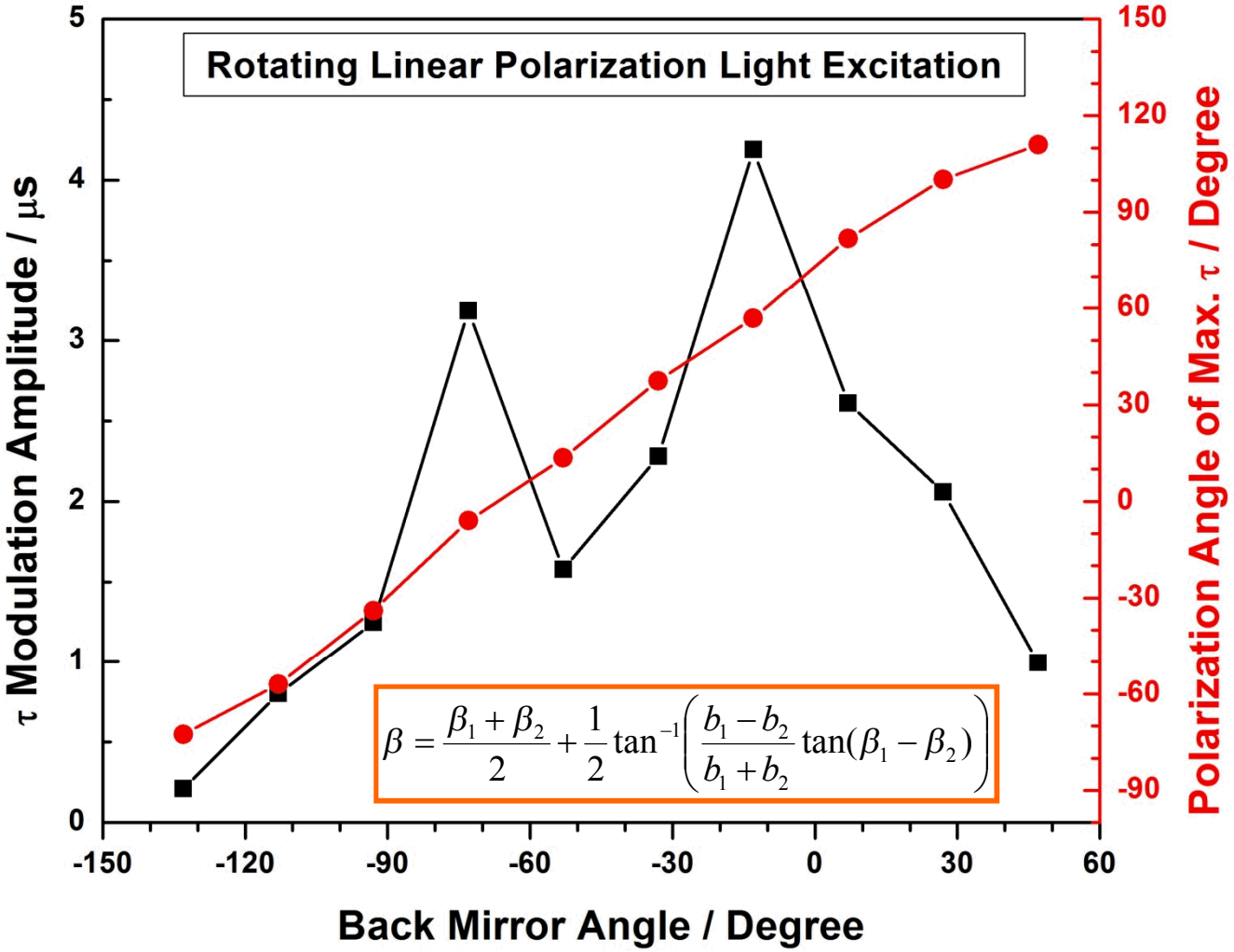

Depolarization the cavity depend on mirror strain conditions.

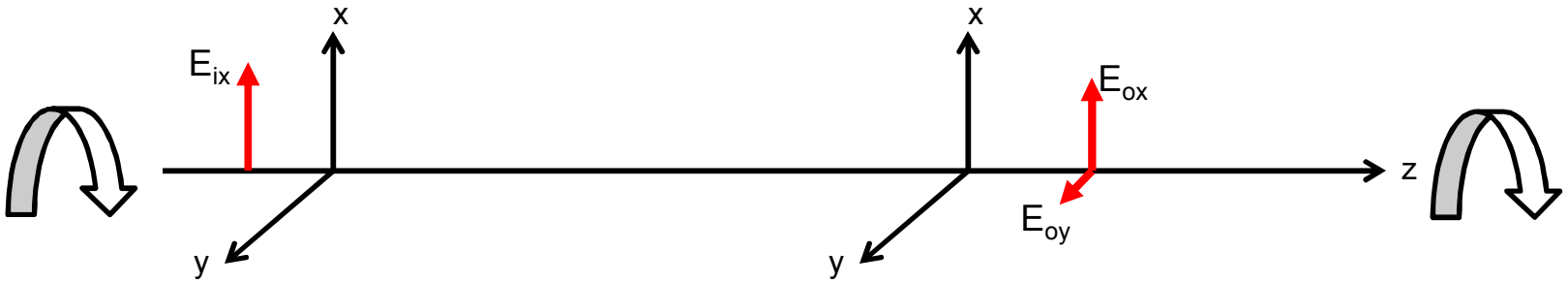

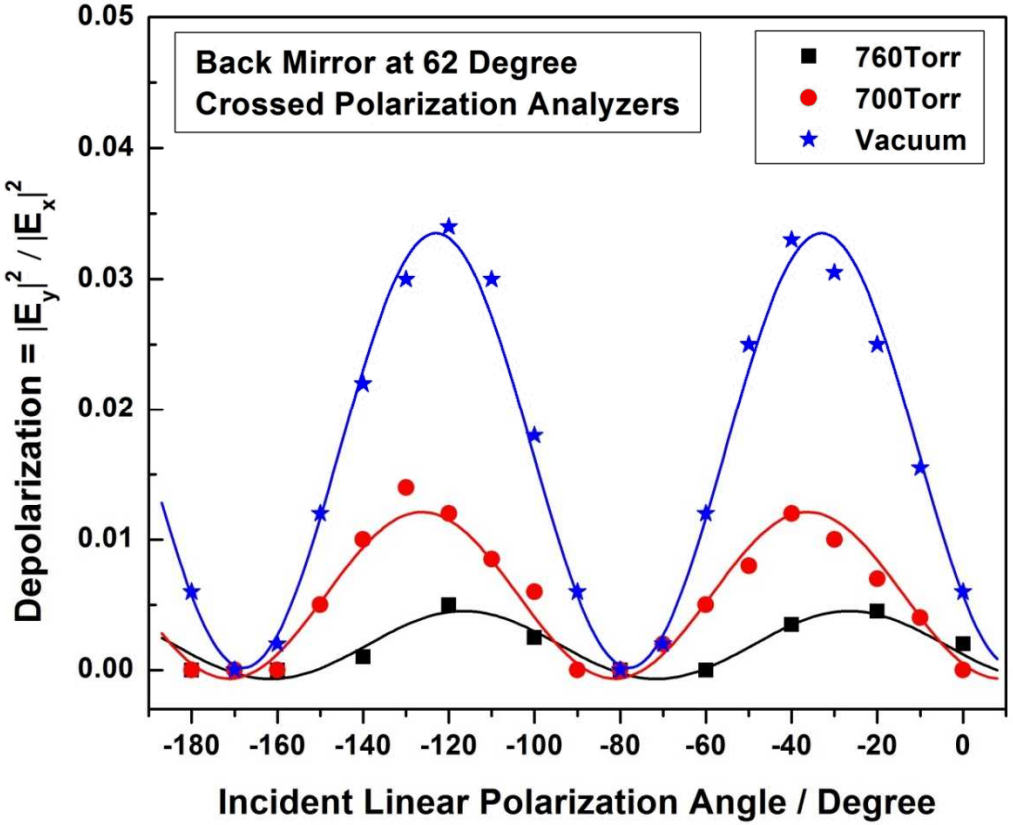

α_1: slow axis angle of mirror 1

$$_2), f = \varepsilon_1/\varepsilon_2 \text{ and } \gamma = \alpha_2 - \alpha_1$$

High strain:

$$\varepsilon_1 \approx 1.0\times10^{-6}\ rad$$
$$\varepsilon_2 \approx 3.1\times10^{-7}\ rad$$

Low strain:

$$\varepsilon_1 \approx 8.3\times10^{-8}\ rad$$
$$\varepsilon_2 \approx 5.0\times10^{-7}\ rad$$

H. Huang and K. K. Lehmann, ***Applied Optics***, **47**(21), 3817-3827 (2008)

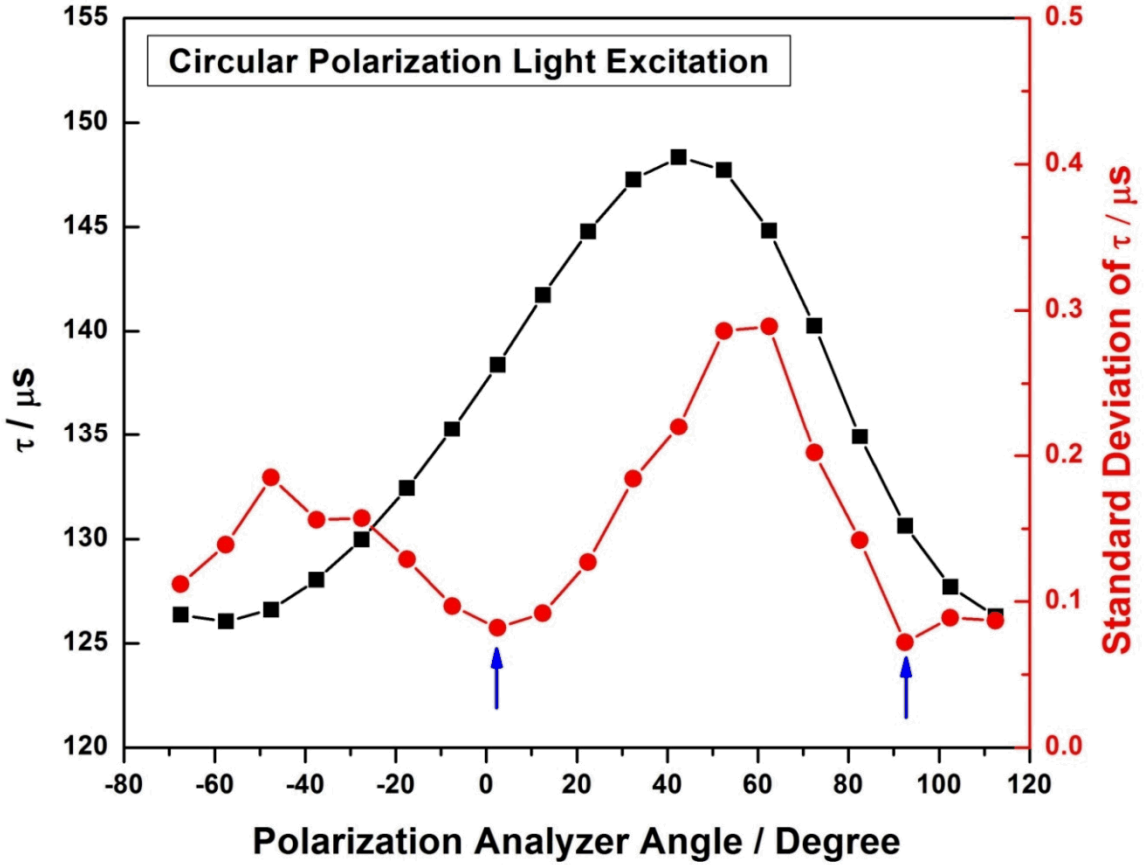

Because the splitting is only **0.1 kHz** and the mode overlap $b / \varepsilon \sim 10^{-2} - 10^{-1}$ is small, it will not cause an observable mode beating effect in ring-down signal.

Practically, linearly polarized incident laser at **two special angles** gives best signal.

However, mismatched polarization discrimination in the detection system will cause severe **mode beating** in ring-down signal, making **reduced $\chi^2 >> 1$**.

H. Huang and K. K. Lehmann, ***Applied Optics***, **47**(21), 3817-3827 (2008)